Asymmetric Pudovik Reaction as a Tool for Functionalizing 3-Formyl Chromones

Synthesis

2026

10.1055/a-2815-1115

ISSN 0039-7881

Paper

Asymmetric Pudovik Reaction as a Tool for Functionalizing 3-Formylchromones

Juan Carlos Morales-Solís[1,2], Mario Ordoñez[2], Eugenia Marqués-López[1], Raquel P. Herrera[1]
Affiliation addresses are listed at the end of the article.

GRAPHICAL ABSTRACT

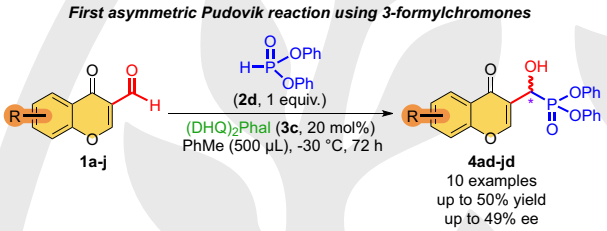

ABSTRACT

We report a preliminary proof of concept for the first asymmetric synthesis of a novel series of chromone-derived compounds via the Pudovik reaction, employing the chiral organocatalyst $(DHQ)_2Phal$. Although only moderate enantiomeric excess values were obtained, the scope of the reaction using different electron-withdrawing and electron-donating groups on substituted 3-formylchromones demonstrated the viability of this methodology. The absolute configuration of the final products was established through NMR analysis of diastereoisomeric derivatives with (*S*)-naproxen, complemented by computational calculations, including a study of the correlation between dipole moment and molecular polarity.

Keywords asymmetric organocatalysis, biscinchona, 3-formylchromones, Pudovik reaction, dipole moment

received December 09, 2025 | **accepted after revision** February 16, 2026 | **accepted manuscript online** February 16, 2026 | **article published online** 2026

Bibliography Synthesis **DOI** 10.1055/a-2815-1115 **Art ID** SS-2025-12-0399-OP

Correspondence Prof. Raquel P. Herrera, Department of Organic Chemistry, Laboratorio de Organocatálisis Asimétrica, Instituto de Síntesis Química y Catálisis Homogénea (CSIC–University of Zaragoza), Zaragoza, Spain, Email: raquelph@unizar.es
Dr. Eugenia Marqués-López, Department of Organic Chemistry, Laboratorio de Organocatálisis Asimétrica, Instituto de Síntesis Química y Catálisis Homogénea (CSIC–University of Zaragoza), Zaragoza, Spain, Email: mmaamarq@unizar.es

Introduction

The Pudovik reaction is a pivotal transformation in organic chemistry,[1] due to its efficiency and versatility constructing carbon–phosphorus bonds. It plays a crucial role in the synthesis of α-amino- and α-hydroxyphosphonates and other phosphorus-containing compounds.[2] This reaction involves the nucleophilic addition of dialkyl or diaryl phosphites, which are the actual reactive species,[3] to electrophilic carbon centers such as imines or carbonyl compounds.[2] This simple transformation offers an efficient route to highly functionalized molecules, making it a valuable tool for developing products with broad applications in medicinal chemistry, agriculture, and materials science.[4]

Among the products derived from the Pudovik reaction, α-hydroxyphosphonates are particularly noteworthy. These compounds possess significant interest in both synthetic and medicinal chemistry.[5] Their functional versatility, particularly the presence of both hydroxyl and phosphonate moieties, allows for further derivatization as important intermediates in organic synthesis, leading to bioactive molecules with potential pharmaceutical applications.[6] In this context, they can act as enzyme inhibitors, herbicides, and as anticancer agents, and some exhibiting antibacterial and antifungal properties (**Fig. 1**).

Therefore, the development of novel synthetic methodologies using this tool still plays a fundamental role in the progress of organic chemistry, particularly in areas such as pharmaceuticals, materials science, and sustainable chemistry.

On the other hand, chromone derivatives are an important class of heterocycles[7] known for their broad pharmacological spectrum, including antioxidant, anti-inflammatory, and anticancer effects.[8] Their structural diversity and biological relevance

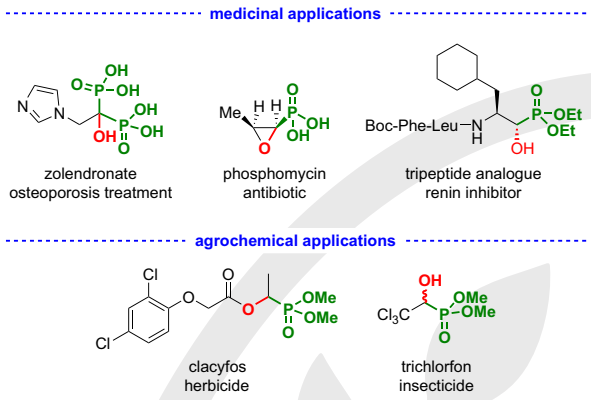

Fig. 1 Examples of biologically active α-hydroxyphosphonates.

have positioned them as valuable scaffolds in drug discovery and development. Additionally, chirality is crucial in medicinal chemistry because stereochemistry can strongly influence biological activity by modulating interactions with chiral targets such as enzymes and receptors.[9] In this context, enantioselective synthetic strategies play a key role in developing biologically active compounds with enhanced efficacy and selectivity. Within this framework, incorporating the Pudovik reaction into chromone-based substrates could represent a notable advancement. To the best of our knowledge, this approach has only been explored from a racemic perspective.[10] Therefore, the first application of this reaction with chromone-derived aldehydes under asymmetric organocatalysis can be regarded as a preliminary step toward expanding the synthetic methodology available for this substrate class. While still at an early stage, this demonstrates that stereoselective control is feasible and may, in the future, enable access to chromone-based compounds with potentially distinctive biological properties. In this sense, the present study contributes to the ongoing development of asymmetric phosphorus chemistry and highlights the relevance of chirality in the design of bioactive molecules.

As part of our efforts to develop a novel enantioselective and organocatalytic Pudovik addition to 3-formylchromones, we began by evaluating a series of chiral organocatalysts. Based on our expertise in hydrophosphonylation reactions[11] and the necessity of a Brønsted base functionality, we selected catalysts from three distinct families: cinchona alkaloids, thioureas, and squaramides (**Scheme 1**, see Supporting Information for additional catalytic structures tested). Initial investigations focused on the model reaction between chromone **1a** and dibenzyl phosphite **2a**.

Although all the tested catalysts were able to promote the reaction to some extent, only biscinchona **3c** afforded a slight and promising 20% of enantiomeric excess (ee). While this level

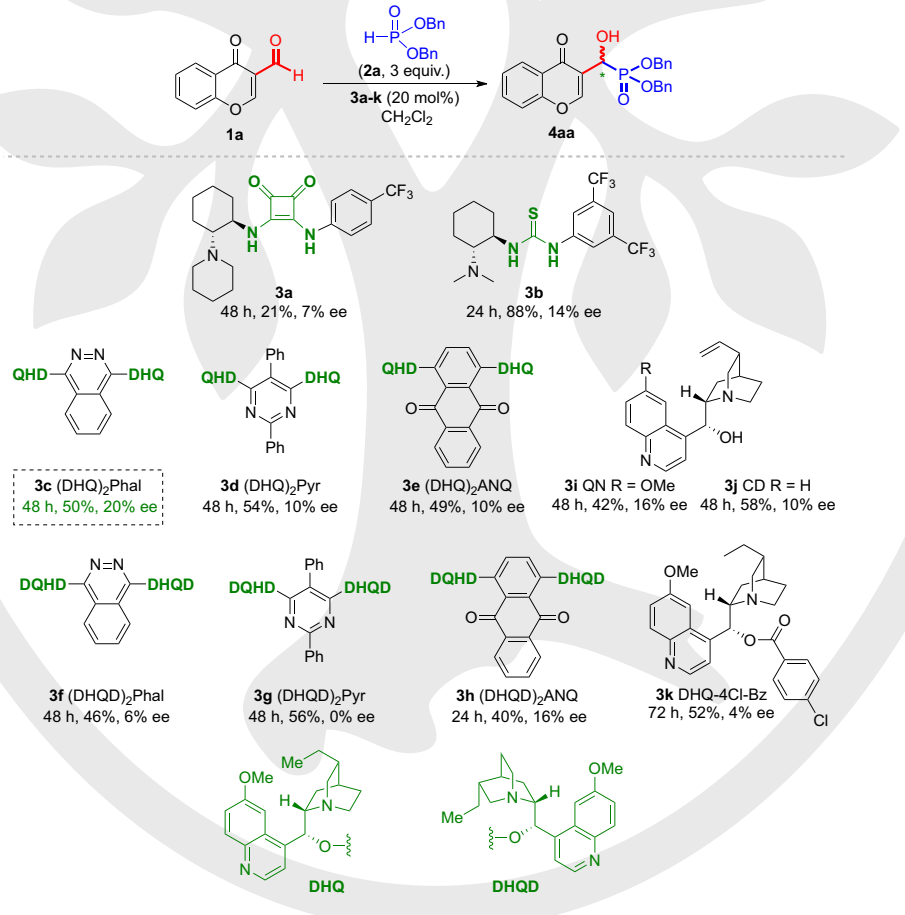

Scheme 1 Exploring the catalytic activity of different chiral Brønsted base derivatives.

of enantioselectivity is modest, this result is noteworthy as it represents the first reported use of 3-formylchromones as substrates under asymmetric conditions. This initial promising outcome highlights the potential for further development and optimization. Encouraged by this result, we proceeded to systematically investigate the reaction parameters using catalyst **3c** in the subsequent experiments, aiming to improve both reactivity and stereoselectivity (**Tables 1 and 2**).

First, we evaluated various reaction parameters, including temperature, solvent, and equivalents of phosphite **2a** and catalyst loading (see Supporting Information for the use of additives and different concentrations). The temperature screening revealed that optimal reaction conditions were achieved at room temperature (entries 1–4), as lower temperatures significantly reduced the yield without substantially improving the ee. Further analysis of the amount of phosphite **2a** indicated that 1 equiv. was sufficient, although it led to a slight decrease in yield, the use of a large excess was not justified (entries 1, 5, and 6). Additionally, solvent exploration demonstrated that toluene was the most effective option, slightly improving the ee of the reaction (entries 6–10). Variation in catalyst loading (30 mol% or 10 mol%) showed no enhancement neither in the reactivity nor in the enantioselectivity of the process (entries 7, 11, and 12). With these optimized conditions established, we proceeded to evaluate the behavior of different phosphites (**Table 2**).

Table 1 Screening of the reaction exploring different parameters.

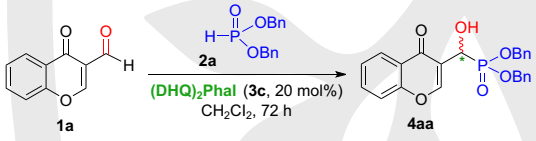

Entry	$HP(O)(OBn)_2$ (2a) (equiv.)	Solvent (500 µL)	Temp. (°C)	Yield (%)[a]	ee (%)[b]
1[c]	3	CH_2Cl_2	r.t.	50	20
2	3	CH_2Cl_2	0	38	26
3	3	CH_2Cl_2	−20	33	24
4	3	CH_2Cl_2	−40	13	20
5	2	CH_2Cl_2	r.t.	38	20
6	1	CH_2Cl_2	r.t.	30	22
7	1	Toluene	r.t.	36	32
8	1	2-MeTHF	r.t.	18	20
9	1	Ethyl L-lactate	r.t.	27	12
10	1	CPME[d]	r.t.	24	28
11[e]	1	Toluene	r.t.	24	27
12[f]	1	Toluene	r.t.	24	34

[a]Yield after purification by column chromatography.
[b]Enantiomeric excess (ee) determined by chiral HPLC [Daicel Chiralpak IF column (*n*-heptane/*i*PrOH = 70:30, flow rate 1 mL min^{-1})].
[c]Reaction stopped after 48 h.
[d]CPME: cyclopentyl methyl ether.
[e]30 mol% of catalyst **3c**.
[f]10 mol% of catalyst **3c**.

Table 2 Screening of different phosphites and temperature effect in the Pudovik reaction.

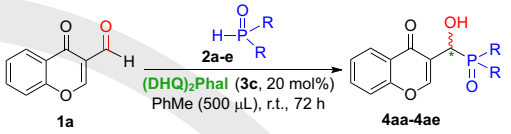

Entry	$HP(O)(R)_2$ (2a–e) (1 equiv.)	Temp. (°C)	Yield (%)[a]	ee (%)[b]
1	R = OBn, **2a**	r.t.	50	20
2	R = OEt, **2b**	r.t.	38	35
3	R = O*i*Pr, **2c**	r.t.	11	26
4	R = OPh, **2d**	r.t.	23	43
5	R = Ph, **2e**	r.t.	69	8
6	R = OPh, **2d**	0	50	28
7	R = OPh, **2d**	−10	50	35
8	R = OPh, **2d**	−20	52	35
9	R = OPh, **2d**	−30	50	43
10[c]	R = OPh, **2d**	−30	50	30
11[d]	R = OPh, **2d**	−30	43	28

[a]Yield after purification by column chromatography.
[b]Enantiomeric excess (ee) determined by chiral HPLC.
[c]2 equiv. of diphenyl phosphite **2d**.
[d]3 equiv. of diphenyl phosphite **2d**.

The evaluation of phosphites **2a–e** under optimal reaction conditions (entries 1–5), as shown in **Table 2**, revealed that diphenyl phosphite (**2d**) afforded the final product **4ad** with the highest enantioselectivity (entry 4). Notably, diphenyl phosphine oxide (**2e**) exhibited the best reactivity, although with lower enantioselectivity (entry 5). Due to the critical role of temperature in asymmetric catalysis, we further investigated its impact again at this stage (entries 6–9). Notably, for diphenyl phosphite (**2d**), the best compromise between reactivity and enantioselectivity was achieved at −30 °C (entry 9). In this sense, we examined the effect of equivalents of diphenyl phosphite (**2d**) at −30 °C (entries 9–11). Significantly, the use of 1 equiv. (entry 9) represented the best option in terms of both yield and enantioselectivity.

Having established the best reactions conditions for the Pudovik addition, the subsequent step involved the synthesis of different 3-formylchromones **1** to complement the commercially available ones. Thus, based on previous reports using Vilsmeier–Haack conditions,[10a,c] we carried out the synthesis described in **Scheme 2**, using 2′-hydroxyacetophenones **5d,e,f,i** as starting materials and the Vilsmeier–Haack reagent formed in situ by the reaction of *N,N*-dimethylformamide (DMF) with $POCl_3$, followed by the hydrolysis which, after the intramolecular cyclization and formylation, afforded four new 3-formylchromones **1d,e,f,i** in good yields. Notably, the efficiency of this approach highlights its suitability for accessing a wide variety of 3-formylchromones, which could be valuable for further functionalization in our methodology.

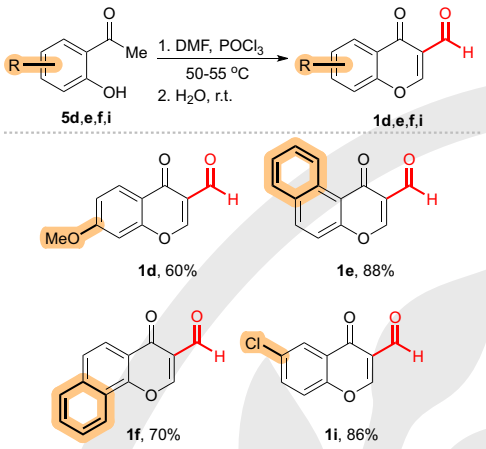

Scheme 2 Synthesis of different 3-formylchromones starting from 2′-hydroxyacetophenones **5d**,**e**,**f**,**i**.

Then, we investigated the scope and limitations of our methodology by employing various 3-formylchromones **1b–j**, as illustrated in **Scheme 3**. In this study, various chromone derivatives were selected with different electronic properties, allowing for an evaluation of their influence on reactivity and enantiomeric excess.

In this sense, the benzene-fused rings (**4ed**,**fd**) gave the best enantioselectivities, with a notably higher yield in the benzene [*f*]-ring (**4ed**). Additionally, electron withdrawing groups as NO_2, Br, and Cl at C-6 position (**4gd**,**hd**,**id**) showed moderated results for both yield and enantioselectivity. However, electron donating groups at C-6 position as methoxy (**4cd**) gave a similar yield but the lowest enantioselectivity, instead of its isomer 7-methoxy (**4dd**), which showed one of the highest enantioselectivities in this work. Finally, methyl group (**4bd**) provided a similar yield and ee that electron withdrawing groups. On the other hand, the double substituted chromone (**4jd**) gave one of the best yields although with low enantioselectivity. This could be attributed to the higher reactivity of the system during the Pudovik addition, which, however, results in lower enantioselectivity (**Scheme 3**). This scope revealed that while our method can be applied to a wide variety of derivatives, both enantioselectivity and reactivity are significantly influenced by the nature of the substituents on the 3-formylchromones **1**.

Furthermore, to establish the absolute configuration of the major α-hydroxyphosphonate obtained from the Pudovik addition, an NMR study was performed.[12] Specifically, α-hydroxyphosphonates **4aa** and **4ad** were derivatized via esterification with (*S*)-naproxen using EDC (*N*-(3-dimethylaminopropyl)-*N*′-ethylcarbodiimide) hydrochloride and DMAP (4-dimethylaminopyridine) in CH_2Cl_2, affording the corresponding α-naproxen-phosphonates **6aa** and **6ad** in 96 and 95% yield, respectively. Both products were obtained as mixtures of the diastereoisomers (*S*,*S*) and (*R*,*S*) (**Scheme 4**). While chromatographic separation of the diastereoisomeric mixture **6ad** proved challenging, the α-naproxen-phosphonates **6aa** were successfully separated by column chromatographic, affording the enantiomerically pure (*S*,*S*)- and (*R*,*S*)-naproxen-phosphonates **6aa** (**Scheme 4**).

With the isolated α-naproxen-phosphonates **6aa** in hand as the most polar and least polar diastereoisomers, we proposed Newman extended projections for each diastereoisomer

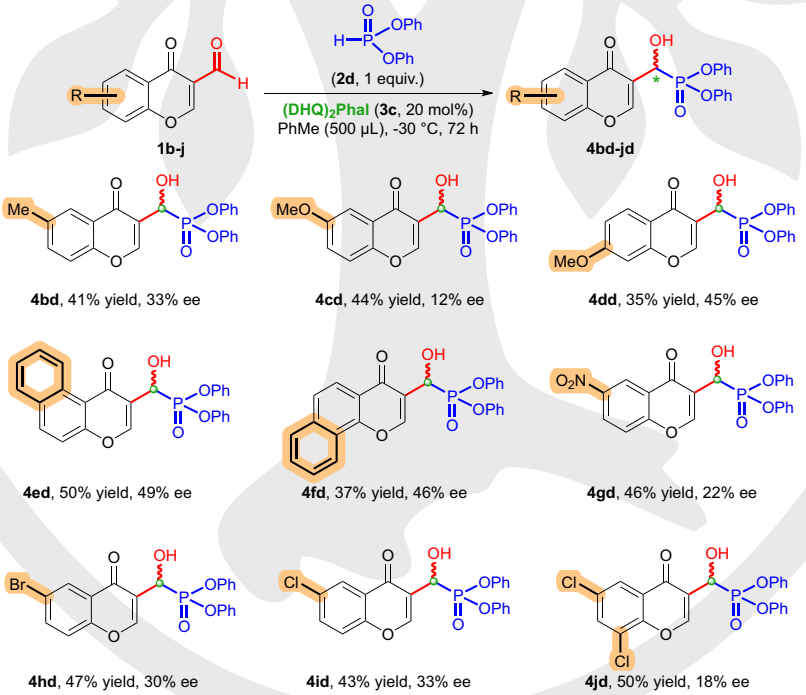

Scheme 3 Scope of the asymmetric Pudovik addition on 3-formylchromones **1b–j**. Yield after purification by column chromatography. Ee% determined by chiral HPLC.

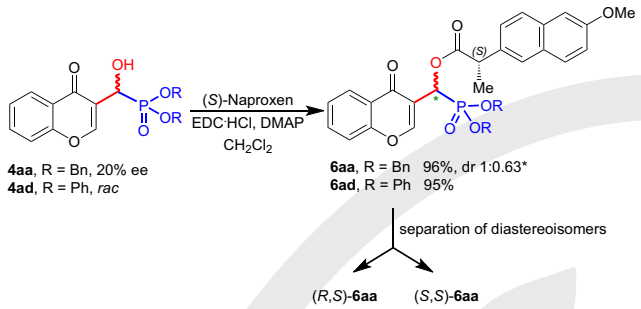

Scheme 4 Esterification of **4aa** and **4ad** with (*S*)-naproxen and diastereoisomeric separation of α-hydroxyphosphonate **4aa**. *Calculated from the ^{1}H NMR spectrum of the mixture of reaction (see Supporting Information).

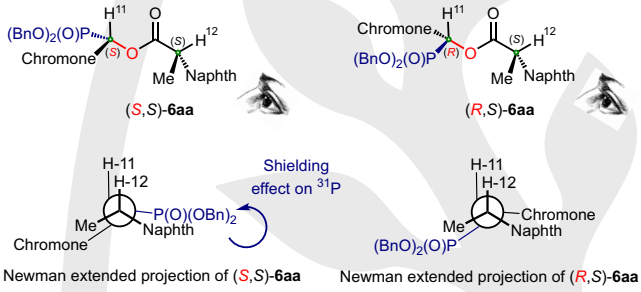

Scheme 5 Newman extended projections of α-naproxen-phosphonates **6aa**.

(**Scheme 5**) based on previous reports on determining absolute configuration of stereogenic carbons by NMR analysis.[13] In these projections, the H-11 on the α-carbon of the α-naproxen-phosphonate **6aa** is eclipsed by the H-12 of the (*S*)-naproxen stereogenic carbon. This arrangement leads to two possible anisotropic effects from the naphthalene ring of (*S*)-naproxen. For the (*S*,*S*)-**6aa**, a shielding effect on the phosphonate group should be observed, as evidence by the difference in ^{31}P{^{1}H} NMR chemical shifts (18.12 ppm for the least polar diastereoisomer and 18.57 ppm for the most polar one. See Supporting Information).

Similarly for ^{1}H NMR, the anisotropic effect on the phosphonate methylene group of the least polar diastereoisomer results in signals at 4.85 ppm (d, *J* = 9.0 Hz, 2H), 4.77 ppm (dd, *J* = 11.8, 9.0 Hz, 1H), and 4.45 ppm (dd, *J* = 11.8, 9.0 Hz, 1H), whereas the most polar product shows two signals at 5.14 ppm (d, *J* = 9.0 Hz, 2H) and 5.06 ppm (d, *J* = 9.0 Hz, 2H). Furthermore, the anisotropic effect of the naphthalene group on the (*R*,*S*)-**6aa** is reflected in the change of chemical shift of the chromone vinyl proton (H-2), at 8.10 ppm (d, *J* = 3.1 Hz) for the least polar diastereoisomer and the signal overlap at lower chemical shift (7.59–7.74 ppm) for the most polar product. Finally, the change in the chemical shift of the naproxen methoxy group may be attributed to a shielding effect of the phosphonate benzyl group in the least polar diastereoisomer (**Fig. 2**).

In addition to NMR experiments, computational calculations were performed to determine the most stable conformer for each α-naproxen-phosphonate **6aa**. The minimum-energy conformation was obtained using the semiempirical PM3 method, followed by geometry optimization using the Hartree–Fock method with 3-21G and 6-31G* basis set (**Fig. 3**).[14,15] Analysis

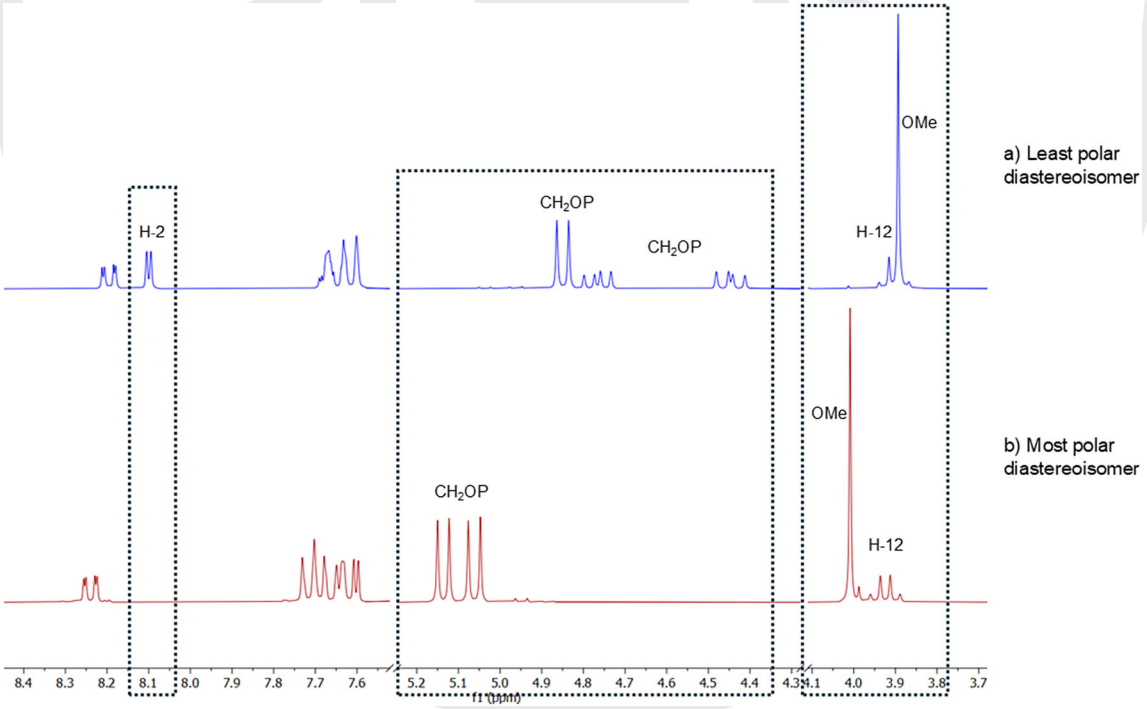

Fig. 2 Anisotropic effect observed in ^{1}H NMR of α-naproxen-phosphonates **6aa**.

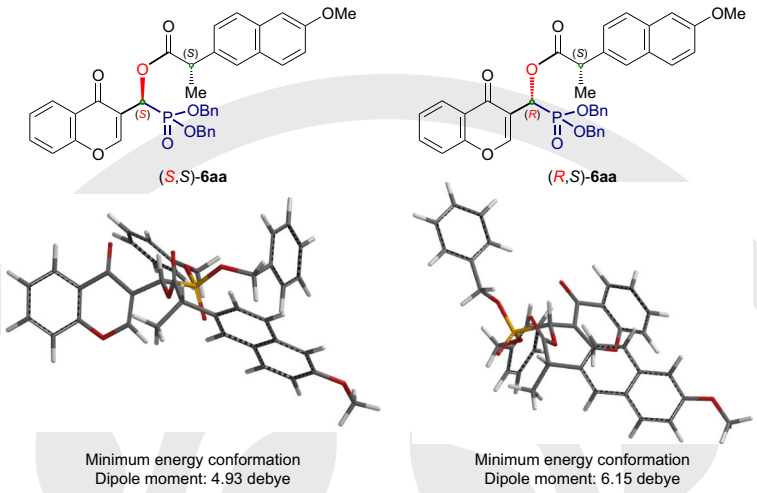

Fig. 3 Minimum-energy conformations of α-naproxen-phosphonates **6aa**.

of the minimum-energy conformations revealed a correlation between dipole moment and polarity. Specifically, the (*S*,*S*)-**6aa** diastereoisomer exhibited a dipole moment of 4.93 Db, consistent with its assignment as the least polar diastereoisomer, whereas the (*R*,*S*)-**6aa** diastereoisomer showed a dipole moment of 6.15 Db, supporting its assignment as the most polar one. Based on these results, the absolute configuration of the least polar diastereoisomer was assigned as (*S*,*S*) and that of the most polar as (*R*,*S*). Subsequently, the major diastereoisomer observed by NMR in the synthesis with (*S*)-naproxen was attributed to (*R*,*S*)-**6aa** (**Scheme 4**). Therefore, the absolute configuration of the major enantiomer in the organocatalytic Pudovik addition has been determined as (*R*).

Based on these results obtained, some aspects can be concluded. While the obtained yields and ee values are low or moderate across the series, this study provides a preliminary proof of concept for the first asymmetric synthesis of these chromone-derived α-hydroxyphosphonates. Rather than representing a fully optimized methodology, the present work demonstrates the fundamental viability of the asymmetric Pudovik reaction with this substrate class and its potential to be further optimized. Despite the moderate enantioselectivity, the results demonstrate how electronic and steric effects contribute to the reactivity and enantioselectivity profile of the process. The study supports that delicate structural modifications play a crucial role in asymmetric induction, offering useful insights for the future design of more efficient catalysts and reaction conditions. Beyond its synthetic implications, this exploratory study expands the scope of access to chromone-derived building blocks, which could be useful for subsequent applications in medicinal chemistry, material science, or bioactive compound development. With this initial asymmetric version now established, it can focus on improving selectivity and yield through alternative catalysts, reaction conditions, or substrate modifications. Moreover, we successfully assigned the absolute configuration of our final products based on (*S*)-naproxen derivatives, supported by NMR experiments and computational calculations, including the correlation between dipole moment and polarity.

General Information on Reagents and Instrumental Techniques Used

Purification of reaction products was carried out by column chromatography using silica gel (0.063–0.200 mm). Analytical thin-layer chromatography was performed on 0.25 mm silica gel 60-F plates. ESI ionization method and MicroTof-Q Bruker mass analyzer were used for the HRMS measurements. HPLC was performed on analytical Waters (Delta 600 Separation Module, 2996 Photodiode Array Detector). NMR spectroscopy was conducted using a Bruker AVANCE–II spectrometer. ^{1}H NMR spectra were recorded at 300 MHz; ^{13}C{^{1}H} NMR spectra were recorded at 75 and 100 MHz; ^{31}P{^{1}H} NMR spectra were recorded at 121 MHz; $CDCl_3$ was used as the deuterated solvent. Chemical shifts were reported in the δ scale relative to residual $CHCl_3$ (7.26 ppm) for ^{1}H NMR and the central line of $CDCl_3$ (77.16 ppm) for ^{13}C{^{1}H} NMR. Melting points were recorded on a Gallenkamp MDP350 Variable Heater melting point apparatus without correction. All commercially available solvents and reagents were used as received.

General Procedure for the Synthesis of 3-Formylchromones 1d,e,f,i

To dry DMF (3.2 mL) in a round flask into an oil bath at 50 °C, was slowly added $POCl_3$ (2.3 mL, 25 mmol) and stirred for 2 h. Then, a solution of 2′-hydroxyacetophenones **5d**,**e**,**f**,**i** (5.0 mmol) in dry DMF (1.8 mL) was slowly added to the reaction mixture and stirred during 2 h at 55 °C. After this time, the reaction was allowed to get room temperature and stirring over night until get a solid. Crushed ice was added and stirred for 4 h. The solid was filtered off and washed with water and ethyl acetate.

7-Methoxy-4-oxo-4*H*-chromene-3-carbaldehyde (1d)

Yield: 0.61 g (60%); yellow powder; mp 180–181 °C.

^{1}H NMR (300 MHz, $CDCl_3$): δ = 10.37 (s, 1H, CHO), 8.46 (s, 1H, H-2), 8.19 (d, *J* = 8.9 Hz, 1H, H-5), 7.04 (dd, *J* = 8.9, 2.4 Hz, 1H, H-6), 6.91 (d, *J* = 2.4 Hz, 1H, H-8), 3.92 (s, 3H, OCH_3) ppm.

^{13}C{^{1}H} NMR (100 MHz, $CDCl_3$): δ = 188.7 (C=O), 175.1 (C=O), 164.7 (C-7), 160.0 (C-2), 157.8 (C-9), 127.4 (C-5), 120.1 (C-10), 118.7 (C-3), 115.3 (C-6), 100.9 (C-8), 55.8 (OCH_3) ppm.

HRMS (ESI^{+}): *m*/*z* [M+Na]$^{+}$ calcd for $C_{11}H_8NaO_4$: 227.0315; found: 227.0334.

4-Oxo-4*H*-benzo[*f*]chromene-3-carbaldehyde (1e)

Yield: 0.99 g (88%); yellow powder; mp 196 °C.

^{1}H NMR (300 MHz, $CDCl_3$): δ = 10.47 (d, *J* = 3.0 Hz, 1H, CHO), 9.95 (d, *J* = 8.7 Hz, 1H, H-11), 8.51 (d, *J* = 3.0 Hz, 1H, H-2), 8.13 (d, *J* = 9.0 Hz, 1H, H-7), 7.92 (d, *J* = 8.0 Hz, 1H, H-14), 7.78 (dd, *J* = 8.7, 7.4 Hz, 1H, H-12), 7.66 (dd, *J* = 8.0, 7.4 Hz, 1H, H-13), 7.51 (d, *J* = 9.1 Hz, 1H, H-8) ppm.

$^{13}C\{^1H\}$ NMR (75 MHz, $CDCl_3$): δ = 189.4 (C=O), 177.9 (C=O), 158.1 (C-2), 157.7 (C-9), 136.7 (C-5), 131.2 (C-7), 130.5 (C-12), 129.9 (C-14), 128.5 (C-6), 127.6 (C-11), 127.1 (C-13), 122.4 (C-10), 119.1 (C-3), 117.4 (C-8) ppm.

HRMS (ESI^+): *m*/*z* $[M+Na]^+$ calcd for $C_{14}H_8NaO_3$: 247.0366; found: 247.0410.

4-Oxo-4*H*-benzo[*h*]chromene-3-carbaldehyde (1f)

Yield: 0.78 g (70%); yellow powder; mp 175–176 °C.

^1H NMR (300 MHz, $CDCl_3$): δ = 10.47 (s, 1H, CHO), 8.71 (s, 1H, H-2), 8.54–8.46 (m, 1H, H-14), 8.21 (d, *J* = 8.7 Hz, 1H, H-5), 8.02–7.94 (m, 1H, H-11), 7.87 (d, *J* = 8.7 Hz, 1H, H-6), 7.82–7.68 (m, 2H, H-12 and H-13) ppm.

$^{13}C\{^1H\}$ NMR (75 MHz, $CDCl_3$): δ = 189.0 (C=O), 175.8 (C=O), 159.7 (C-2), 154.5 (C-9), 136.5 (C-7), 130.2 (C-12), 128.4 (C-11), 128.0 (C-13), 126.9 (C-5), 124.1 (C-6), 122.3 (C-14), 122.2 (C-8), 121.5 (C-10), 120.6 (C-3) ppm.

HRMS (ESI^+): *m*/*z* $[M+Na]^+$ calcd for $C_{14}H_8NaO_3$: 247.0366; found: 247.0453.

6-Chloro-4-oxo-4*H*-chromene-3-carbaldehyde (1i)

Yield: 0.97 g (86%); yellow powder; mp 167–168 °C.

^1H NMR (300 MHz, $CDCl_3$): δ = 10.33 (s, 1H, CHO), 8.52 (s, 1H, H-2), 8.21 (d, *J* = 2.6 Hz, 1H, H-5), 7.68 (dd, *J* = 8.9, 2.6 Hz, 1H, H-7), 7.50 (d, *J* = 8.9 Hz, 1H, H-8) ppm.

$^{13}C\{^1H\}$ NMR (75 MHz, $CDCl_3$): δ = 188.2 (C=O), 174.9 (C=O), 160.8 (C-2), 154.6 (C-9), 135.1 (C-7), 132.9 (C-6), 126.4 (C-10), 125.7 (C-5), 120.4 (C-8), 120.4 (C-3) ppm.

HRMS (ESI^+): *m*/*z* $[M+Na]^+$ calcd for $C_{10}H_5ClNaO_3$: 230.9825; found: 230.9820.

General Procedure for the Synthesis of (Hydroxy(4-oxo-4*H*-chromen-3-yl)methyl)phosphonate 4aa–4ae

To a stirred solution of the organocatalyst $(DHQ)_2Phal$ **3c** (20 mol%) in toluene (500 µL), was added 3-formylchromone **1a** (0.1 mmol) and phosphites **2a–2e** (0.1 mmol). The reaction mixture was stirred at room temperature for 72 h and then purified by column chromatography using EtOAc:Hex 50:50.

Dibenzyl (Hydroxy(4-oxo-4*H*-chromen-3-yl)methyl)phosphonate (4aa)

Yield: 21.8 mg (50%); white solid.

^1H NMR (300 MHz, $CDCl_3$): δ = 8.02 (dd, *J* = 7.9, 1.1 Hz, 1H, H-5), 7.90 (dd, *J* = 3.4, 0.8 Hz, 1H, H-2), 7.53 (ddd, *J* = 8.7, 7.1, 1.8 Hz, 1H, H-7), 7.33–7.21 (m, 2H, H-6 and H-8), 7.20–7.01 (m, 10H, H_{arom}), 5.16 (d, *J* = 11.4 Hz, 1H, H-11), 5.08–4.80 (m, 4H, CH_2OP), 4.62 (s, 1H, OH) ppm.

$^{13}C\{^1H\}$ NMR (75 MHz, $CDCl_3$): δ = 177.0 (d, *J* = 3.8 Hz, C=O), 156.3 (C-9), 155.3 (d, *J* = 7.6 Hz, C-2), 136.2 (d, *J* = 5.3 Hz, C_{ipso}), 136.1 (d, *J* = 5.3 Hz, C_{ipso}), 134.1 (C-7), 128.6 (d, *J* = 3.8 Hz, Ph), 128.5 (d, *J* = 0.8 Hz, Ph), 128.2 (d, *J* = 5.5 Hz, Ph), 126.0 (C-5), 125.6 (C-6), 123.8 (C-10), 119.8 (C-8), 118.4 (C-3), 68.8 (d, *J* = 11.3 Hz, CH_2OP), 68.7 (d, *J* = 11.3 Hz, CH_2OP), 64.7 (d, *J* = 220.4 Hz, C-11) ppm.

$^{31}P\{^1H\}$ NMR (121 MHz, $CDCl_3$): δ = 21.8 ppm.

HRMS (ESI^+): *m*/*z* $[M+Na]^+$ calcd for $C_{24}H_{21}NaO_6P$: 459.0968; found: 459.0974.

HPLC: 20% ee. Daicel Chiralpak IF column (*n*-heptane/*i*PrOH = 70:30, flow rate 1 mL min^{-1}).

Diethyl (Hydroxy(4-oxo-4*H*-chromen-3-yl)methyl)phosphonate (4ab)

Yield: 11.9 mg (38%); white solid.

^1H NMR (300 MHz, $CDCl_3$): δ = 8.22 (dd, *J* = 8.0, 1.7 Hz, 1H, H-5), 8.18 (dd, *J* = 3.2, 0.8 Hz, 1H, H-2), 7.71 (ddd, *J* = 8.7, 7.1, 1.8 Hz, 1H, H-7), 7.49 (dd, *J* = 8.5, 1.5 Hz, 1H, H-8), 7.44 (ddd, *J* = 8.1, 7.1, 1.1 Hz, 1H, H-6), 5.23 (dd, *J* = 11.7, 6.8 Hz, 1H, H-11), 4.44 (dd, *J* = 6.9, 6.9 Hz, 1H, OH) 4.32–4.10 (m, 4H, CH_2OP), 1.34 (dd, *J* = 7.3, 7.3 Hz, 3H, CH_3), 1.31 (dd, *J* = 7.3, 7.3 Hz, 3H, CH_3) ppm.

$^{13}C\{^1H\}$ NMR (75 MHz, $CDCl_3$): δ = 177.3 (d, *J* = 3.0 Hz, C=O), 156.3 (C-9), 155.2 (d, *J* = 7.6 Hz, C-2), 134.3 (C-7), 126.0 (C-5), 125.7 (C-6), 123.8 (C-10), 120.0 (C-8), 118.4 (C-3), 64.5 (d, *J* = 165.3 Hz, C-11), 63.7 (d, *J* = 6.8 Hz, CH_2OP), 63.5 (d, *J* = 6.8 Hz, CH_2OP), 16.6 (d, *J* = 1.5 Hz, CH_3), 16.6 (d, *J* = 1.5 Hz, CH_3) ppm.

$^{31}P\{^1H\}$ NMR (121 MHz, $CDCl_3$): δ = 20.8 ppm.

HRMS (ESI^+): *m*/*z* $[M+Na]^+$ calcd for $C_{14}H_{17}NaO_6P$: 335.0655; found: 335.0653.

HPLC: 35% ee. Daicel Chiralpak IC column (*n*-heptane/*i*PrOH = 70:30, flow rate 1 mL min^{-1}).

Di*iso*propyl (Hydroxy(4-oxo-4*H*-chromen-3-yl)methyl)phosphonate (4ac)

Yield: 3.7 mg (11%); white solid.

^1H NMR (300 MHz, $CDCl_3$): δ = 8.22 (dd, *J* = 8.0, 1.7 Hz, 1H, H-5), 8.19 (d, *J* = 3.2 Hz, 1H, H-2), 7.70 (ddd, *J* = 8.7, 7.1, 1.7 Hz, 1H, H-7), 7.48 (dd, *J* = 8.5, 1.2 Hz, 1H, H-8), 7.43 (ddd, *J* = 8.1, 7.1, 1.1 Hz, 1H, H-6), 5.18 (dd, *J* =11.6, 4.7 Hz, 1H, H-11), 4.90–4.65 (m, 2H, CHOP), 4.29 (dd, *J* = 9.0, 6.0 Hz, 1H, OH), 1.39–1.20 (m, 12H, CH_3) ppm.

$^{13}C\{^1H\}$ NMR (75 MHz, $CDCl_3$): δ = 177.2 (d, *J* = 3.8 Hz, C=O), 156.3 (C-9), 155.2 (d, *J* = 6.8 Hz, C-2), 134.1 (C-7), 126.0 (C-5), 125.6 (C-6), 123.9 (C-10), 120.2 (C-8), 118.4 (C-3), 72.4 (d, *J* = 6.8 Hz, CHOP), 72.1 (d, *J* = 6.8 Hz, CHOP), 64.7 (d, *J* = 166.1 Hz, C-11), 24.4 (d, *J* = 5.3 Hz, CH_3), 24.3 (d, *J* = 5.3 Hz, CH_3), 24.1 (d, *J* = 5.3 Hz, CH_3), 24.0 (d, *J* = 5.3 Hz, CH_3) ppm.

$^{31}P\{^1H\}$ NMR (121 MHz, $CDCl_3$): δ = 19.0 ppm.

HRMS (ESI^+): *m*/*z* $[M+Na]^+$ calcd for $C_{16}H_{21}NaO_6P$: 363.0968; found: 363.0973.

HPLC: 26% ee. Daicel Chiralpak IF column (*n*-heptane/*i*PrOH = 80:20, flow rate 1 mL min^{-1}).

Diphenyl (Hydroxy(4-oxo-4*H*-chromen-3-yl)methyl)phosphonate (4ad)

Yield at r.t: 9.4 mg (23%); Yield at −30 °C: 20.4 mg (50%); white solid.

^1H NMR (300 MHz, $CDCl_3$): δ = 8.27–8.19 (m, 2H, H-5 and H-2), 7.71 (ddd, *J* = 8.7, 7.1, 1.8 Hz, 1H, H-7), 7.48 (d, *J* = 7.6 Hz, 1H, H-8), 7.45 (ddd, *J* = 8.1, 7.1, 1.1 Hz, 1H, H-6), 7.34–7.09 (m, 10H, H_{arom}), 5.52 (dd, *J* =10.9, 6.9 Hz, 1H, H-11), 4.90 (dd, *J* = 6.9, 6.9 Hz, 1H, OH) ppm.

$^{13}C\{^1H\}$ NMR (75 MHz, $CDCl_3$): δ = 177.2 (d, *J* = 4.5 Hz, C=O), 156.3 (C-9), 155.7 (d, *J* = 8.3 Hz, C-2), 150.5 (d, *J* = 9.8 Hz, C_{ipso}), 150.4 (d, *J* = 9.8 Hz, C_{ipso}), 134.4 (C-7), 129.9 (d, *J* = 3.4 Hz, Ph), 126.0 (C-5), 125.9 (Ph), 125.5 (C-10), 123.8 (C-6), 120.8 (d, *J* = 7.5 Hz, Ph), 120.7 (d, *J* = 7.5 Hz, Ph), 119.0 (C-8), 118.4 (C-3), 64.7 (d, *J* = 168.3 Hz, C-11) ppm.

$^{31}P\{^1H\}$ NMR (121 MHz, $CDCl_3$): δ = 13.8 ppm.

HRMS (ESI^+): *m*/*z* $[M+Na]^+$ calcd for $C_{22}H_{17}NaO_6P$: 431.0655; found: 431.0671.

HPLC: 43% ee. Daicel Chiralpak IC column (*n*-heptane/*i*PrOH = 80:20, flow rate 1 mL min^{-1}, λ = 241.3 nm): τ_{major} = 32.5 min; τ_{minor} = 38.0 min.

Diphenyl (Hydroxy(4-oxo-4*H*-chromen-3-yl)methyl)phosphine oxide (4ae)

Yield: 25.9 mg (69%); white solid.

^1H NMR (300 MHz, $CDCl_3$): δ = 8.30 (d, *J* = 4.2 Hz, 1H, H-2), 8.02–7.89 (m, H_{arom}), 7.88–7.78 (m, 2H, H_{arom}), 7.65 (ddd, *J* = 8.7, 7.1, 1.8 Hz, 1H, H-6), 7.61–7.31 (m, 8H, H_{arom}), 5.82 (d, *J* = 3.7 Hz, 1H, H-11) ppm.

$^{13}C\{^1H\}$ NMR (75 MHz, $CDCl_3$): δ = 177.4 (d, *J* = 3.0 Hz, C=O), 156.1 (C-9), 155.7 (d, *J* = 6.0 Hz, C-2), 134.1 (C-7), 132.5 (d, *J* = 3.0 Hz, Ph), 132.1 (d, *J* = 30.2 Hz, C_{ipso}), 131.8 (d, *J* = 30.2 Hz, C_{ipso}), 128.7 (d, *J* = 22.6 Hz, Ph), 128.6 (Ph), 125.7 (C-5), 125.6 (C-6), 123.5 (C-10), 119.4 (C-3), 118.4 (C-8), 62.5 (d, *J* = 80 Hz, C-11) ppm.

$^{31}P\{^1H\}$ NMR (121 MHz, $CDCl_3$): δ = 30.7 ppm.

HRMS (ESI^+): *m*/*z* $[M+Na]^+$ calcd for $C_{22}H_{17}NaO_4P$: 399.0757; found: 399.0747.

HPLC: 8% ee. Daicel Chiralpak IF column (*n*-heptane/*i*PrOH = 60:40, flow rate 1 mL min^{-1}).

General Procedure for the Synthesis of Diphenyl (Hydroxy(4-oxo-4*H*-chromen-3-yl)methyl)phosphonates 4bd–4jd

To a stirred solution of the organocatalyst $(DHQ)_2Phal$ **3c** (20 mol%) in toluene (500 µL) at −30 °C, was added 3-formylchromones **1b–1j** (0.1 mmol) and diphenyl phosphite **2d** (75% purity, 23 µL, 0.1 mmol). After 72 h, the reaction mixture was purified in column chromatography using EtOAc:Hex 50:50.

Diphenyl (Hydroxy(6-methyl-4-oxo-4*H*-chromen-3-yl)methyl) phosphonate (4bd)

Yield: 17.3 mg (41%); white powder.

^1H NMR (300 MHz, $CDCl_3$): δ = 8.21 (d, *J* = 3.4 Hz, 1H, H-2), 8.01 (d, *J* = 2.3 Hz, 1H, H-5), 7.52 (dd, *J* = 8.6, 2.3 Hz, 1H, H-7), 7.38 (d, *J* = 8.6 Hz, 1H, H-8), 7.33–7.09 (m, 10 H, H_{arom}), 5.51 (d, *J* = 10.9 Hz, 1H, H-11), 2.47 (s, 3H, CH_3) ppm.

$^{13}C\{^1H\}$ NMR (100 MHz, $CDCl_3$): δ = 177.5 (d, *J* = 4.0 Hz, C=O), 155.5 (d, *J* = 8.0 Hz, C-2), 154.6 (C-9), 150.6 (d, *J* =10.1 Hz, C_{ipso}), 150.4 (d, *J* =10.1 Hz, C_{ipso}), 136.0 (C-7), 135.7 (C-5), 129.9 (d, *J* = 6.0 Hz, Ph), 125.5 (d, *J* = 5.0 Hz, Ph), 125.3 (C-6), 123.5 (C-10), 120.8 (d, *J* = 2.2 Hz, Ph), 120.8 (d, *J* = 2.2 Hz, Ph),118.5 (C-3), 118.2 (C-8), 65.1 (d, *J* = 168.1 Hz, C-11), 21.1 (CH_3) ppm.

$^{31}P\{^1H\}$ NMR (121 MHz, $CDCl_3$): δ = 13.9 ppm.

HRMS (ESI^+): *m*/*z* $[M+Na]^+$ calcd for $C_{23}H_{19}NaO_6P$: 445.0811; found: 445.0819.

HPLC: 33% ee. Daicel Chiralpak IC column (*n*-heptane/*i*PrOH = 70:30, flow rate 1 mL min^{-1}, λ = 231.5 nm): τ_{major} = 18.7 min; τ_{minor} = 14.4 min.

Diphenyl (Hydroxy(6-methoxy-4-oxo-4*H*-chromen-3-yl)methyl) phosphonate (4cd)

Yield: 19.3 mg (44%); light yellow powder.

^{1}H NMR (300 MHz, $CDCl_3$): δ = 8.21 (dd, *J* = 3.4, 0.7 Hz, 1H, C-2), 7.57 (d, *J* = 3.1 Hz, 1H, H-5), 7.42 (d, *J* = 9.2 Hz, 1H, H-8), 7.35–7.08 (m, 11H, H-7 and H_{arom}), 5.52 (dd, *J* = 10.9, 0.8 Hz, 1H, H-11), 3.90 (s, 3H, OCH_3) ppm.

^{13}C{^{1}H} NMR (75 MHz, $CDCl_3$): δ = 177.2 (d, *J* = 3.8 Hz, C=O), 157.5 (C-6), 155.3 (d, *J* = 7.6 Hz, C-2), 151.2 (C-9), 150.5 (d, *J* = 9.8 Hz, C_{ipso}), 150.4 (d, *J* = 9.8 Hz, C_{ipso}), 129.9 (d, *J* = 4.5 Hz, Ph), 125.5 (d, *J* = 1.1 Hz, Ph), 125.5 (d, *J* = 1.1 Hz, Ph),124.6 (C-7), 12.4 (C-10), 120.8 (d, *J* = 3.8 Hz, Ph), 120.8 (d, *J* = 3.8 Hz, Ph),119.9 (C-8), 118.0 (C-3), 104.9 (C-5), 65.0 (d, *J* = 168.3 Hz, C-11), 56.1 (OCH_3) ppm.

^{31}P{^{1}H} NMR (121 MHz, $CDCl_3$): δ = 13.9 ppm.

HRMS (ESI$^+$): *m*/*z* [M+Na]$^+$ calcd for $C_{23}H_{19}NaO_7P$: 461.0761; found: 461.0761.

HPLC: 12% ee. Daicel Chiralpak IC column (*n*-heptane/*i*PrOH = 70:30, flow rate 1 mL min^{-1}, λ = 238.5 nm): τ_{major} = 33.0 min; τ_{minor} = 36.7 min.

Diphenyl (Hydroxy(7-methoxy-4-oxo-4*H*-chromen-3-yl)methyl) phosphonate (4dd)

Yield: 15.3 mg (35%); light yellow powder.

^{1}H NMR (300 MHz, $CDCl_3$): δ = 8.13 (d, *J* = 3.5 Hz, 1H, H-2), 8.12 (d, *J* = 6.3 Hz, 1H, H-5), 7.36–7.08 (m, 10 H, H_{arom}), 7.00 (dd, *J* = 8.9, 2.4 Hz, 1H, H-6), 6.85 (d, *J* = 2.4 Hz, 1H, H-8), 5.6 (d, *J* = 10.6 Hz, 1H, H-11), 5.05 (br s, OH), 3.91 (s, 3H, OCH_3) ppm.

^{13}C{^{1}H} NMR (75 MHz, $CDCl_3$): δ = 176.9 (d, *J* = 3.8 Hz, C=O), 164.7 (C-7), 158.1 (C-9), 155.0 (d, *J* = 8.3 Hz, C-2), 150.5 (d, *J* = 11.3 Hz, C_{ipso}), 150.4 (d, *J* = 11.3 Hz, C_{ipso}), 129.9 (d, *J* = 5.3 Hz, Ph), 127.4 (C-5), 125.5 (d, *J* = 4.5 Hz, Ph), 120.8 (d, *J* = 3.8 Hz, Ph), 118.4 (C-10), 117.7 (C-3), 115.4 (C-6), 100.4 (C-8), 65.3 (d, *J* = 167.6 Hz, C-11), 56.1 (OCH_3) ppm.

^{31}P{^{1}H} NMR (121 MHz, $CDCl_3$): δ = 13.8 ppm.

HRMS (ESI$^+$): *m*/*z* [M+Na]$^+$ calcd for $C_{23}H_{19}NaO_7P$: 461.0761; found: 461.0786.

HPLC: 45% ee. Daicel Chiralpak ID column (*n*-heptane/*i*PrOH = 60:40, flow rate 1 mL min^{-1}, λ = 210.7 nm): τ_{major} = 42.4 min; τ_{minor} = 58.2 min.

Diphenyl (Hydroxy(4-oxo-4*H*-benzo[*f*]chromen-3-yl)methyl) phosphonate (4ed)

Yield: 22.9 mg (50%); white powder.

^{1}H NMR (300 MHz, $CDCl_3$): δ = 9.98 (dd, *J* = 8.7, 1.3 Hz, 1H, H-12), 8.28 (dd, *J* = 3.5, 0.7 Hz, 1H, H-2), 8.10 (d, *J* = 9.1 Hz, 1H, H-7), 7.91 (dd, *J* = 8.1, 1.5 Hz, 1H, H-15), 7.77 (ddd, *J* = 8.6, 7.0, 1.5 Hz, 1H, H-13), 7.64 (ddd, *J* = 8.1, 7.0, 1.3 Hz, 1H, H-14), 7.49 (d, *J* = 9.1 Hz, 1H, H-8), 7.33–7.05 (m, 10H, H_{arom}), 5.63 (dd, *J* = 11.4, 0.8 Hz, 1H, H-11) ppm.

^{13}C{^{1}H} NMR (75 MHz, $CDCl_3$): δ = 178.9 (d, *J* = 3.8 Hz, C=O), 157.7 (C-9), 153.2 (d, *J* = 8.3 Hz, C-2), 150.6 (d, *J* = 9.8 Hz, C_{ipso}), 150.4 (d, *J* = 9.8 Hz, C_{ipso}), 136.3 (C-7), 130.9 (C-5), 130.5 (C-13), 129.8 (d, *J* = 3.7 Hz, Ph), 129.7 (C-15), 128.5 (C-6), 127.3 (C-12), 127.1 (C-14), 125.4 (C-8), 121.4 (C-10), 120.8 (d, *J* = 4.5 Hz, Ph), 120.7 (d, *J* = 5.3 Hz, Ph), 117.6 (C-3), 65.1 (d, *J* = 168.3 Hz, C-11) ppm.

^{31}P{^{1}H} NMR (121 MHz, $CDCl_3$): δ = 14.0 ppm.

HRMS (ESI$^+$): *m*/*z* [M+Na]$^+$ calcd for $C_{26}H_{19}NaO_6P$: 481.0811; found: 481.0833.

HPLC: 49% ee. Daicel Chiralpak IA column (*n*-heptane/*i*PrOH = 60:40, flow rate 1 mL min^{-1}, λ = 260.9 nm): τ_{major} = 31.7 min; τ_{minor} = 35.4 min.

Diphenyl (Hydroxy(4-oxo-4*H*-benzo[*h*]chromen-3-yl)methyl) phosphonate (4fd)

Yield: 16.9 mg (37%); white powder.

^{1}H NMR (300 MHz, $CDCl_3$): δ = 8.50–8.41 (m, 2H, H-15 and H-2), 8.15 (d, *J* = 8.8 Hz, 1H, H-5), 7.94 (dd, *J* = 7.4, 1.8 Hz, H-12), 7.80 (d, *J* = 8.8 Hz, 1H, H-6), 7.77–7.62 (m, 2H, H-13 and H-14), 7.33–7.07 (m, 10H, H_{arom}), 5.62 (d, *J* = 11.2 Hz, 1H, H-11), 5.24 (br s, 1H, OH) ppm.

^{13}C{^{1}H} NMR (75 MHz, $CDCl_3$): δ = 177.1 (d, *J* = 4.5 Hz, C=O), 154.8 (d, *J* = 8.3 Hz, C-2), 154.0 (C-9), 150.5 (d, *J* = 10.6 Hz, C_{ipso}), 150.4 (d, *J* = 10.6 Hz, C_{ipso}), 136.1 (C-7), 129.8 (d, *J* = 3.7 Hz, Ph), 128.3 (C-13), 127.6 (C-12), 126.1 (C-14), 125.5 (d, *J* = 2.3 Hz, Ph), 123.9 (C-15), 122.5 (C-8), 120.8 (d, *J* = 2.4 Hz, Ph), 120.8 (d, *J* = 2.3 Hz, Ph),120.6 (C-5), 120.4 (C-10), 120.2 (C-3), 68.8 (d, *J* = 167.6 Hz, C-11) ppm.

^{31}P{^{1}H} NMR (121 MHz, $CDCl_3$): δ = 13.8 ppm.

HRMS (ESI$^+$): *m*/*z* [M+H]$^+$ calcd for $C_{26}H_{20}O_6P$: 459.0997; found: 459.1274.

HPLC: 46% ee. Daicel Chiralpak ID column (*n*-heptane/*i*PrOH = 70:30, flow rate 1 mL min^{-1}, λ = 231.8 nm): τ_{major} = 44.2 min; τ_{minor} = 64.5 min.

Diphenyl (Hydroxy(6-nitro-4-oxo-4*H*-chromen-3-yl)methyl) phosphonate (4gd)

Yield: 20.9 mg (46%); light orange powder.

^{1}H NMR (300 MHz, $CDCl_3$): δ = 9.11 (d, *J* = 2.7 Hz, 1H, H-5), 8.53 (dd, *J* = 9.2, 2.7 Hz, 1H, H-7), 8.32 (dd, *J* = 3.7, 0.8 Hz, 1H, H-2), 7.64 (d, *J* = 9.2 Hz, 1H, H-8), 7.38–7.09 (m, 10H, H_{arom}), 5.60 (d, *J* = 10.9 Hz, 1H, H-11), 4.49 (br s, 1H, OH) ppm.

^{13}C{^{1}H} NMR (125 MHz, $CDCl_3$): δ = 175.2 (C=O), 159.0 (C-9), 156.4 (d, *J* = 7.0 Hz, C-2), 150.3 (d, *J* = 10.9 Hz, C_{ipso}), 150.2 (d, *J* = 10.9 Hz, C_{ipso}), 145.2 (C-6), 130.0 (Ph), 130.0 (d, *J* = 3.6 Hz, Ph), 128.6 (C-7), 125.7 (d, *J* = 3.6 Hz, C-10), 123.9 (C-5), 122.9 (C-8), 120.8 (d, *J* = 4.4 Hz, Ph), 120.7 (d, *J* = 3.8 Hz, Ph), 120.3 (C-3), 63.7 (d, *J* = 166.9 Hz, C-11) ppm.

^{31}P{^{1}H} NMR (121 MHz, $CDCl_3$): δ = 13.1 ppm.

HRMS (ESI$^+$): *m*/*z* [M+Na]$^+$ calcd for $C_{22}H_{16}NNaO_8P$: 476.0506; found: 476.0526.

HPLC: 22% ee. Daicel Chiralpak IC column (*n*-heptane/*i*PrOH = 70:30, flow rate 1 mL min^{-1}, λ = 210.4 nm): τ_{major} = 27.9 min; τ_{minor} = 32.1 min.

Diphenyl (Hydroxy(6-bromo-4-oxo-4*H*-chromen-3-yl)methyl) phosphonate (4hd)

Yield: 22.9 mg (47%); white powder.

^{1}H NMR (300 MHz, $CDCl_3$): δ = 8.35 (d, *J* = 2.5 Hz, 1H, H-5), 8.24 (dd, *J* = 3.5, 0.8 Hz, 1H, H-7), 7.79 (dd, *J* = 8.9, 2.5 Hz, 1H, H-2), 7.38 (d, *J* = 8.9 Hz, 1H, H-8), 7.35–7.09 (m, 10H, H_{arom}), 5.53 (d, *J* = 11.0 Hz, 1H, H-11), 4.63 (br s, 1H, OH) ppm.

^{13}C{^{1}H} NMR (100 MHz, $CDCl_3$): δ = 175.6 (d, *J* = 4.2 Hz, C=O), 156.0 (d, *J* = 7.6 Hz, C-2), 155.0 (C-9), 150.4 (d, *J* = 10.9 Hz, C_{ipso}), 150.3 (d, *J* = 10.1 Hz, C_{ipso}), 137.3 (C-7), 129.9 (d, *J* = 3.8 Hz, Ph), 128.7 (C-5), 125.6 (C-10), 125.0 (C-8), 120.8 (d, *J* = 4.2 Hz, Ph), 120.7 (d, *J* = 4.2 Hz, Ph), 120.4 (C-3), 119.7 (d, *J* = 4.7 Hz, Ph), 119.3 (C-6), 64.1 (d, *J* = 167.7 Hz, C-11) ppm.

^{31}P{^{1}H} NMR (121 MHz, $CDCl_3$): δ = 13.5 ppm.

HRMS (ESI$^+$): *m*/*z* [M+H]$^+$ calcd for $C_{22}H_{17}BrO_6P$: 486.9946; found: 486.9949.

HPLC: 30% ee. Daicel Chiralpak IC column (*n*-heptane/*i*PrOH = 70:30, flow rate 1 mL min^{-1}, λ = 233.8 nm): τ_{major} = 14.7 min; τ_{minor} = 17.9 min.

Diphenyl (Hydroxy(6-chloro-4-oxo-4*H*-chromen-3-yl)methyl) phosphonate (4id)

Yield: 19.0 mg (43%); white powder.

^{1}H NMR (300 MHz, $CDCl_3$): δ = 8.26 (d, *J* = 4.2 Hz, 1H, H-2), 8.19 (d, *J* = 2.5 Hz, 1H, H-5), 7.64 (dd, *J* = 8.9, 2.5 Hz, 1H, H-7), 7.44 (d, *J* = 8.9 Hz, 1H, H-8), 7.35–7.07 (m, 10H, H_{arom}), 5.57 (d, *J* = 10.8 Hz, 1H, H-11) ppm.

^{13}C{^{1}H} NMR (75 MHz, $CDCl_3$): δ = 175.7 (d, *J* = 4.5 Hz, C=O), 155.9 (d, *J* = 7.5 Hz, C-2), 154.6 (C-9), 150.4 (d, *J* = 9.1 Hz, C_{ipso}), 150.3 (d, *J* = 9.1 Hz, C_{ipso}), 134.6 (C-7), 131.9 (C-5), 129.9 (d, *J* = 2.8 Hz, Ph), 125.5 (d, *J* = 7.6 Hz, Ph), 124.7 (C-10), 120.8 (d, *J* = 4.6 Hz, Ph), 120.7 (d, *J* = 4.6 Hz, Ph), 120.2 (C-8), 119.6 (C-3), 64.1 (d, *J* = 167.6 Hz, C-11) ppm.

^{31}P{^{1}H} NMR (121 MHz, $CDCl_3$): δ = 13.6 ppm.

HRMS (ESI$^+$): *m*/*z* [M+Na]$^+$ calcd for $C_{22}H_{16}ClNaO_6P$: 465.0265; found: 465.0274.

HPLC: 33% ee. Daicel Chiralpak IC column (*n*-heptane/*i*PrOH = 80:20, flow rate 1 mL min^{-1}, λ = 233.8 nm): τ_{major} = 22.3 min; τ_{minor} = 27.7 min.

Diphenyl (Hydroxy(6,8-dichloro-4-oxo-4*H*-chromen-3-yl)methyl) phosphonate (4jd)

Yield: 23.9 mg (50%); white powder.

^{1}H NMR (300 MHz, $CDCl_3$): δ = 8.34 (dd, *J* = 3.7, 0.8 Hz, 1H, H-2), 8.10 (d, *J* = 2.5 Hz, 1H, H-5), 7.74 (d, *J* = 2.5 Hz, 1H, H-7), 7.37–7.08 (m, 10H, H_{arom}), 5.60 (dd, *J* = 10.6, 0.8 Hz, H-11) ppm.

^{13}C{^{1}H} NMR (75 MHz, $CDCl_3$): δ = 174.7 (d, *J* = 4.5 Hz, C=O), 155.9 (d, *J* = 6.8 Hz, C-2), 150.7 (C-9), 150.4 (d, *J* = 6.0 Hz, C_{ipso}), 150.3 (d, *J* = 6.0 Hz, C_{ipso}), 134.4 (C-7), 131.5 (C-6), 130.0–129.9 (m, Ph), 125.7–125.5 (m, Ph), 125.5 (C-3), 124.8 (C-5), 124.2 (C-10), 120.8 (d, *J* = 4.2 Hz, Ph), 120.7 (d, *J* = 4.2 Hz, Ph), 120.5 (C-8), 63.4 (d, *J* = 167.6 Hz, C-11) ppm.

^{31}P{^{1}H} NMR (121 MHz, $CDCl_3$): δ = 13.3 ppm.

HRMS (ESI$^+$): *m*/*z* [M+Na]$^+$ calcd for $C_{22}H_{15}Cl_2NaO_6P$: 498.9876; found: 498.9915.

HPLC: 18% ee. Daicel Chiralpak IC column (*n*-heptane/*i*PrOH = 80:20, flow rate 1 mL min^{-1}, λ = 236.2 nm): τ_{major} = 18.3 min; τ_{minor} = 32.5 min.

General Procedure for the Synthesis of (Bis(benzyloxy)phosphoryl)(4-oxo-4*H*-chromen-3-yl)methyl 2-(6-Methoxynaphthalen-2-yl) propanoate (*R*,*S*)-6aa and (*S*,*S*)-6aa

To a stirred solution of α-hydroxyphosphonate **4aa** (43.6 mg, 0.1 mmol) (20% ee), DMAP (1.2 mg, 10 mol%) and (*S*)-naproxen (23.3 mg, 0.1 mmol) in CH_2Cl_2 (500 µL) at 0 °C, was added EDC hydrochloride (21.5 mg, 0.11 mmol), and the reaction mixture was allowed to warm to room temperature. After 2 h, the reaction mixture was extracted with CH_2Cl_2 (2 × 20 mL) and the organic phase was washed successively with sat. aq. $NaHCO_3$ (20 mL), sat. aq. NH_4Cl (20 mL), and brine (20 mL), then filtered through anhydrous Na_2SO_4 and evaporated under reduced pressure. The crude product was purified by column chromatographic using EtOAc:Hex (50:50) as eluent, affording the α-naproxen-phosphonate **6aa** as white solid in 96% yield as mixture of both diastereoisomers. The NMR of this mixture give a ratio 1.00:0.63 as expected from the %ee measured by HPLC (see Supporting Information for the NMR of this mixture). The diastereoisomers were subsequently isolated by column chromatographic using CH_2Cl_2:Et_2O (90:10) as eluent, giving as the major diastereoisomer the most polar one with absolute configuration (*R*,*S*).

(*S*)-(Bis(benzyloxy)phosphoryl)(4-oxo-4*H*-chromen-3-yl)methyl (*S*)-2-(6-Methoxynaphthalen-2-yl)propanoate (6aa) (Least Polar)

^{1}H NMR (300 MHz, $CDCl_3$): δ = 8.20 (dd, *J* = 8.3, 1.7 Hz, 1H, H-5), 8.10 (d, *J* = 3.1 Hz, 1H, H-2), 7.73–7.56 (m, 4H, H_{arom}), 7.45–7.34 (m, 3H, H_{arom}), 7.22–7.01 (m, 10H, H_{arom}), 6.95–6.88 (m, 2H, H_{arom}), 6.72 (dd, *J* = 12.6, 0.6 Hz, 1H, H-11), 4.85 (d, *J* = 9.0 Hz, 2H, CH_2OP), 4.77 (dd, *J* = 11.8, 9.0 Hz, 1H, CH_2OP), 4.45 (dd, *J* = 11.8, 9.0 Hz, 1H, CH_2OP), 3.90 (q, *J* = 7.1 Hz, 1H, H-12), 3.89 (s, 3H, OCH_3), 1.56 (d, *J* = 7.1 Hz, 3H, CH_3) ppm.

^{13}C{^{1}H} NMR (75 MHz, $CDCl_3$): δ = 174.7 (d, *J* = 6.0 Hz, C=O), 172.5 (d, *J* = 8.3 Hz, C=O), 157.9 (C-18), 156.4 (d, *J* = 5.3 Hz, C-2), 156.2 (C-9), 135.8 (d, *J* = 6.0 Hz, C_{ipso}), 135.7 (d, *J* = 6.0 Hz, C_{ipso}), 134.9 (C-7), 133.9 (C-14), 133.9 (C-22), 129.4 (C-20), 129.0 (C-21), 128.5 (Ph), 128.4 (d, *J* = 5.3 Hz, Ph), 128.3 (C-16), 128.0 (C-15), 127.7 (C-13), 127.4 (C-5), 126.4 (d, *J* = 3.8 Hz, Ph), 125.6 (C-10), 123.9 (C-6), 119.3 (C-3), 118.7 (C-19), 118.3 (C-8), 105.7 (C-17), 68.7 (d, *J* = 6.8 Hz, CH_2OP), 61.7 (d, *J* = 174.3 Hz, C-11), 55.4 (OCH_3), 45.4 (C-12), 18.5 (CH_3) ppm.

^{31}P{^{1}H} NMR (121 MHz, $CDCl_3$): δ 18.1 ppm.

HRMS (ESI$^+$): *m*/*z* [M+Na]$^+$ calcd for $C_{38}H_{33}NaO_8P$: 671.1805; found: 671.1805.

(*R*)-(Bis(benzyloxy)phosphoryl)(4-oxo-4*H*-chromen-3-yl)methyl (*S*)-2-(6-Methoxynaphthalen-2-yl)propanoate (6aa) (Most Polar)

^{1}H NMR (300 MHz, $CDCl_3$): δ = 8.24 (dd, *J* = 8.0, 1.7 Hz, 1H, H-5), 7.76–7.58 (m, 5H, H_{arom}), 7.46 (dd, *J* = 8.1, 7.8 Hz, 1H, H-6), 7.42i-7.32 (m, 7H, H_{arom}), 7.23–7.15 (m, 2H, H_{arom}), 6.78 (dd, *J* = 12.6, 0.7 Hz, 1H, H-11), 5.14 (d, *J* = 9.0 Hz, 2H, CH_2OP), 5.06 (d, *J* = 9.0 Hz, 2H, CH_2OP), 4.01 (s, 3H, OCH_3), 3.92 (q, *J* = 7.2 Hz, 1H, H-12), 1.60 (d, *J* = 7.1 Hz, 3H, CH_3) ppm.

^{13}C{^{1}H} NMR (75 MHz, $CDCl_3$): δ = 174.6 (d, *J* = 5.3 Hz, C=O), 172.2 (d, *J* = 9.8 Hz, C=O), 157.9 (C-18), 156.0 (C-9), 155.7 (d, *J* = 5.3 Hz, C-2), 136.0 (d, *J* = 5.3 Hz, C_{ipso}), 135.7 (d, *J* = 5.3 Hz, C_{ipso}), 134.8 (C-7), 133.9 (C-14), 133.8 (C-22), 129.3 (C-20), 129.0 (C-21), 128.6 (d, *J* = 9.8 Hz, Ph), 128.5 (d, *J* = 5.3 Hz, Ph), 128.1 (d, *J* = 7.5 Hz, Ph), 127.4 (C-16), 126.3 (C-15), 126.2 (C-13), 126.1 (C-5), 125.5 (C-10), 123.7 (C-6), 119.2 (C-3), 118.4 (C-19), 118.2 (C-8), 105.7 (C-17), 61.8 (d, *J* = 175.1 Hz, C-11), 68.8 (d, *J* = 6.0 Hz, CH_2OP), 55.4 (OCH_3), 45.2 (C-12), 18.3 (CH_3) ppm.

^{31}P{^{1}H} NMR (121 MHz, $CDCl_3$): δ = 18.6 ppm.

HRMS (ESI$^+$): *m*/*z* [M+Na]$^+$ calcd for $C_{38}H_{33}NaO_8P$: 671.1805; found: 671.1804.

Author Affiliations

1 Department of Organic Chemistry, Laboratorio de Organocatálisis Asimétrica, Instituto de Síntesis Química y Catálisis Homogénea (CSIC–University of Zaragoza), Zaragoza, Spain

2 Centro de Investigaciones Químicas-IICAB, Universidad Autónoma del Estado de Morelos, Cuernavaca, Mexico

Statements and Additional Information

Conflict of Interest The authors declare that they have no conflict of interest.

Acknowledgment The authors would like to thank the Research Support Service of CEQMA (CSIC) and SAI (Universidad de Zaragoza). The authors would also like to thank ArtsyBee for the image of the eye in **Scheme 5**, downloaded from Pixabay.

Funding Information The authors thank Ministerio de Ciencia, Innovación y Universidades and Agencia Estatal de investigación for the project PID2023-147471NB-I00 funded by MICIU/AEI10.13039/501100011033, Gobierno de Aragón-Fondo Social Europeo (Research Group E07_23R) and Secretaría de Ciencia, Humanidades, Tecnología e Innovación (SECIHTI) for financial support through projects CBF-2025-I-1963 and 286614. J.C.M.S. also thanks SECIHTI for predoctoral scholarship 1004402.

Contributors' Statement J.C.M.-S.: Conceptualization, Data curation, Formal analysis, Investigation, Methodology, Validation, Writing – original draft, Writing – review & editing. M.O.: Conceptualization, Data curation, Formal analysis, Funding acquisition, Investigation, Methodology, Project administration, Resources, Software, Supervision, Validation, Visualization, Writing – original draft, Writing – review & editing. E.M.L.: Conceptualization, Data curation, Formal analysis, Funding acquisition, Investigation, Methodology, Project administration, Resources, Software, Supervision, Validation, Visualization, Writing – original draft, Writing – review & editing. R.P.H.: Conceptualization, Data curation, Formal analysis, Funding acquisition, Investigation, Methodology, Project administration, Resources, Software, Supervision, Validation, Visualization, Writing – original draft, Writing – review & editing.

Supplementary Material is available online at https://doi.org/10.1055/a-2815-1115

References

1 Pudovik AN, Konovalova IV. Synthesis 1979: 81–96

2 (a) Gröger H, Hammer B. Chem Eur J 2000; 6: 943–948 (b) Kolodiazhnyi OI. Tetrahedron Asymmetry 2005; 16: 3295–3340 (c) Ma J-A. Chem Soc Rev 2006; 35: 630–636 (d) Depeng Z, Wang R. Chem Soc Rev 2012; 41: 2095–2108 (e) Merino P, Marqués-López E, Herrera RP. Adv Synth Catal 2008; 350: 1195–1208 (f) Bhadury PS, Li H. Synlett 2012; 23: 1108–1131 (g) Phillips AMF. Mini Rev Org Chem 2014; 11: 164–185 (h) Spilling CD, Malla RK. Top Curr Chem 2015; 361: 83–136 (i) Viveros-Ceballos JL, Ordoñez M, Sayago FJ, Cativiela C. Molecules 2016; 21: 1141 (j) Ordoñez M, Viveros-Ceballos JL, Romero-Estudillo I. Chapter 6 Stereoselective synthesis of α-aminophosphonic acids through Pudovik and Kabachnik fields-reaction. In: Amino Acid-New Insights and Roles in Plant and Animal; Asao T, Asaduzzaman MD, eds. Rijeka: InTech; 2017: 127 (k) Ordoñez M, Viveros-Ceballos JL, Sayago FJ, Cativiela C. Synthesis 2017; 49: 987–997 For requested cites, see also: (l) Sun L, Guo Q-P, Li X et al. Asian J Org Chem 2013; 2: 1031–1035 (m) Ying S, Huang X, Guo X, Yang S. Green Synth Catal 2021; 2: 315–319

3 Springs B, Haake P. J Org Chem 1977; 42: 472–474

4 (a) Ordoñez M, Rojas-Cabrera H, Cativiela C. Tetrahedron 2009; 65: 17–49 (b) Ordoñez M, Sayago FJ, Cativiela C. Tetrahedron 2012; 68: 6369–6412 (c) Ordoñez M, Viveros-Ceballos JL, Cativiela C, Sayago FJ. Tetrahedron 2015; 71: 1745–1784 (d) Zhang S, Zhang M-H, Feng S et al. Chem Pap 2024; 78: 4045–4056 (e) Kumar A, Mukhopadhyay J, Bhagat S. ChemistrySelect 2024; 9: e202404258

5 Kaboudin B, Daliri P, Faghih S, Esfandiari H. Front Chem 2022; 10: 890696

6 (a) Herrera RP. Chem Rec 2017; 17: 833–840 (b) Rádai Z, Keglevich G. Molecules 2018; 23: 1493 (c) Rádai Z. Phosphorus Sulfur Silicon Relat Elem 2019; 194: 425–437 (d) Plouard P, de Zordo-Banliat A, Clarion L, Loiseau S, Virieux D, Ayad T. ChemCatChem 2024; 16: e202400824

7 (a) Zhang M, Gong Y, Zhou W, Zhou Y, Liu X-L. Org Chem Front 2021; 8: 3968–3989 (b) Langer P. Beilstein J Org Chem 2024; 20: 1256–1269 (c) Benny AT, Radhakrishnan EK. RSC Adv 2022; 12: 3343–3358 (d) Morales-Solís JC, Ordoñez M, Marqués-López E, Herrera RP. Org Biomol Chem 2025; 23: 10420–10436

8 (a) Emami S, Ghanbarimasir Z. Eur J Med Chem 2015; 93: 539–563 (b) Costa M, Dias TA, Brito A, Proença F. Eur J Med Chem 2016; 123: 487–507 (c) Yang J, Lai J, Kong W, Li S. J Agric Food Chem 2022; 70: 3409–3419 (d) Kamboj S, Singh R. Arab J Sci Eng 2022; 47: 75–111

9 (a) Brooks WH, Guida WC, Daniel KG. Curr Top Med Chem 2011; 11: 760–770 (b) Scott KA, Ropek N, Melillo B, Schreiber SL, Cravatt BF, Vinogradova EV. Curr Res Chem Biol 2022; 2: 100028 (c) Ceramella J, Iacopetta D, Franchini A et al. Appl Sci 2022; 12: 10909 (d) Senkuttuvan N, Komarasamy B, Krishnamoorthy R, Sarkar S, Dhanasekaran S, Anaikutti P. RSC Adv 2024; 14: 33429–33448

10 (a) Nohara A, Umetani T, Sanno Y. Tetrahedron 1974; 30: 3553–3561 (b) Machida Y, Nomoto S, Negi S, Ikuta H, Saito I. Synth Commun 1980; 10: 889–895 (c) Khan KM, Ambreen N, Hussain S, Perveen S, Choudhary MI. Bioorg Med Chem 2009; 17: 2983–2988 (d) Kumar L, Verma N, Kumar N, Sehrawat H, Kumar R, Chandra R. New J Chem 2022; 46: 20580–20591

11 (a) Pettersen D, Marcolini M, Bernardi L et al. J Org Chem 2006; 71: 6269–6272 (b) Alcaine A, Marqués-López E, Merino P, Tejero T, Herrera RP. Org Biomol Chem 2011; 9: 2777–2783 (c) Alegre-Requena JV, Marqués-López E, Miguel PJS, Herrera RP. Org Biomol Chem 2014; 12: 1258–1264 (d) Ardevines S, Horn D, Alegre-Requena JV et al. Adv Synth Catal 2023; 365: 2152–2158 (e) Marqués-López E, Sonsona IG, Garcés-Marín M, Gimeno MC, Herrera RP. Adv Synth Catal 2023; 365: 3234–3240 (f) Ascaso-Alegre C, Herrera RP, Mangas-Sanchez J. ChemCatChem 2024; 16: e202400817

12 Seco JM, Quiñoá E, Riguera R. Chem Rev 2004; 104: 17–117

13 (a) Hammerschmidt F, Li Y-F. Tetrahedron 1994; 50: 10253–10264 (b) Hoye TR, Jeffrey CS, Shao F. Nat Protoc 2007; 2: 2451–2458 (c) Rojas-Cabrera H, Fernández-Zertuche M, García-Barradas O, Muñoz-Muñiz O, Ordoñez M. Tetrahedron Asymmetry 2007; 18: 142–148 (d) Ordoñez M, González-Morales A, Ruíz-Marcial CA, De la Cruz-Cordero R, Fernández-Zertuche M. Tetrahedron Asymmetry 2003; 14: 1775–1779

14 [Software] Spartan. Wavefunction'08 Version 1.1.1; Wavefunction, Inc; 2008

15 Matta CF. J Comput Chem 2010; 31: 1297–1311

Asymmetric Pudovik Reaction as a Tool for Functionalizing 3-Formyl Chromones

Juan Carlos Morales-Solís,[a,b] Mario Ordoñez,[b] Eugenia Marqués-López,[a]* Raquel P. Herrera[a]*

[a] Department of Organic Chemistry. Laboratorio de Organocatálisis Asimétrica. Instituto de Síntesis Química y Catálisis Homogénea (CSIC-University of Zaragoza). C/ Pedro Cerbuna 12, 50009 Zaragoza, Spain.

[b] Centro de Investigaciones Químicas-IICBA, Universidad Autónoma del Estado de Morelos, Av. Universidad 1001, 62209 Cuernavaca, Morelos, México.

Corresponding author´s e-mail: mmaamarq@unizar.es & raquelph@unizar.es

Table of Contents

Synthesis | DOI 10.1055/a-2815-1115 |

1. Screening of reaction conditions

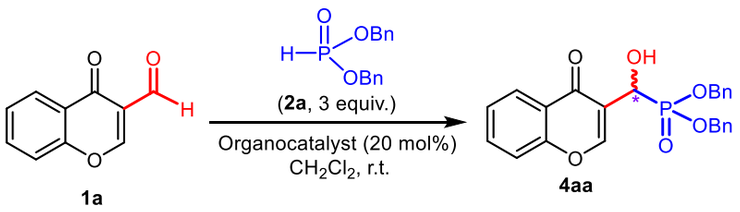

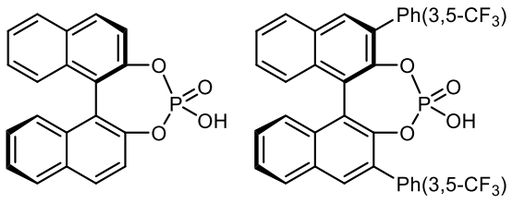

3l, 48 h
46%, 4% ee

3m, 48 h
15%, 8% ee

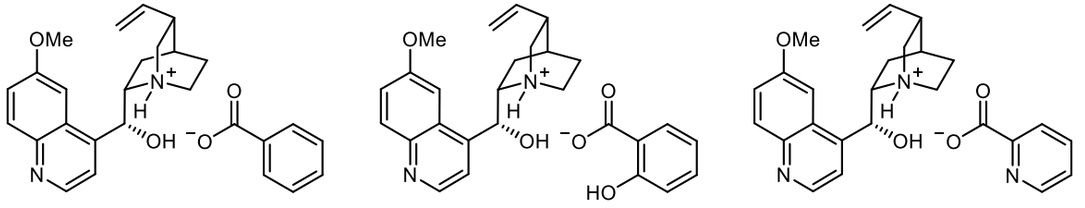

3n, 48 h
40%, 14% ee

3o, 6 d
38%, 12% ee

3p 6 d
52%, 14% ee

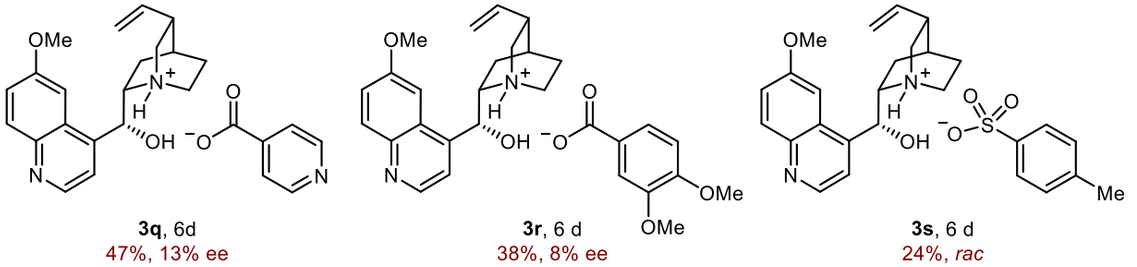

3q, 6d
47%, 13% ee

3r, 6 d
38%, 8% ee

3s, 6 d
24%, *rac*

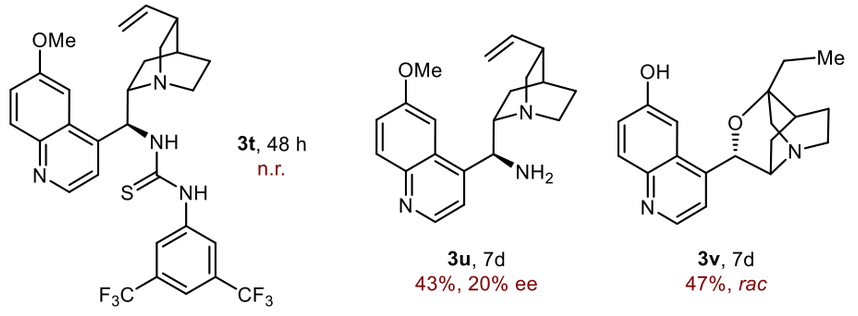

3t, 48 h
n.r.

3u, 7d
43%, 20% ee

3v, 7d
47%, *rac*

Scheme S1. Additional organocatalysts **3l-3v** tested in the model reaction.[1] n.r. = no reaction.

[1] The chiral proton catalyst structures derived from cinchona were synthesized according to our own procedure: F. Auria-Luna, E. Marqués-López, M. C. Gimeno, J. V. Alegre-Requena, R. P. Herrera, *Adv. Synth. Catal.* **2025**, *367*, e202401458.

Synthesis | DOI 10.1055/a-2815-1115 |

Table S1. Effect of additive in the Pudovik reaction with catalyst **3c**.

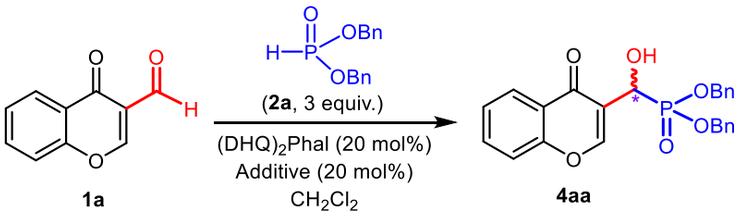

Entry	Additive	Temperature	Yield (%)[a)]	ee (%)[b)]
1	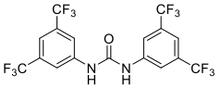	r.t.[c)]	58	16
2	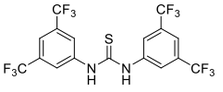	r.t.[c)]	60	13
3	ZnI_2	r.t.[c)]	49	8
4	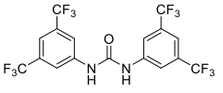	-20 °C	23	20
5	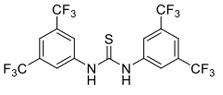	-20 °C	25	18
6	ZnI_2	-20 °C	n.r.[d)]	n.r.[d)]
7	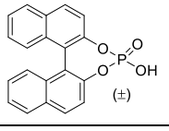	r.t.[c)]	33	32

[a)] Yield after purification by column chromatography. [b)] Enantiomeric excess (ee) determined by chiral HPLC (Daicel chiralpak IF). [c)] r.t. = room temperature. [d)] n.r. = no reaction.

Table S2. Effect of catalyst loading and concentration in Pudovik addition.

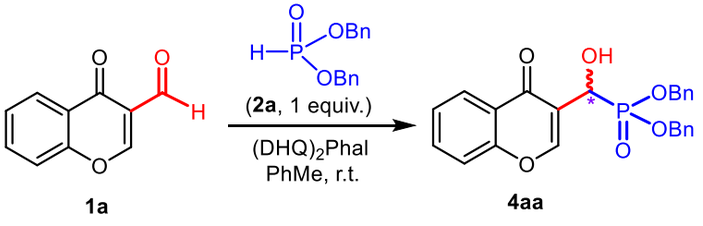

Entry	$(DHQD)_2Phal$	Solvent (µL)	Yield (%)[a)]	ee (%)[b)]
1	30 mol%	500	24	27
2	10 mol%	500	24	34
3	20 mol%	500	36	32
4	20 mol%	750	36	32
5	20 mol%	250	41	28

[a)] Yield after purification by column chromatography. [b)] Enantiomeric excess (ee) determined by chiral HPLC (Daicel chiralpak IF).

Synthesis | DOI 10.1055/a-2815-1115 |

2. NMR spectra of 3-formyl chromones 1d,e,f,i

Figure S1. ^{1}H NMR (300 MHz, $CDCl_3$) spectrum of 7-methoxy-4-oxo-4*H*-chromene-3-carbaldehyde (**1d**).

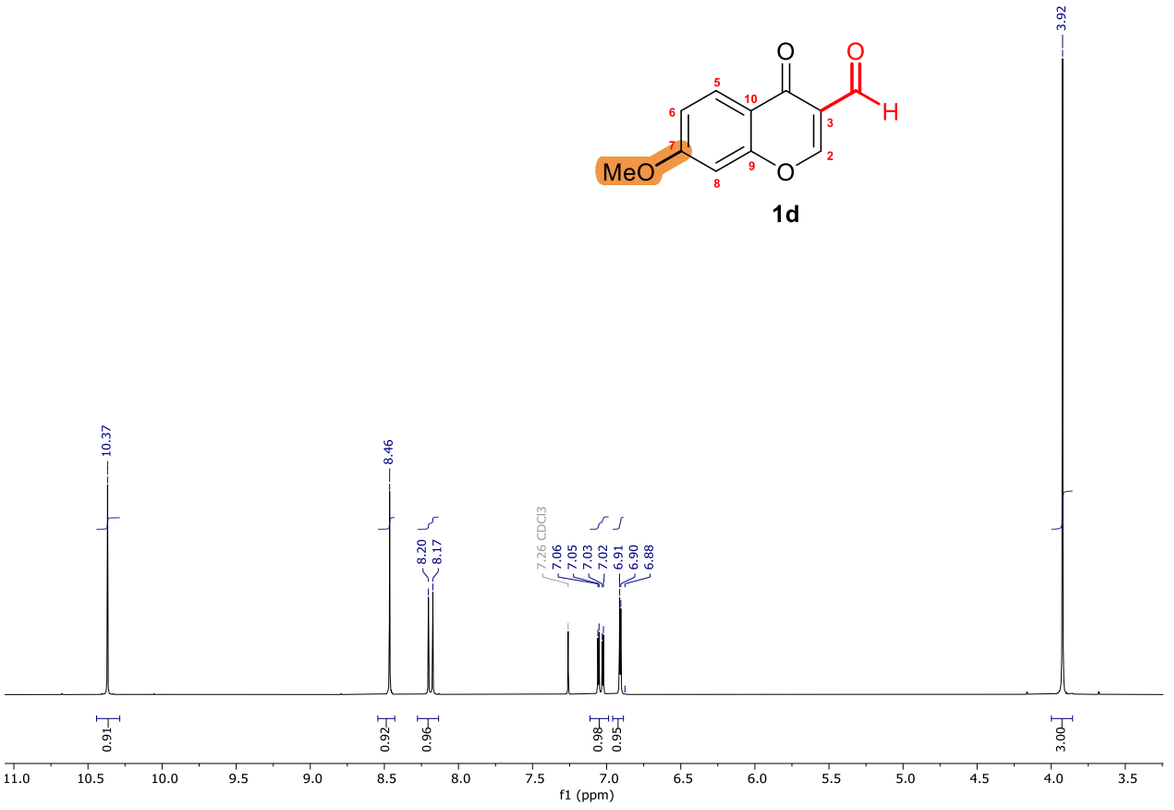

Figure S2. $^{13}C\{^{1}H\}$ NMR (100 MHz, $CDCl_3$) spectrum of **1d**.

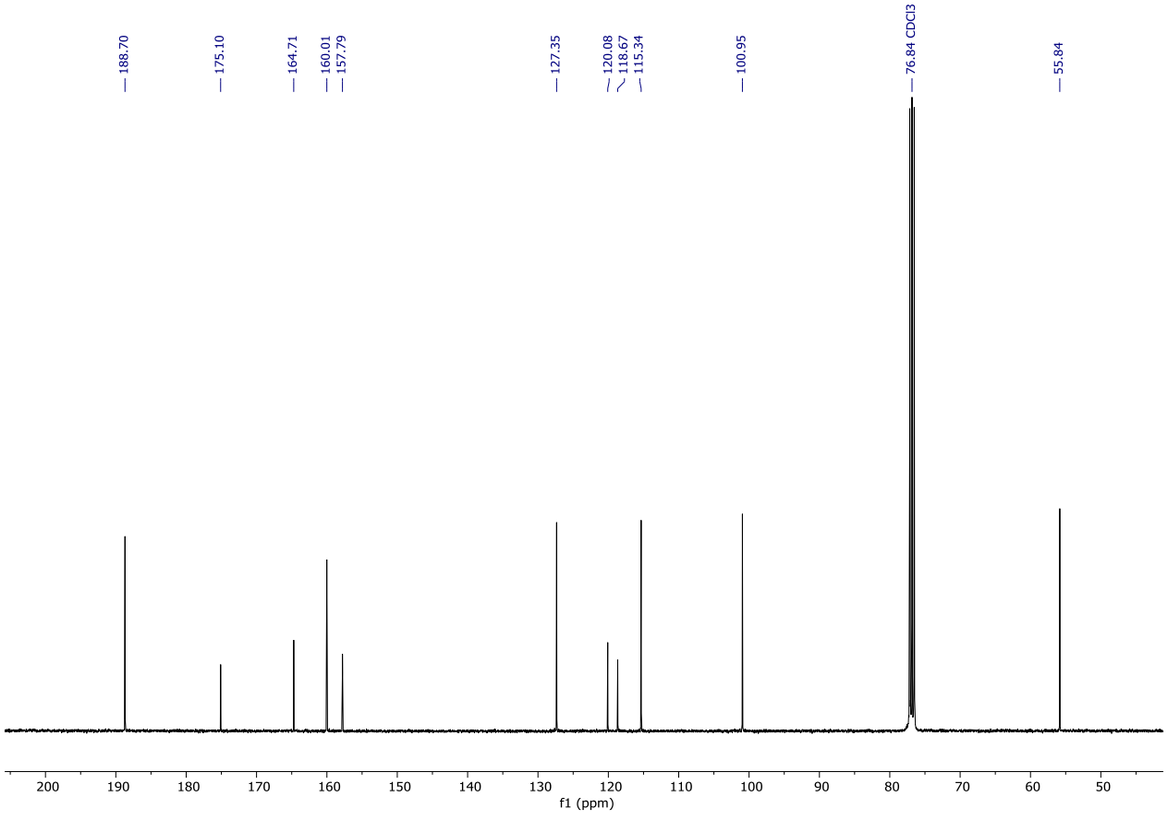

Figure S3. ^{1}H NMR (300 MHz, $CDCl_3$) spectrum of 4-oxo-4*H*-benzo[*f*]chromene-3-carbaldehyde (**1e**).

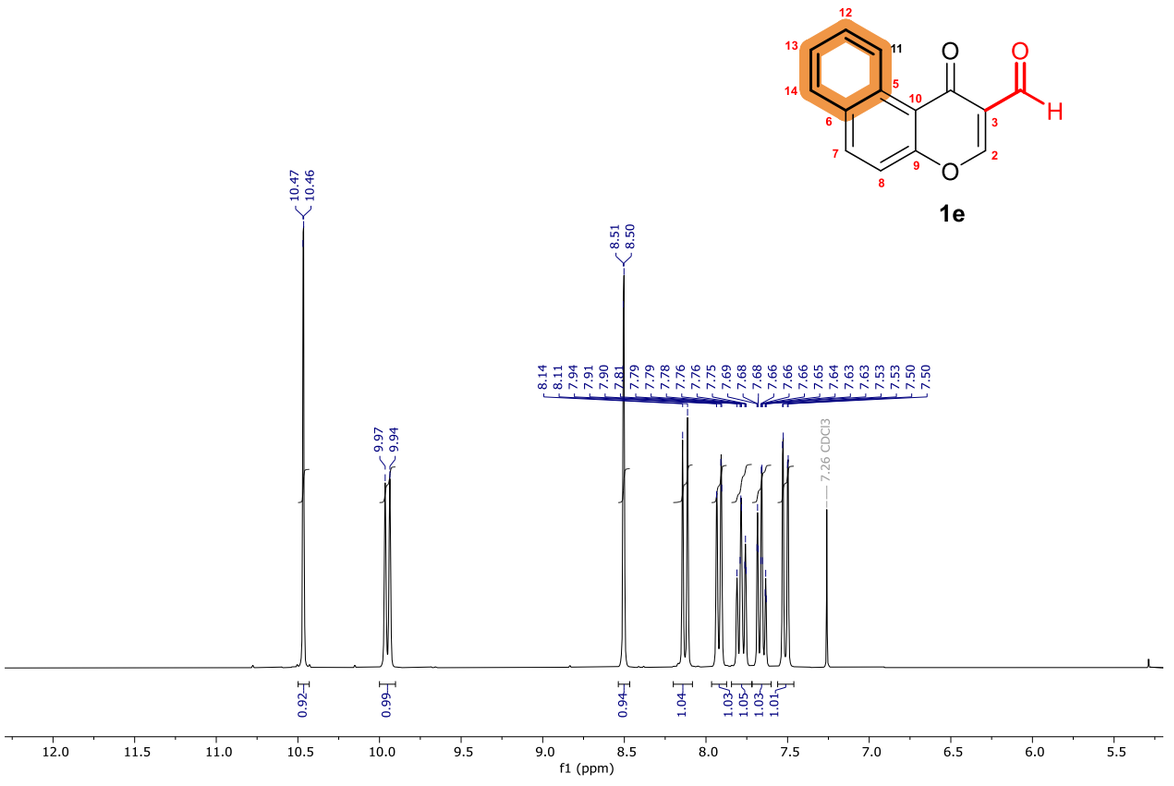

Figure S4. $^{13}C\{^{1}H\}$ NMR (75 MHz, $CDCl_3$) spectrum of **1e**.

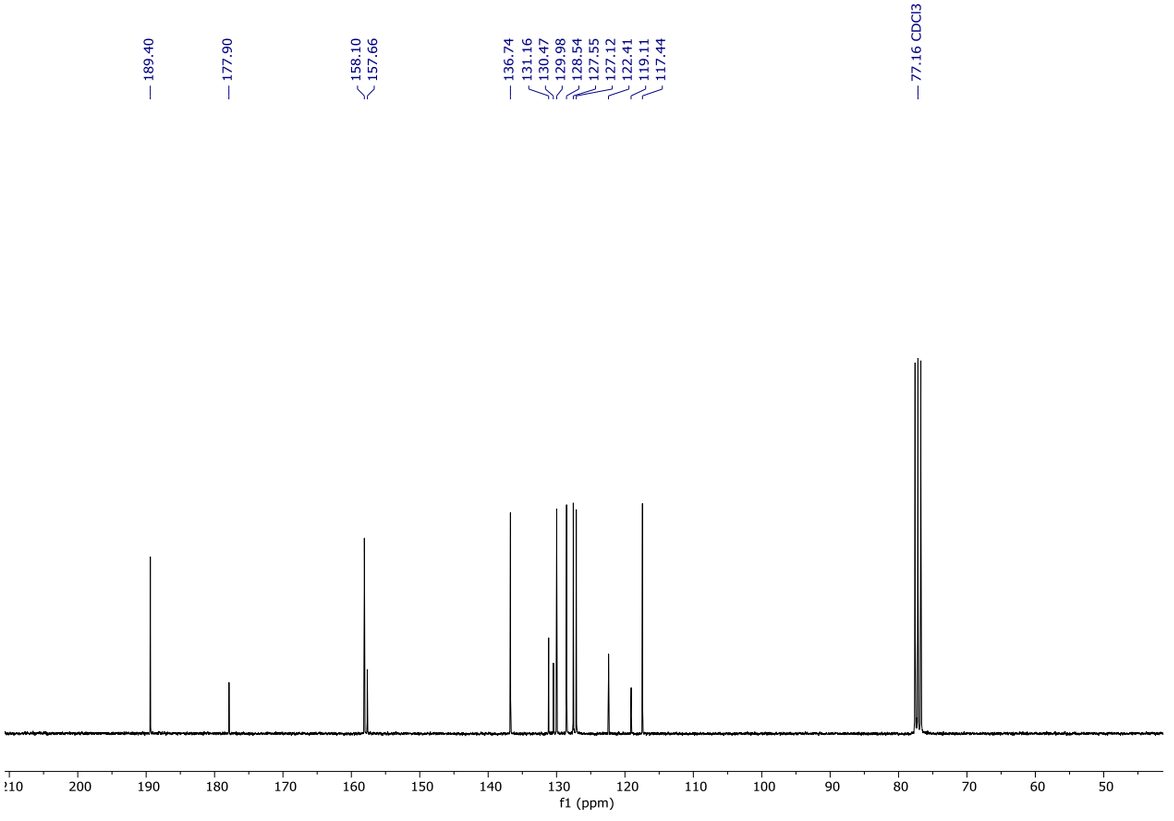

Synthesis | DOI 10.1055/a-2815-1115 |

Figure S5. ^{1}H NMR (300 MHz, $CDCl_3$) spectrum of 4-oxo-4*H*-benzo[*h*]chromene-3-carbaldehyde (**1f**).

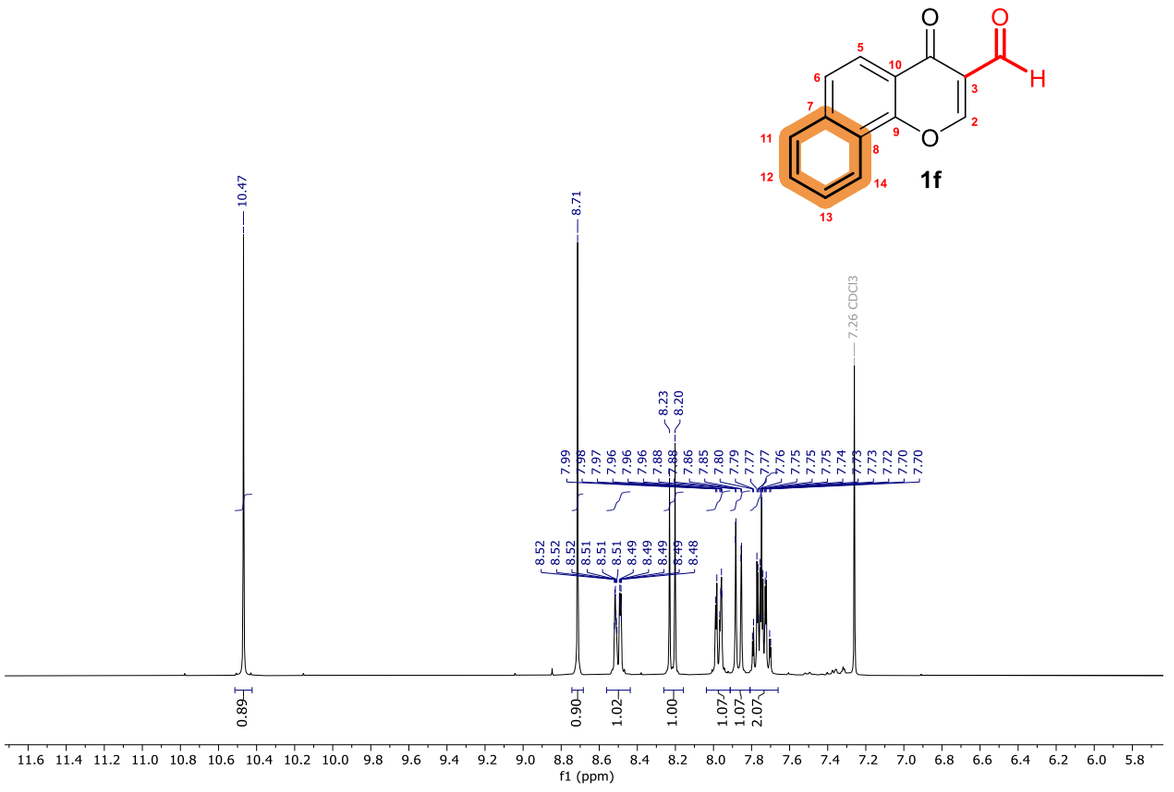

Figure S6. $^{13}C\{^{1}H\}$ NMR (75 MHz, $CDCl_3$) spectrum of **1f**.

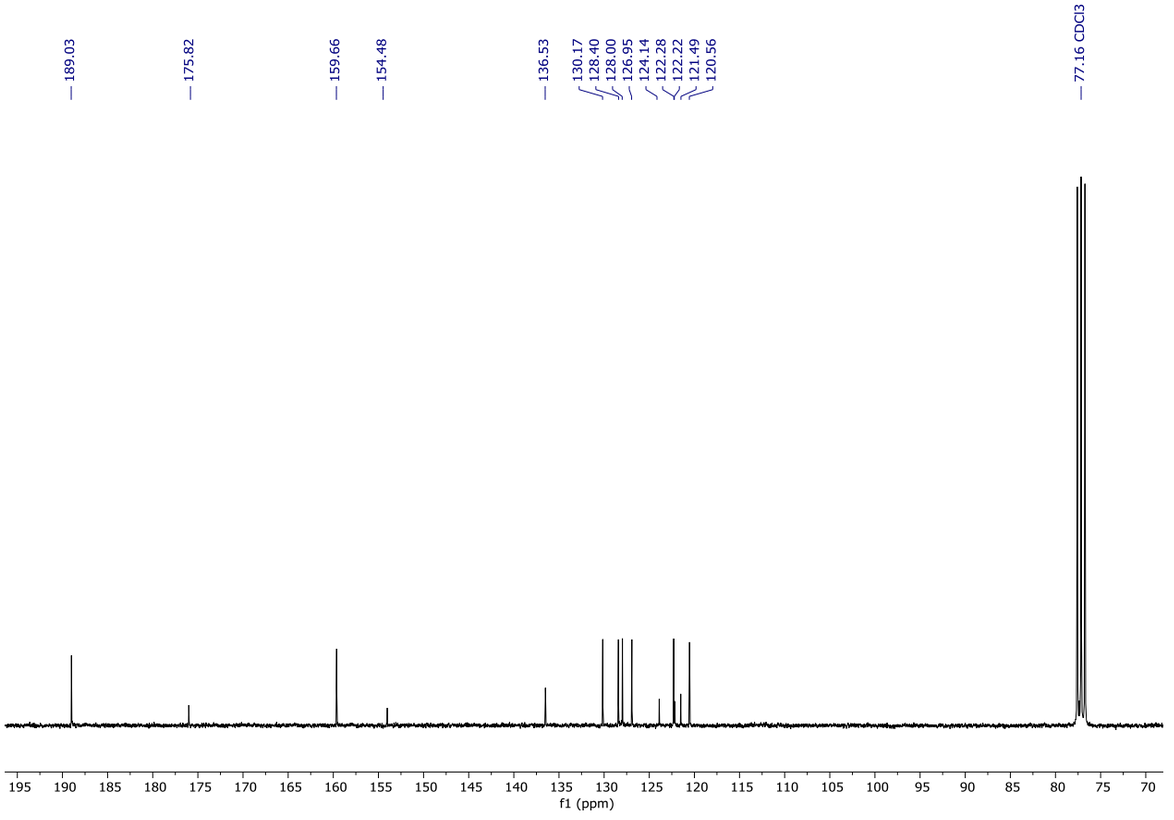

Synthesis | DOI 10.1055/a-2815-1115 |

Figure S7. ^{1}H NMR (300 MHz, $CDCl_3$) spectrum of 6-chloro-4-oxo-4*H*-chromene-3-carbaldehyde (**1i**).

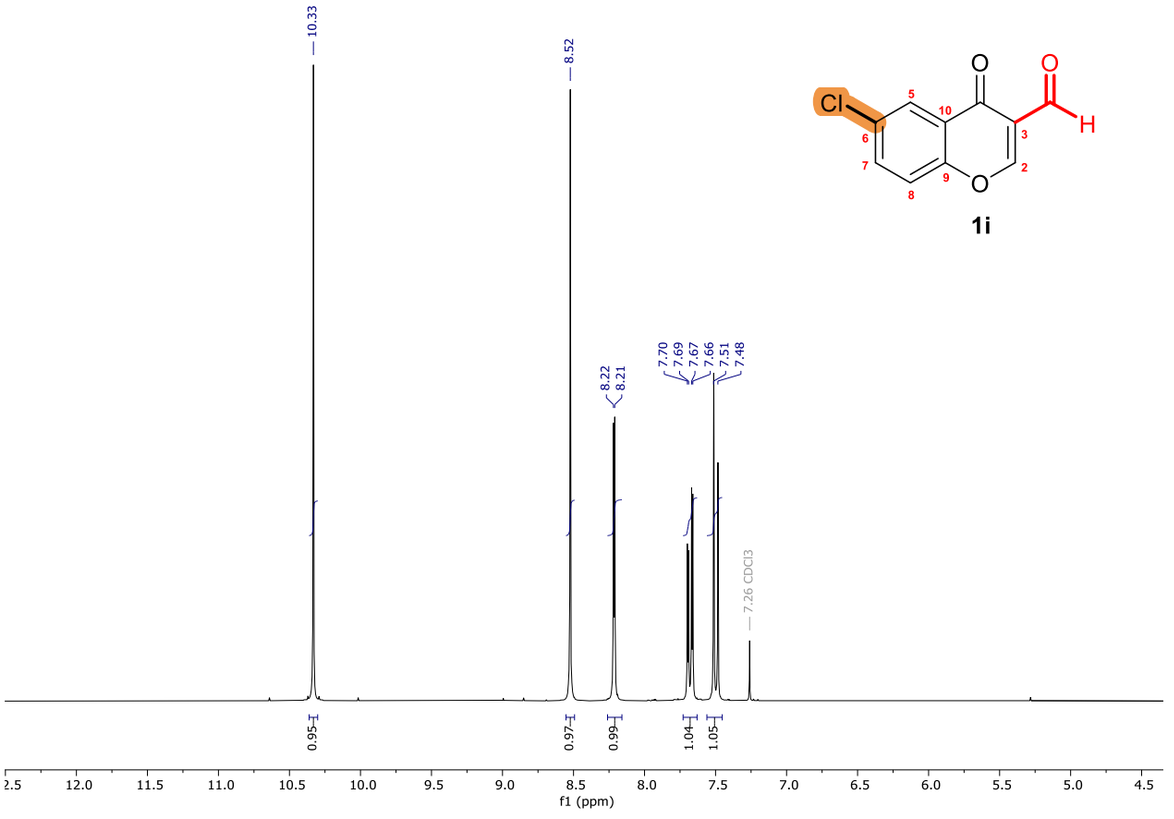

Figure S8. $^{13}C\{^{1}H\}$ NMR (75 MHz, $CDCl_3$) spectrum of **1i**.

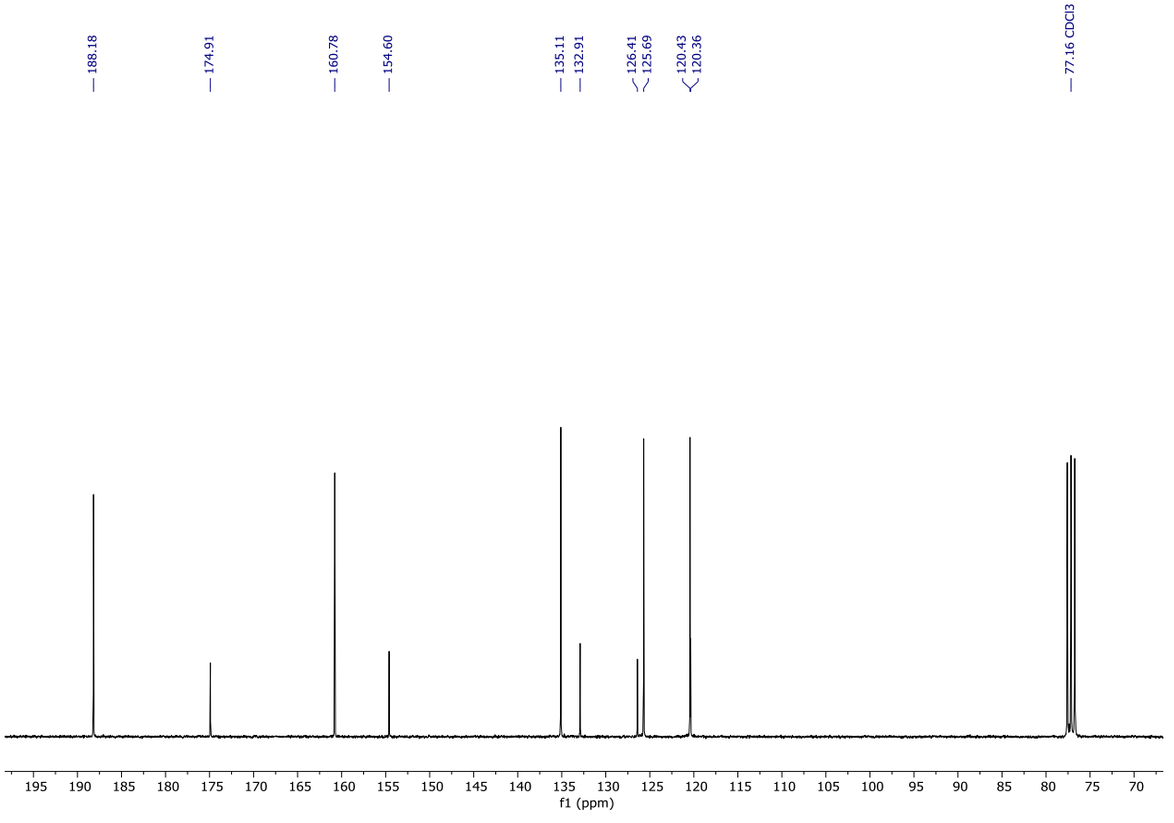

Synthesis | DOI 10.1055/a-2815-1115 |

3. NMR spectra of hydroxy phosphonates 4

Figure S9. ^{1}H NMR (300 MHz, $CDCl_3$) spectrum of dibenzyl (hydroxy(4-oxo-4*H*-chromen-3-yl)methyl)phosphonate (**4aa**).

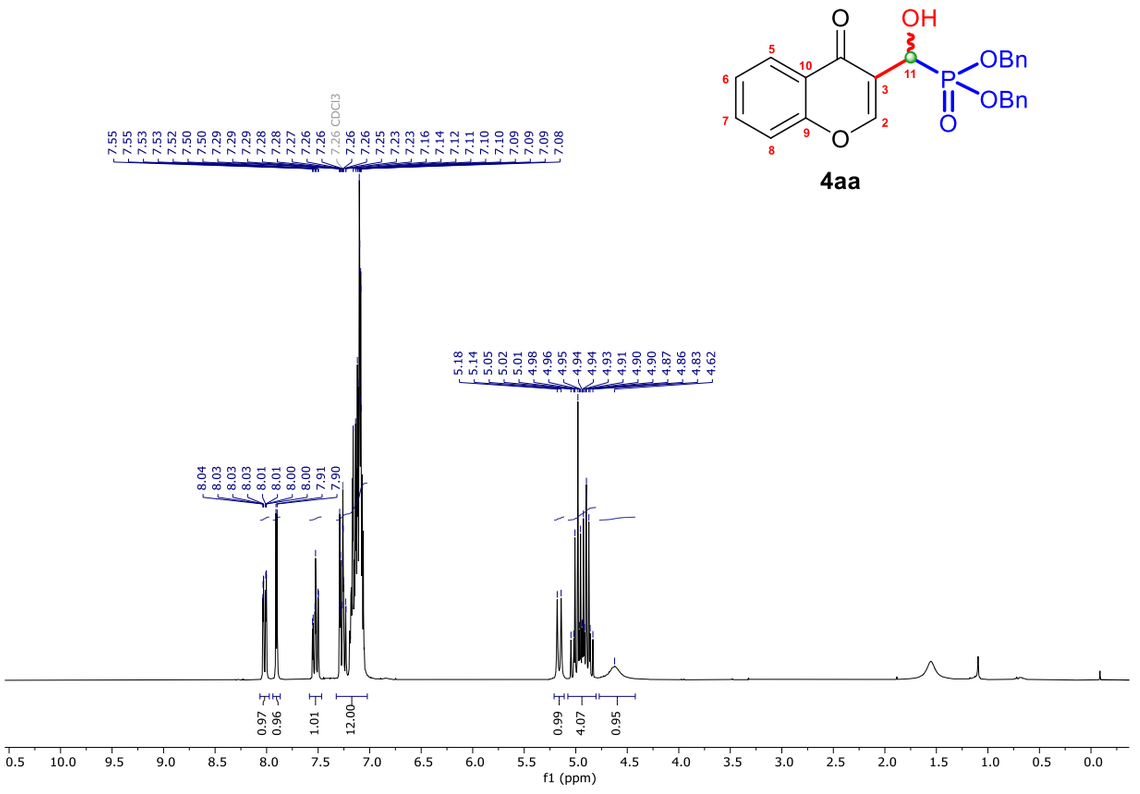

Synthesis | DOI 10.1055/a-2815-1115 |

Figure S10. $^{13}C\{^{1}H\}$ NMR (75 MHz, $CDCl_3$) spectrum of **4aa**.

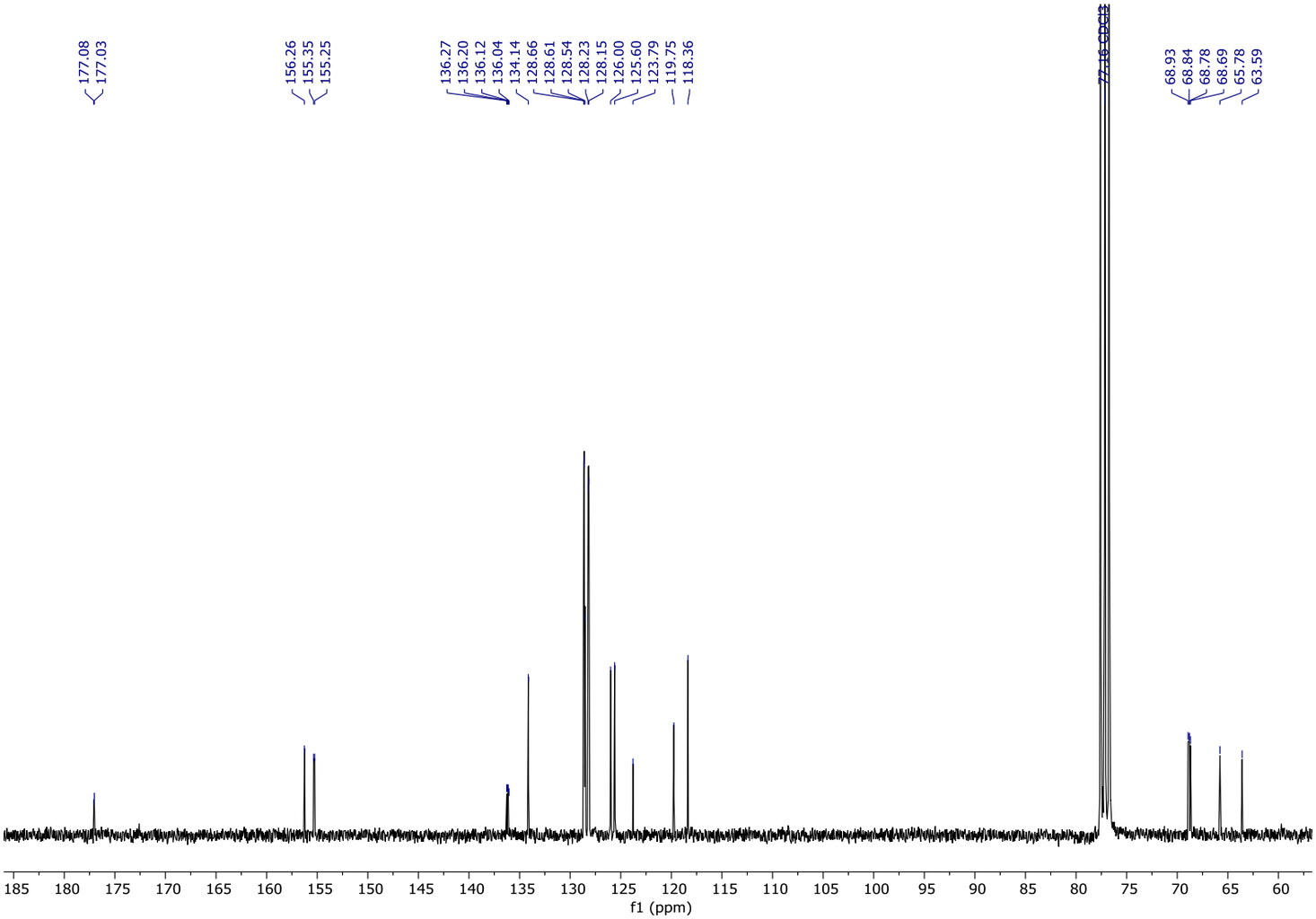

Synthesis | DOI 10.1055/a-2815-1115 |

Figure S11. $^{31}P\{^{1}H\}$ NMR (121 MHz, $CDCl_3$) spectrum of **4aa**.

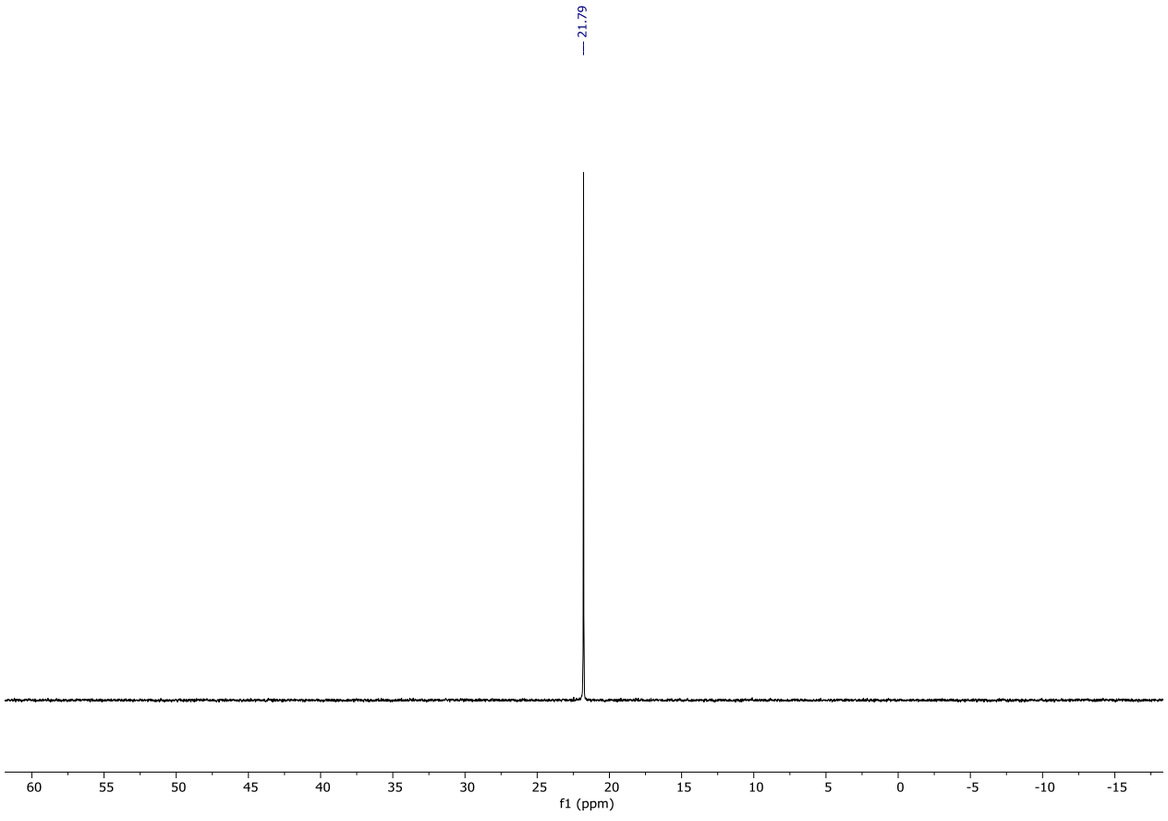

Figure S12. ^{1}H NMR (300 MHz, $CDCl_3$) spectrum of diethyl (hydroxy(4-oxo-4*H*-chromen-3-yl)methyl)phosphonate (**4ab**).

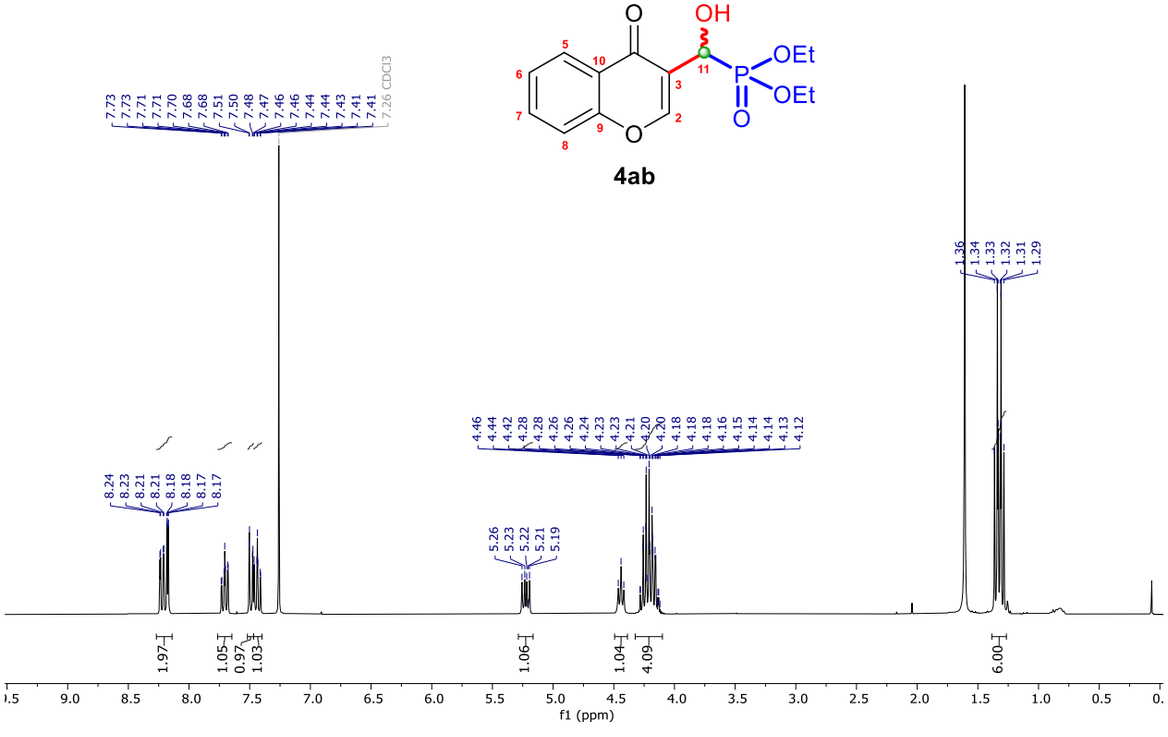

Synthesis | DOI 10.1055/a-2815-1115 |

Figure S13. $^{13}C\{^{1}H\}$ NMR (75 MHz, $CDCl_3$) spectrum of **4ab**.

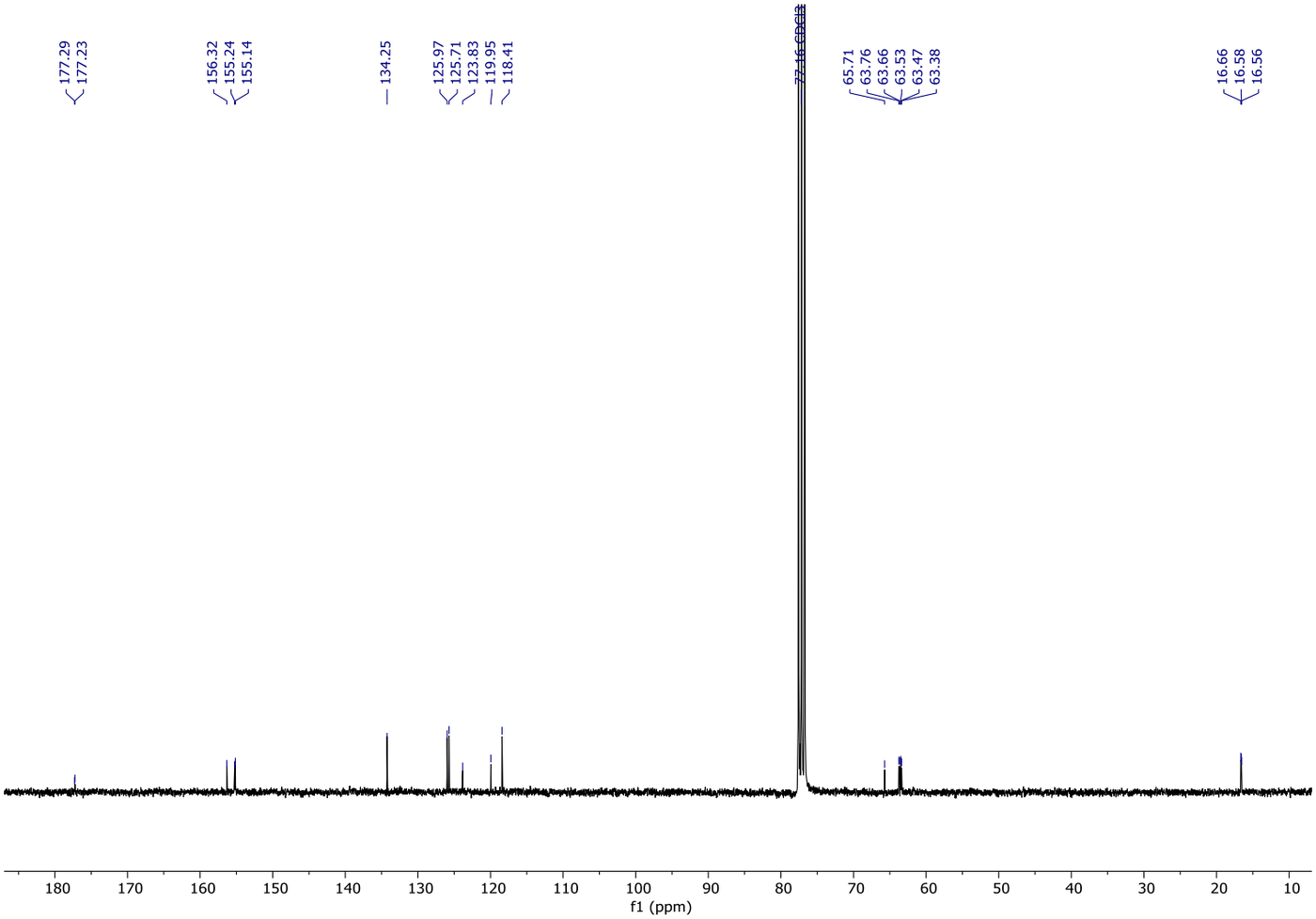

Figure S14. $^{31}P\{^{1}H\}$ NMR (121 MHz, $CDCl_3$) spectrum of **4ab**.

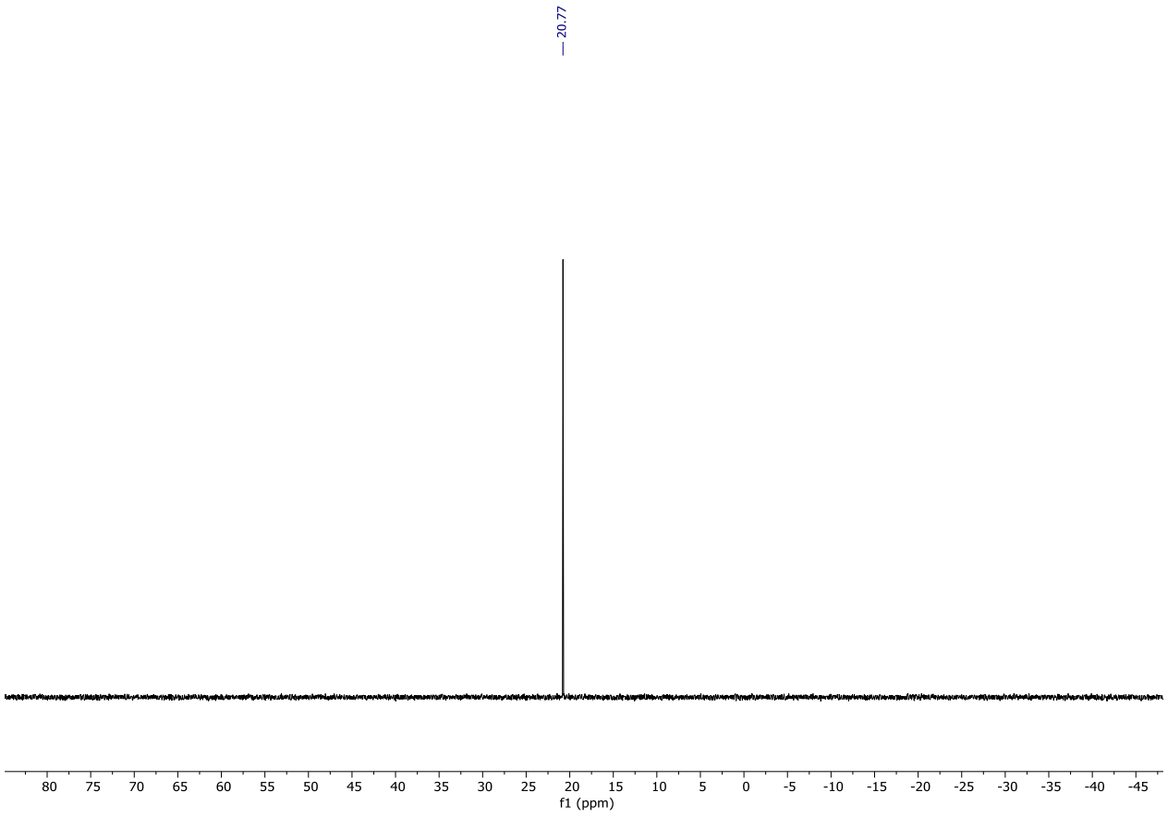

Figure S15. ^{1}H NMR (300 MHz, $CDCl_3$) spectrum of di*iso*propyl (hydroxy(4-oxo-4*H*-chromen-3-yl)methyl)phosphonate (**4ac**).

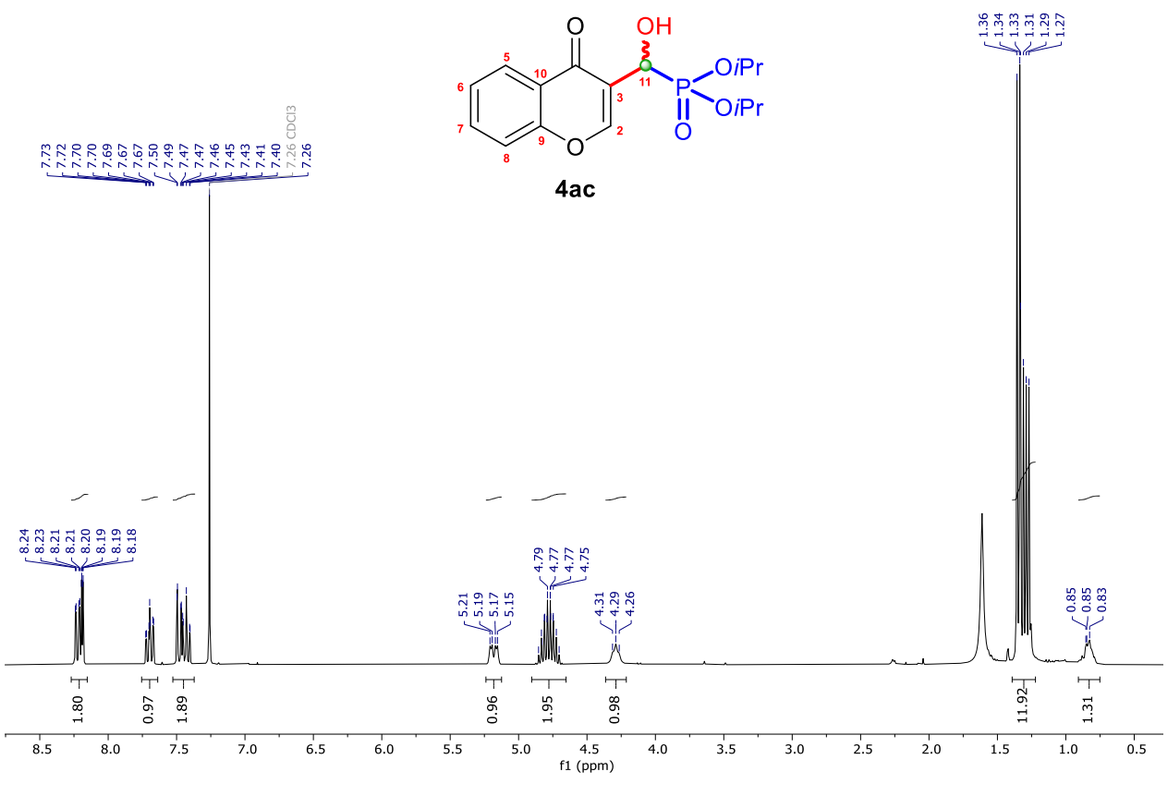

Synthesis | DOI 10.1055/a-2815-1115 |

Figure S16. $^{13}C\{^{1}H\}$ NMR (75 MHz, $CDCl_3$) spectrum of **4ac**.

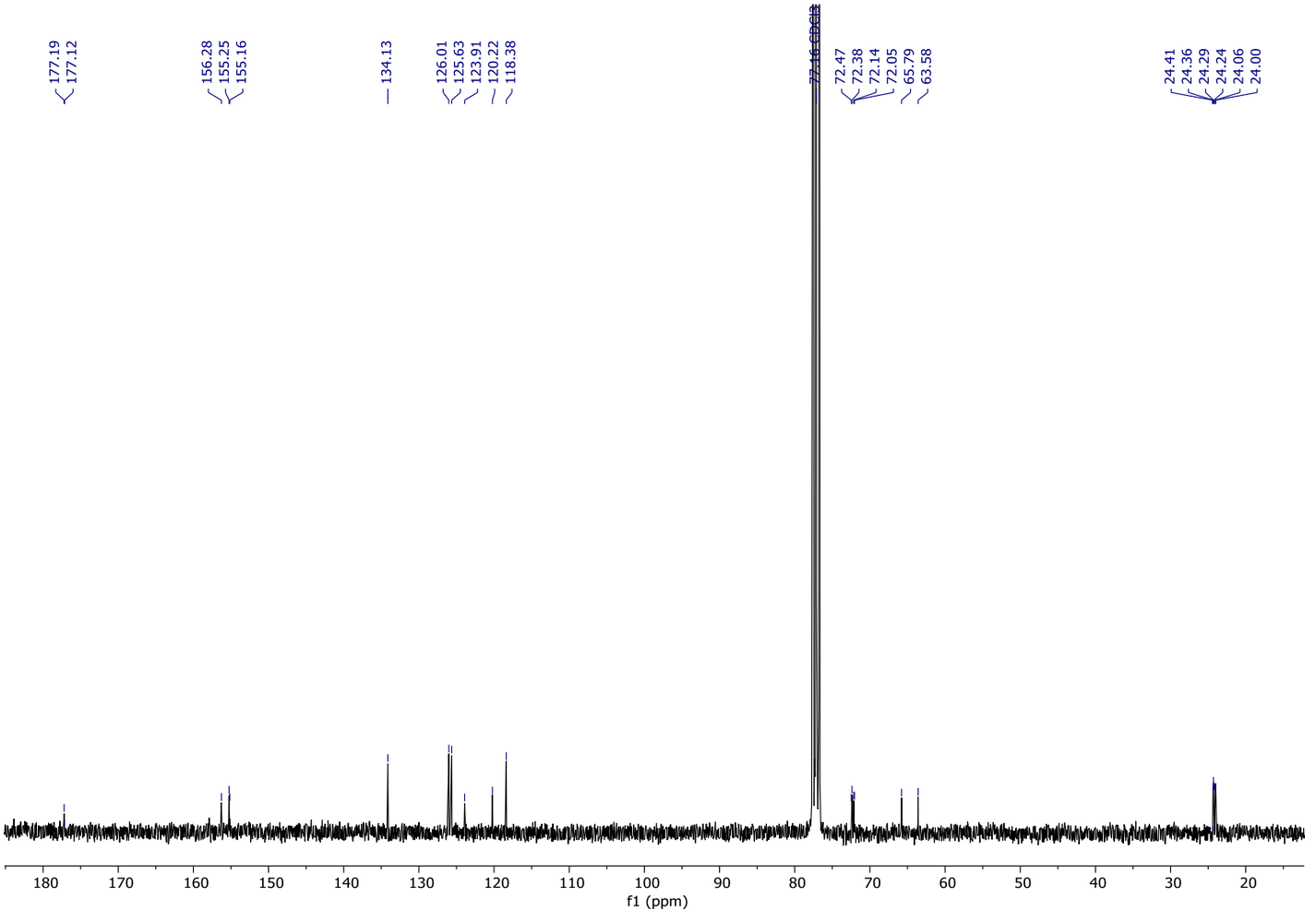

Figure S17. $^{31}P\{^{1}H\}$ NMR (121 MHz, $CDCl_3$) spectrum of **4ac**.

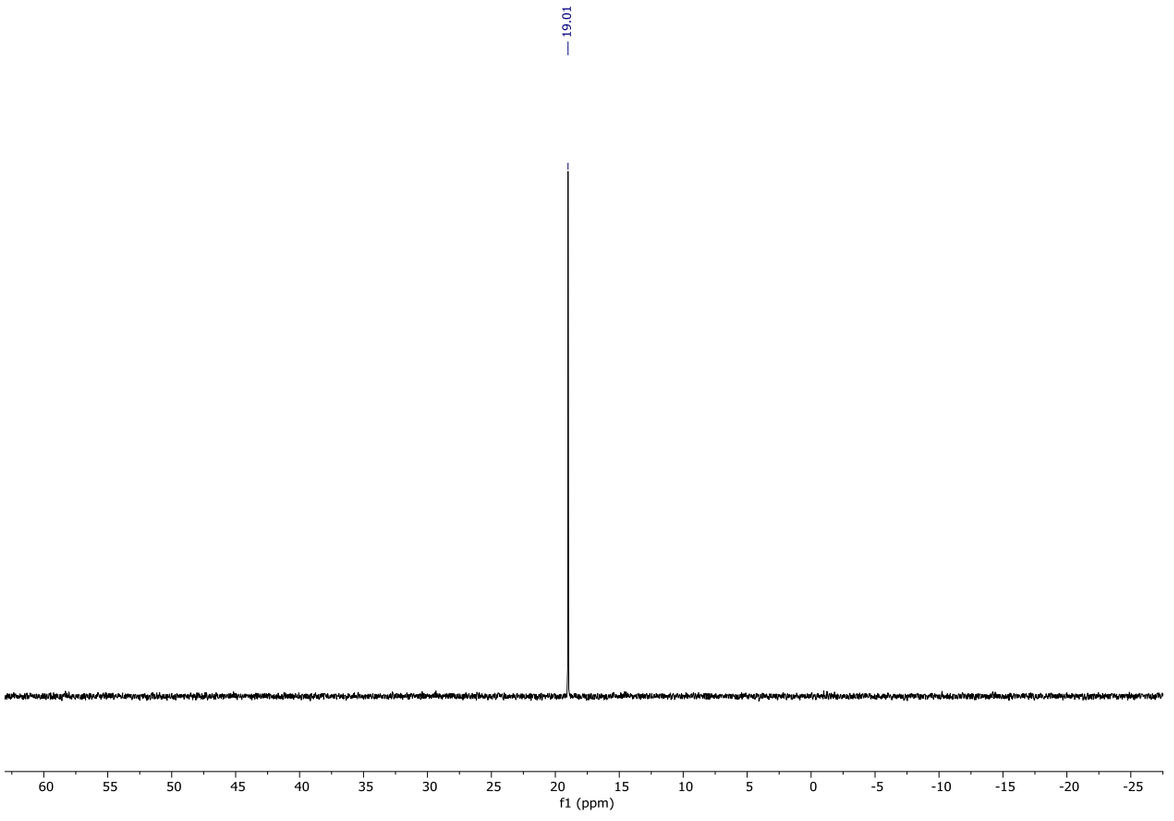

Figure S18. ^{1}H NMR (300 MHz, $CDCl_3$) spectrum of diphenyl (hydroxy(4-oxo-4*H*-chromen-3-yl)methyl)phosphonate (**4ad**).

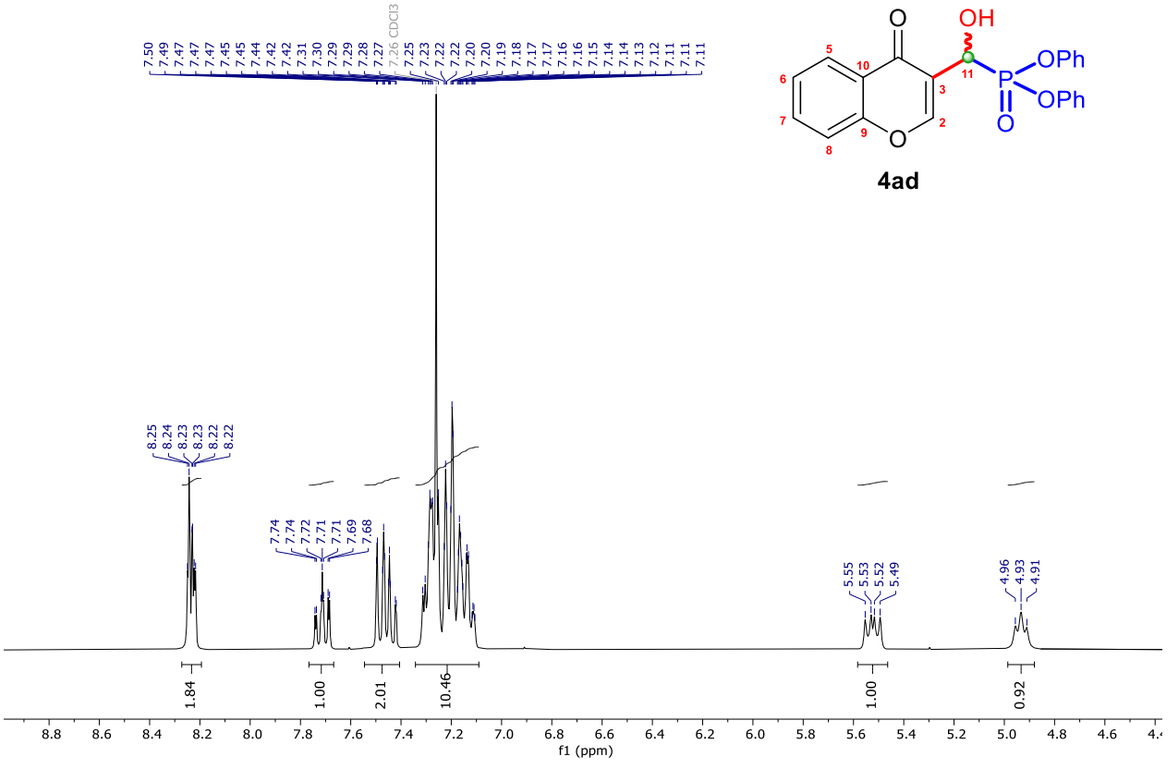

Synthesis | DOI 10.1055/a-2815-1115 |

Figure S19. $^{13}C\{^{1}H\}$ NMR (75 MHz, $CDCl_3$) spectrum of **4ad**.

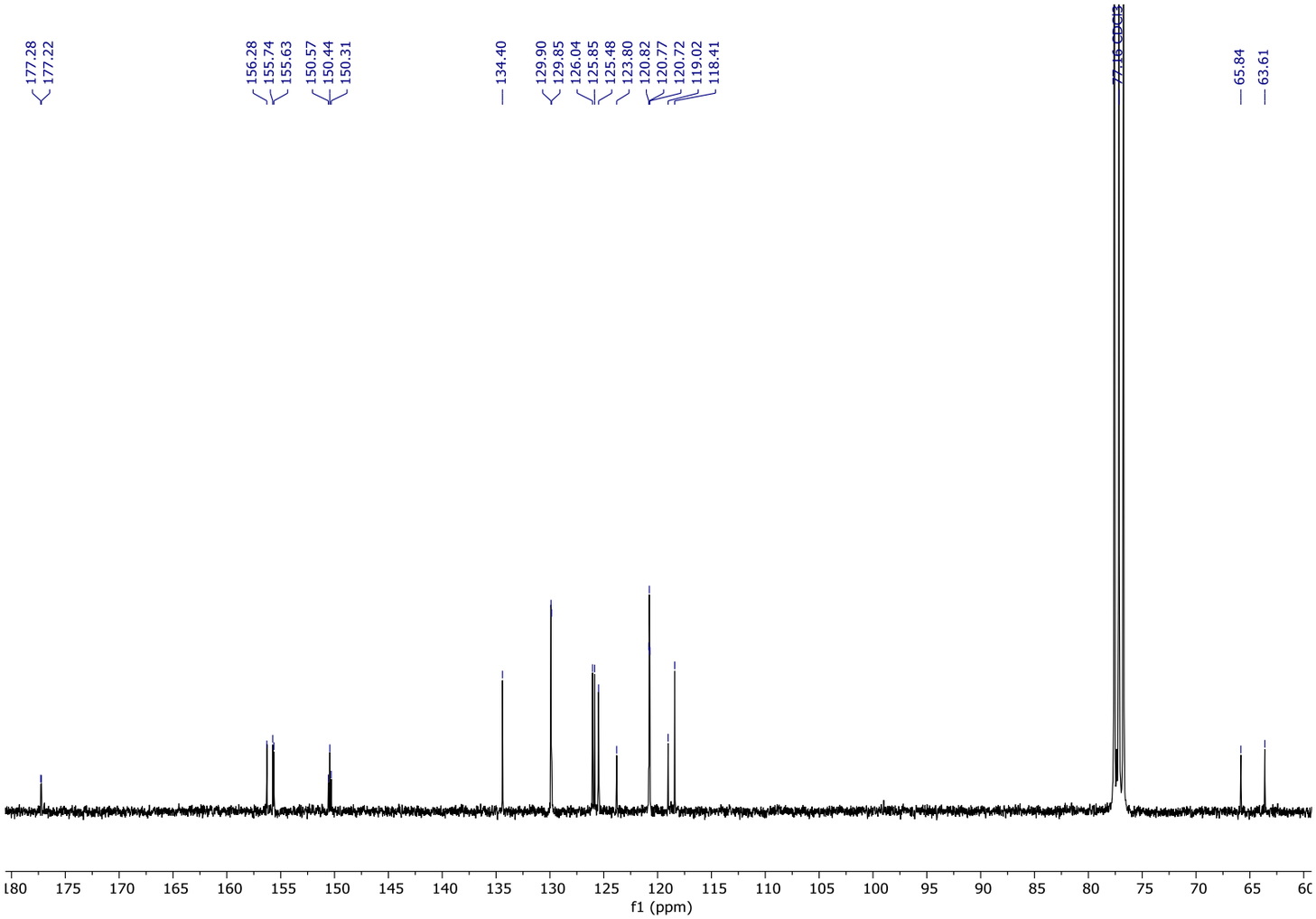

Figure S20. $^{31}P\{^{1}H\}$ NMR (121 MHz, $CDCl_3$) spectrum of **4ad**.

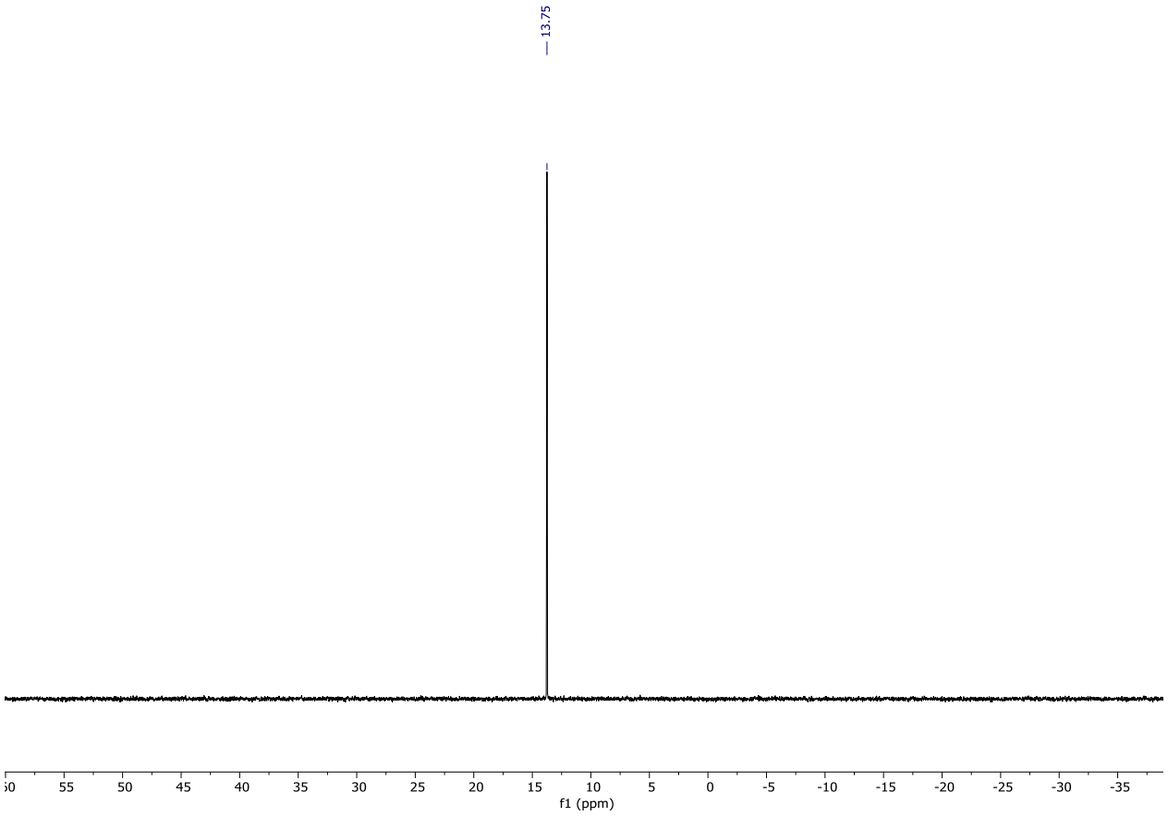

Figure S21. ^{1}H NMR (300 MHz, $CDCl_3$) spectrum of diphenyl (hydroxy(4-oxo-4*H*-chromen-3-yl)methyl)phosphine oxide (**4ae**).

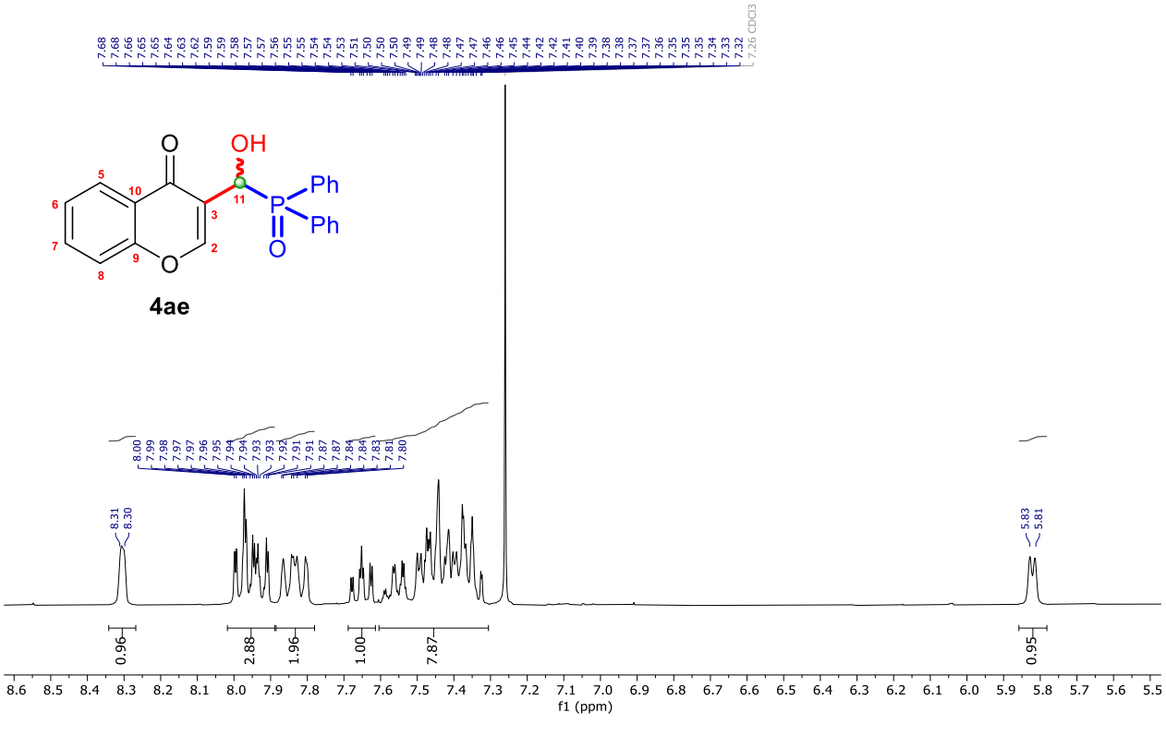

Figure S22. $^{13}C\{^{1}H\}$ NMR (75 MHz, $CDCl_3$) spectrum of **4ae**.

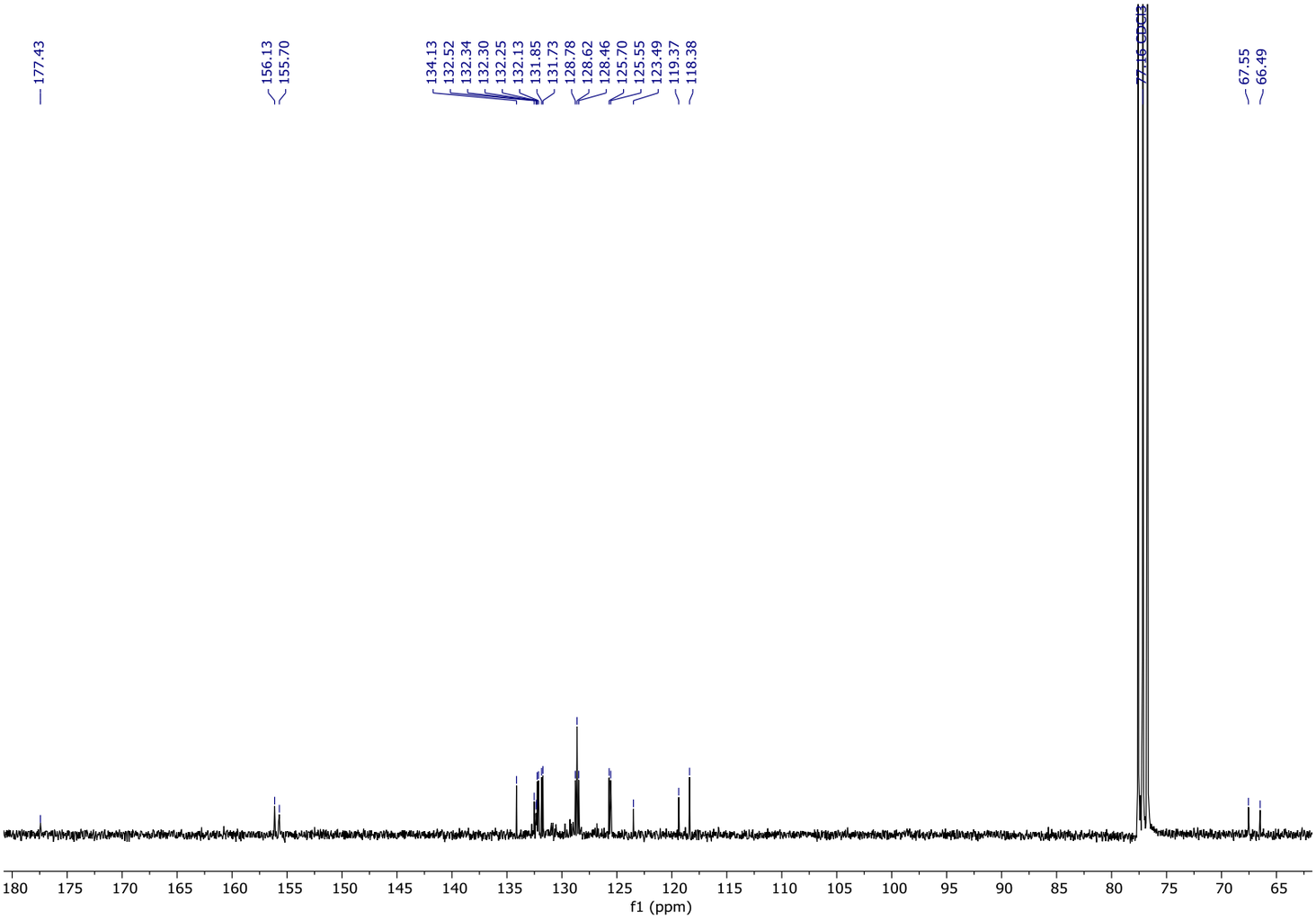

Figure S23. $^{31}P\{^{1}H\}$ NMR (121 MHz, $CDCl_3$) spectrum of **4ae**.

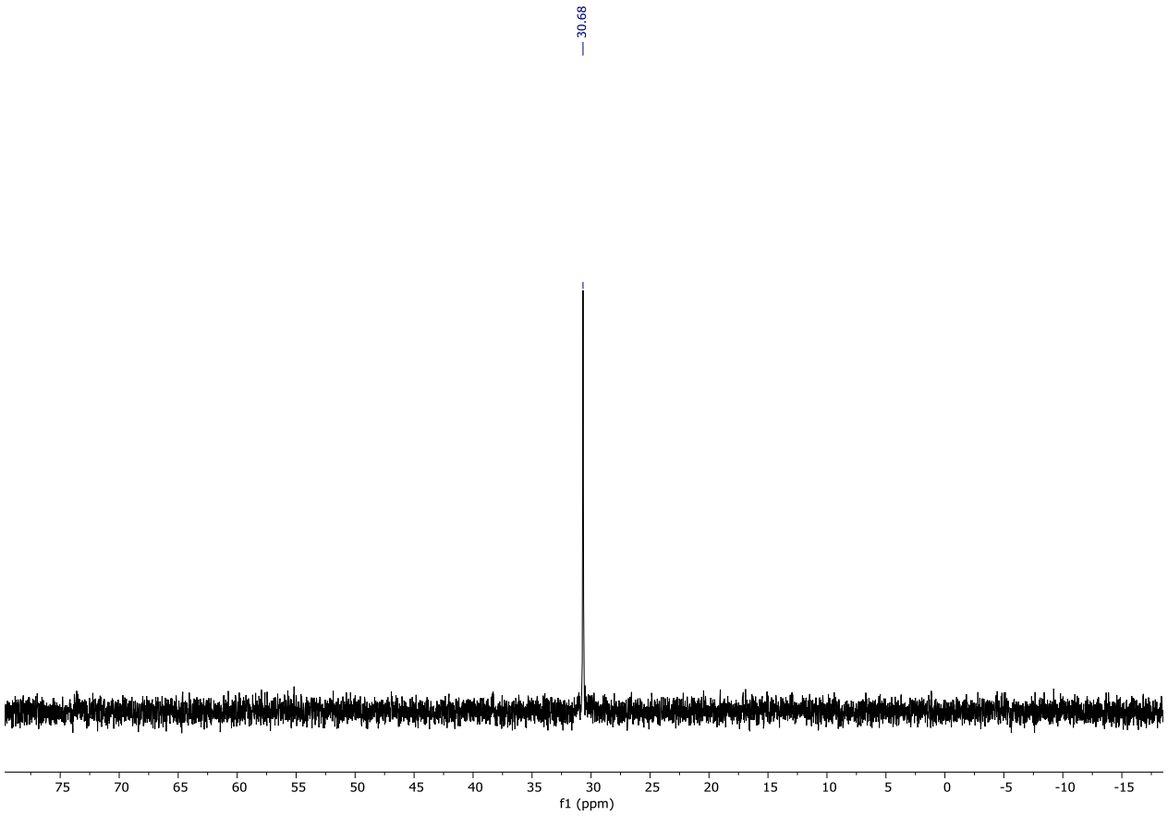

Figure S24. ^{1}H NMR (300 MHz, $CDCl_3$) spectrum of diphenyl (hydroxy(6-methyl-4-oxo-4*H*-chromen-3-yl)methyl)phosphonate (**4bd**).

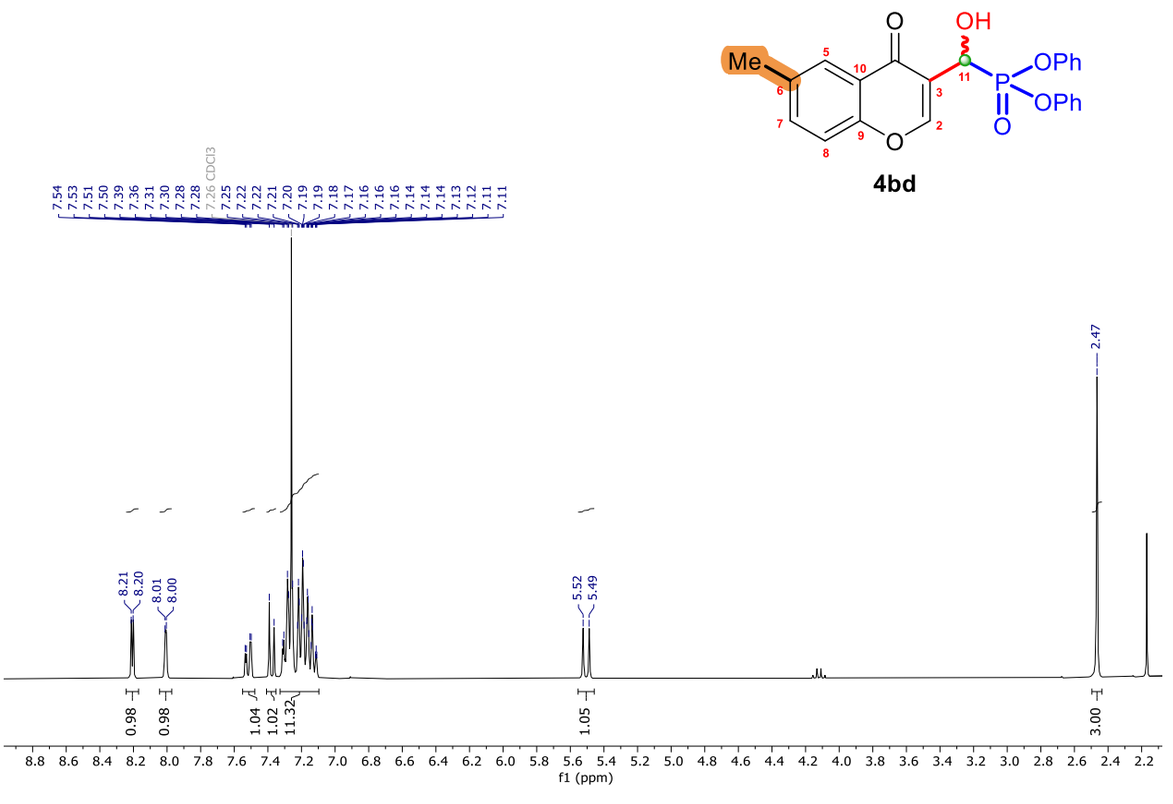

Figure S25. $^{13}C\{^{1}H\}$ NMR (100 MHz, $CDCl_3$) spectrum of **4bd**.

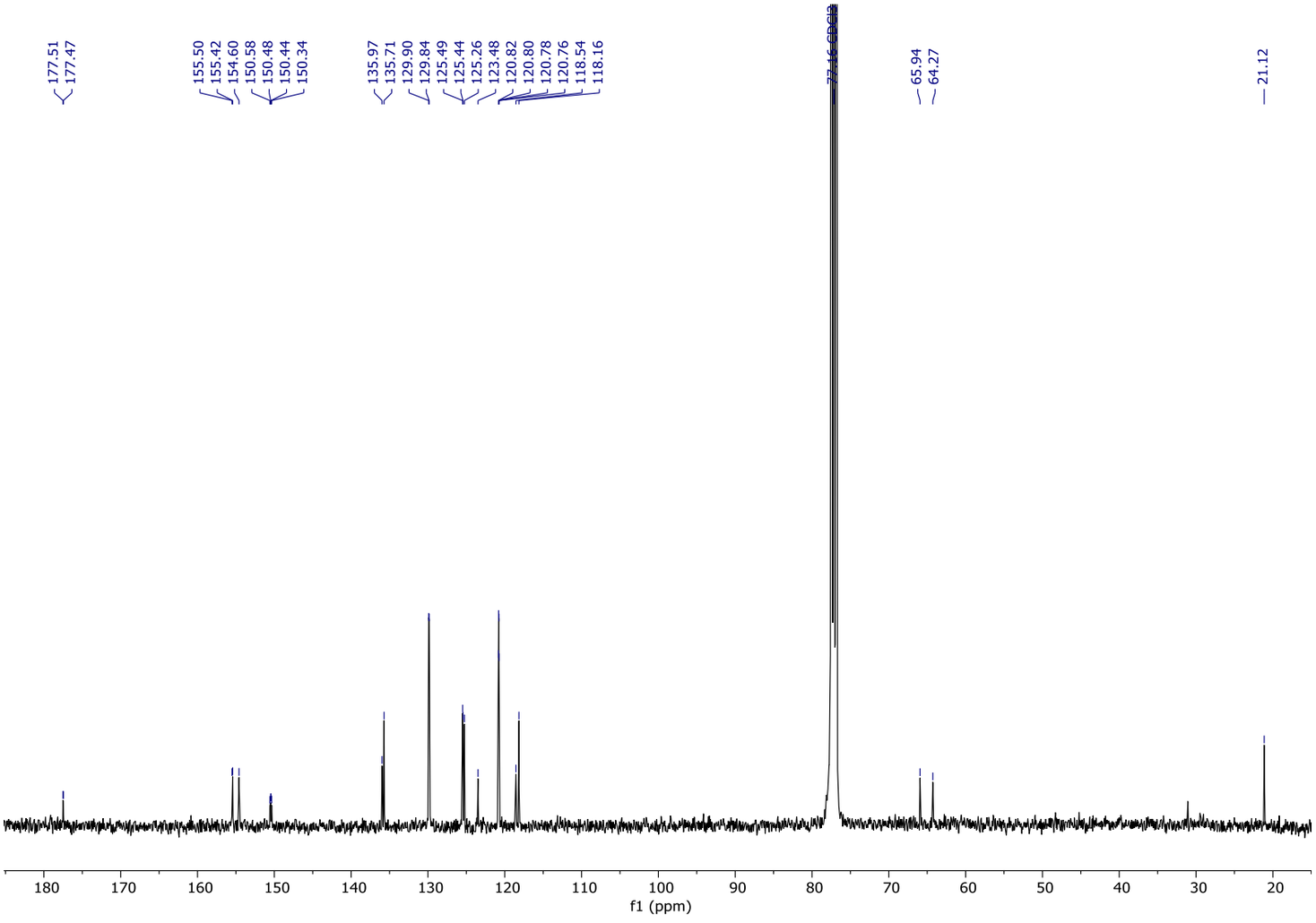

Figure S26. $^{31}P\{^{1}H\}$ NMR (121 MHz, $CDCl_3$) spectrum of **4bd**.

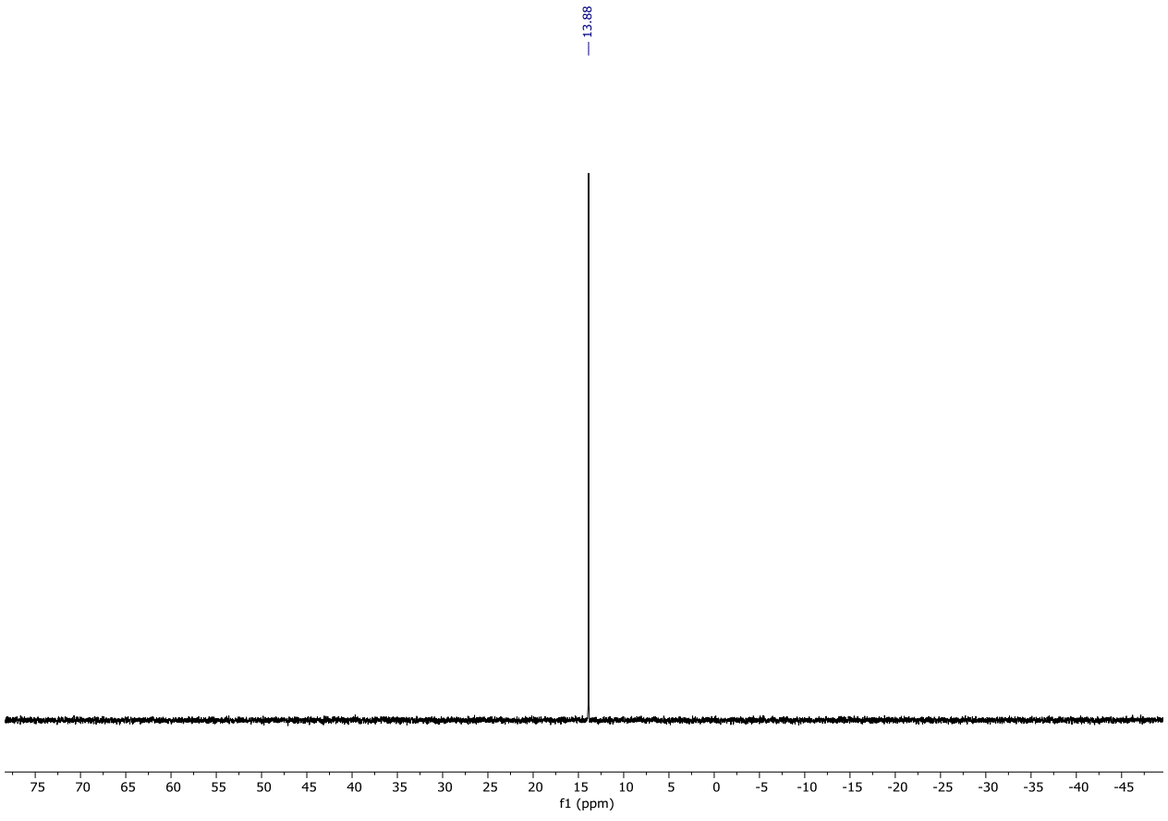

Figure S27. ^{1}H NMR (300 MHz, $CDCl_3$) spectrum of diphenyl (hydroxy(6-methoxy-4-oxo-4*H*-chromen-3-yl)methyl)phosphonate (**4cd**).

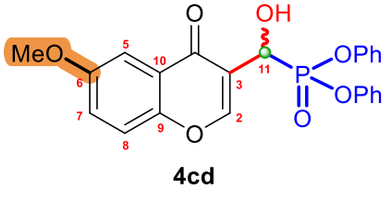

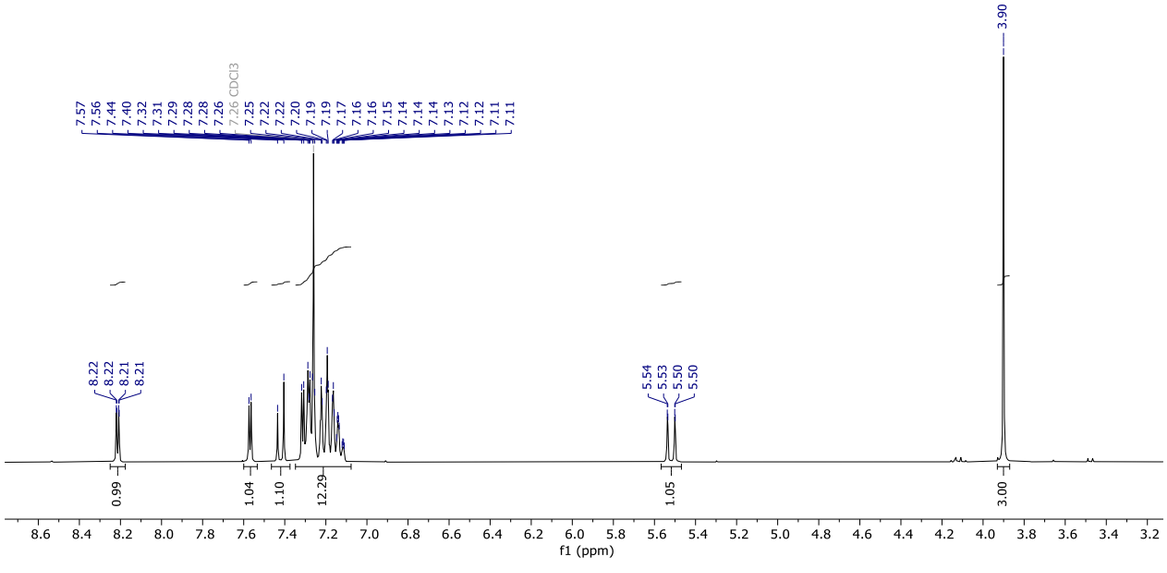

Figure S28. $^{13}C\{^{1}H\}$ NMR (75 MHz, $CDCl_3$) spectrum of **4cd**.

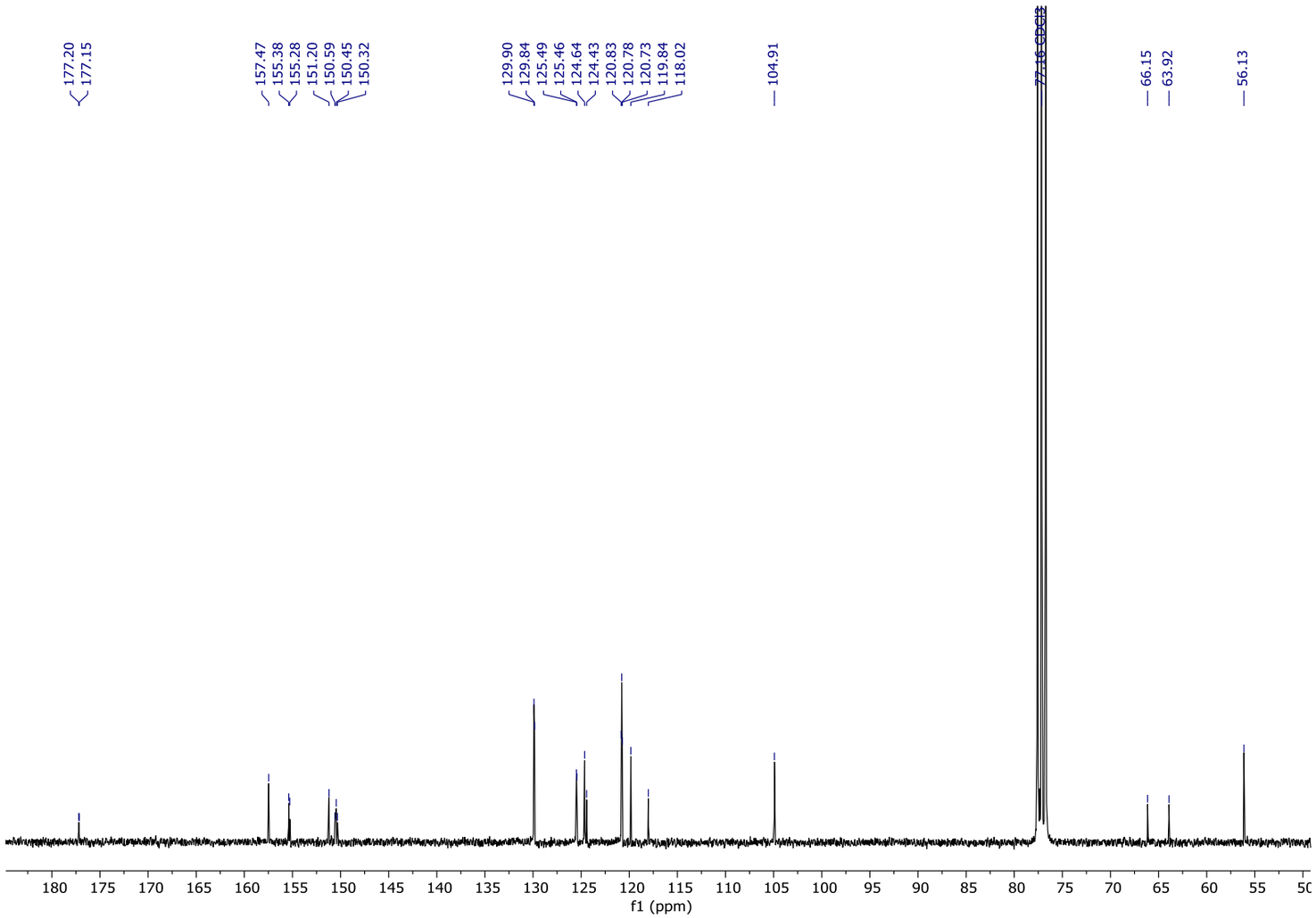

Figure S29. $^{31}P\{^{1}H\}$ NMR (121 MHz, $CDCl_3$) spectrum of **4cd**.

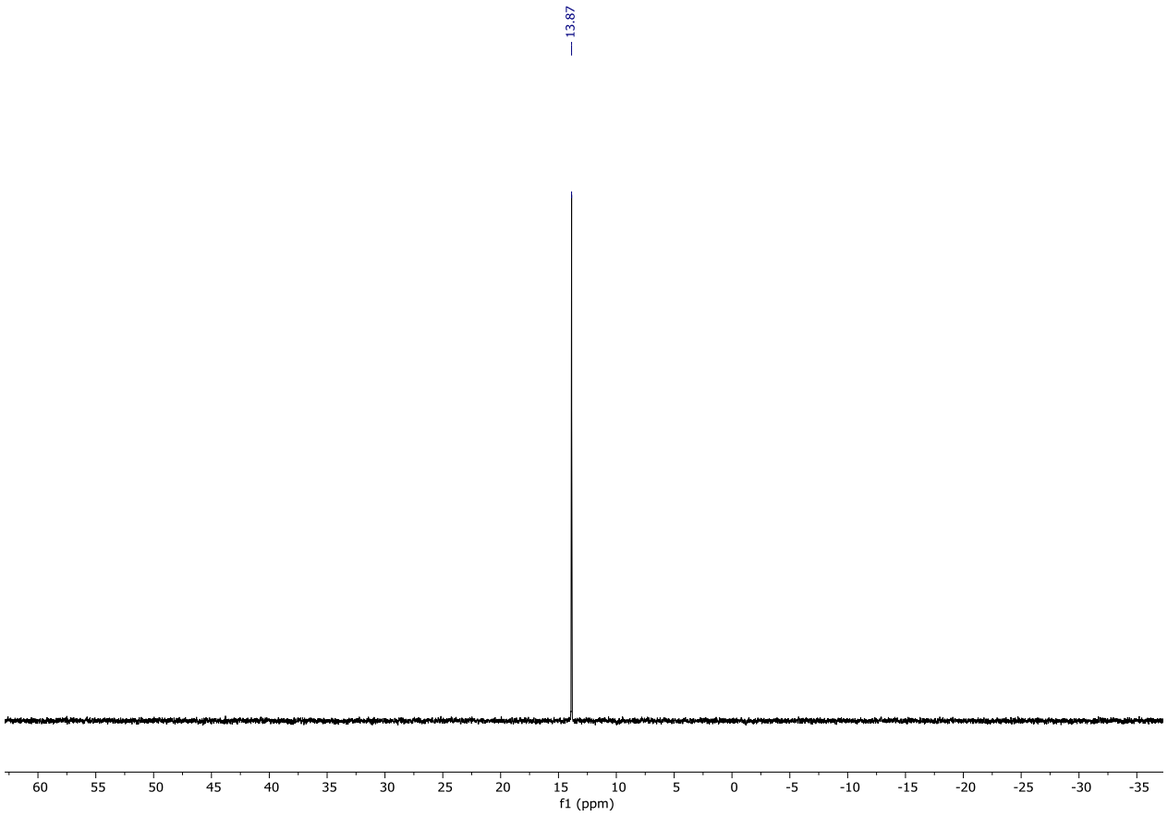

Figure S30. ^{1}H NMR (300 MHz, $CDCl_3$) spectrum of Diphenyl (hydroxy(7-methoxy-4-oxo-4*H*-chromen-3-yl)methyl)phosphonate (**4dd**).

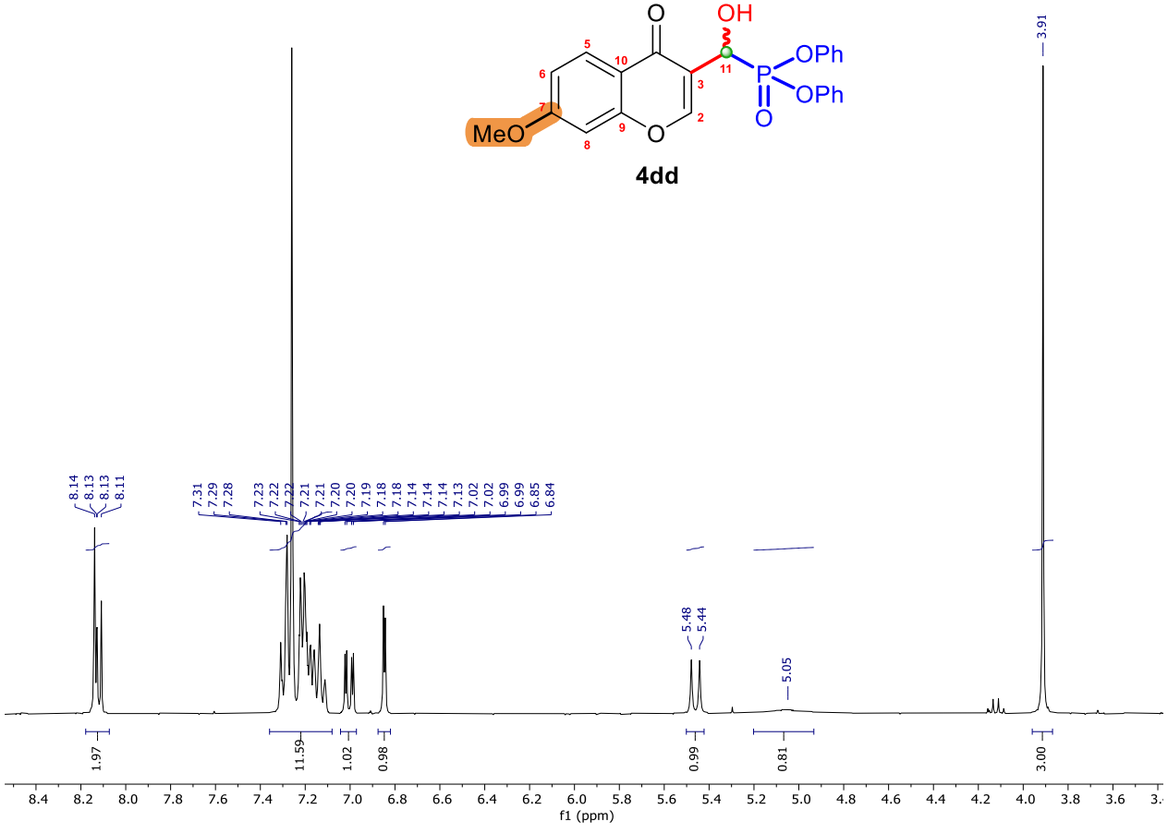

Synthesis | DOI 10.1055/a-2815-1115 |

Figure S31. $^{13}C\{^{1}H\}$ NMR (75 MHz, $CDCl_3$) spectrum of **4dd**.

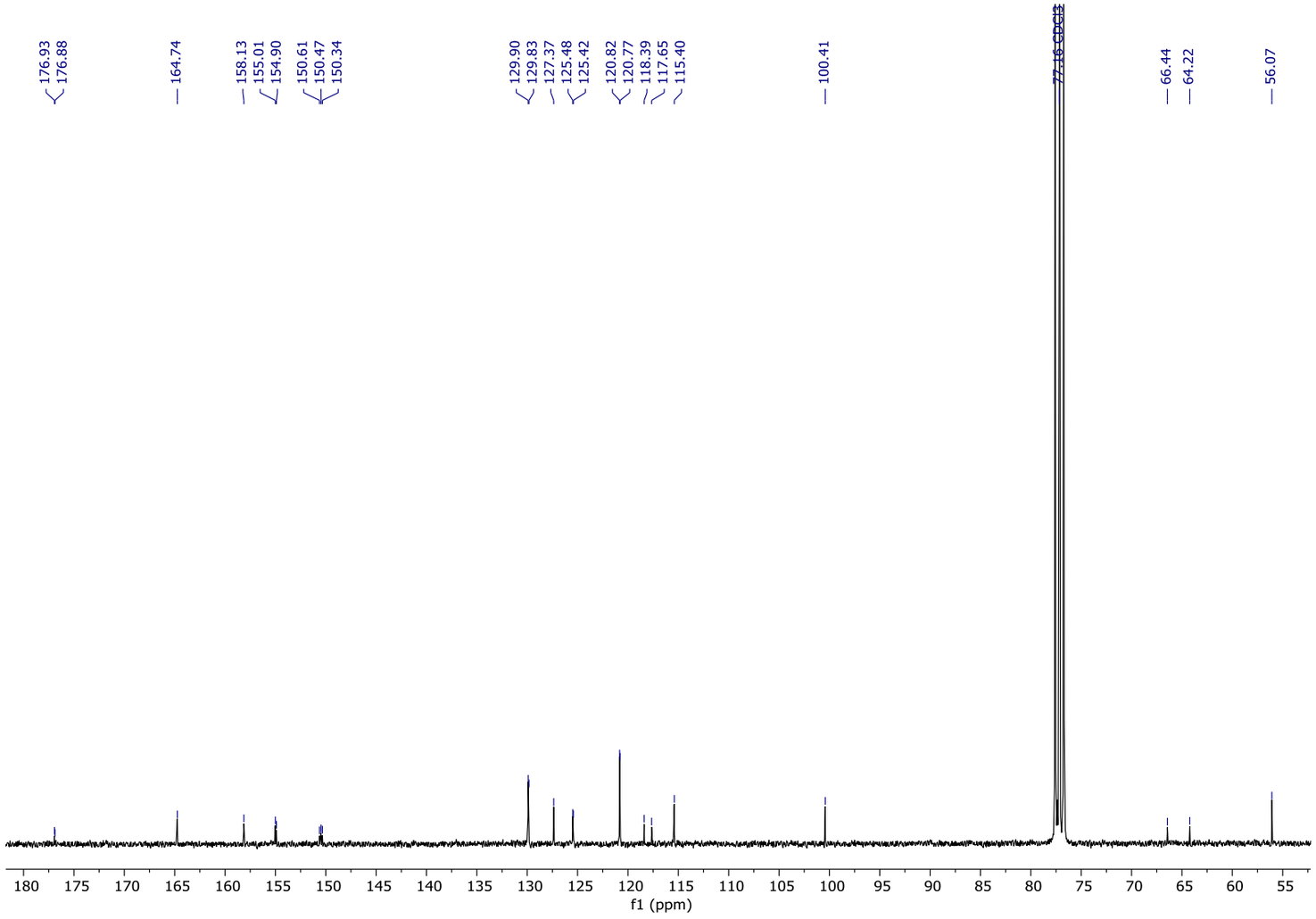

Figure S32. $^{31}P\{^{1}H\}$ NMR (121 MHz, $CDCl_3$) spectrum of **4dd**.

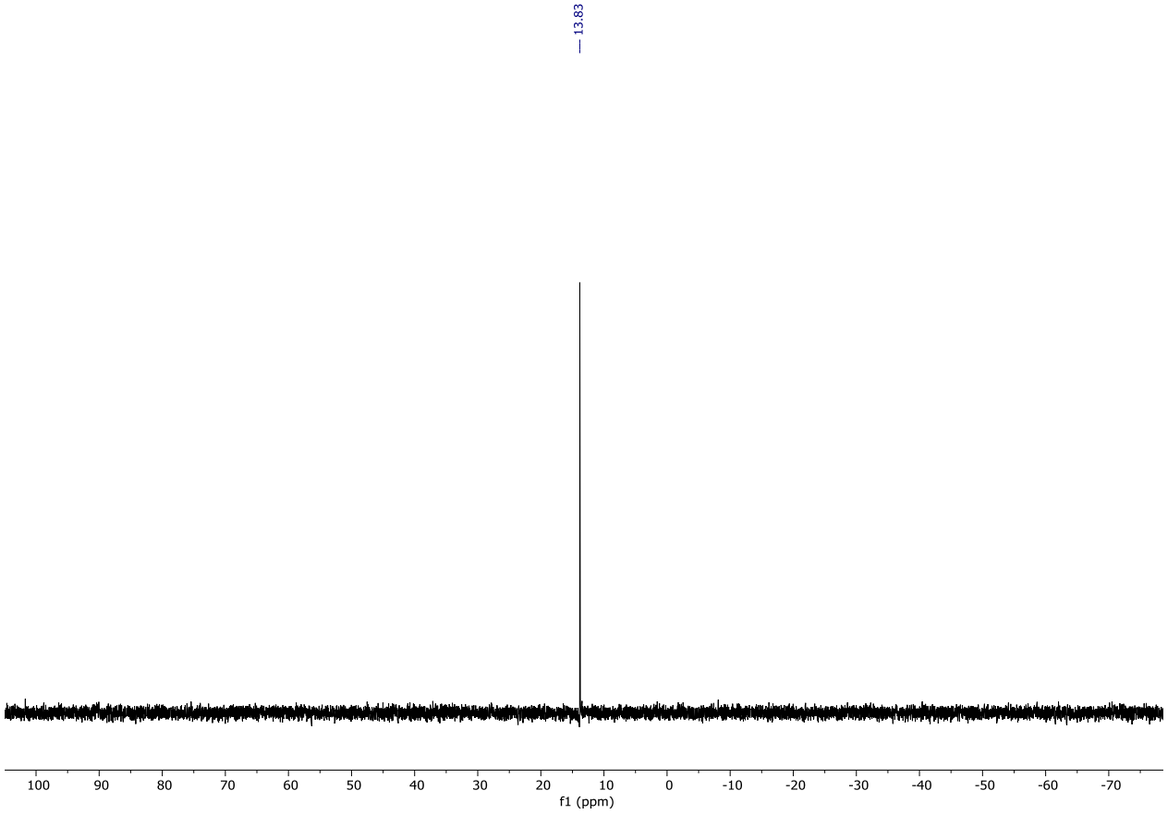

Figure S33. ^{1}H NMR (300 MHz, $CDCl_3$) spectrum of diphenyl (hydroxy(4-oxo-4*H*-benzo[*f*]chromen-3-yl)methyl)phosphonate (**4ed**).

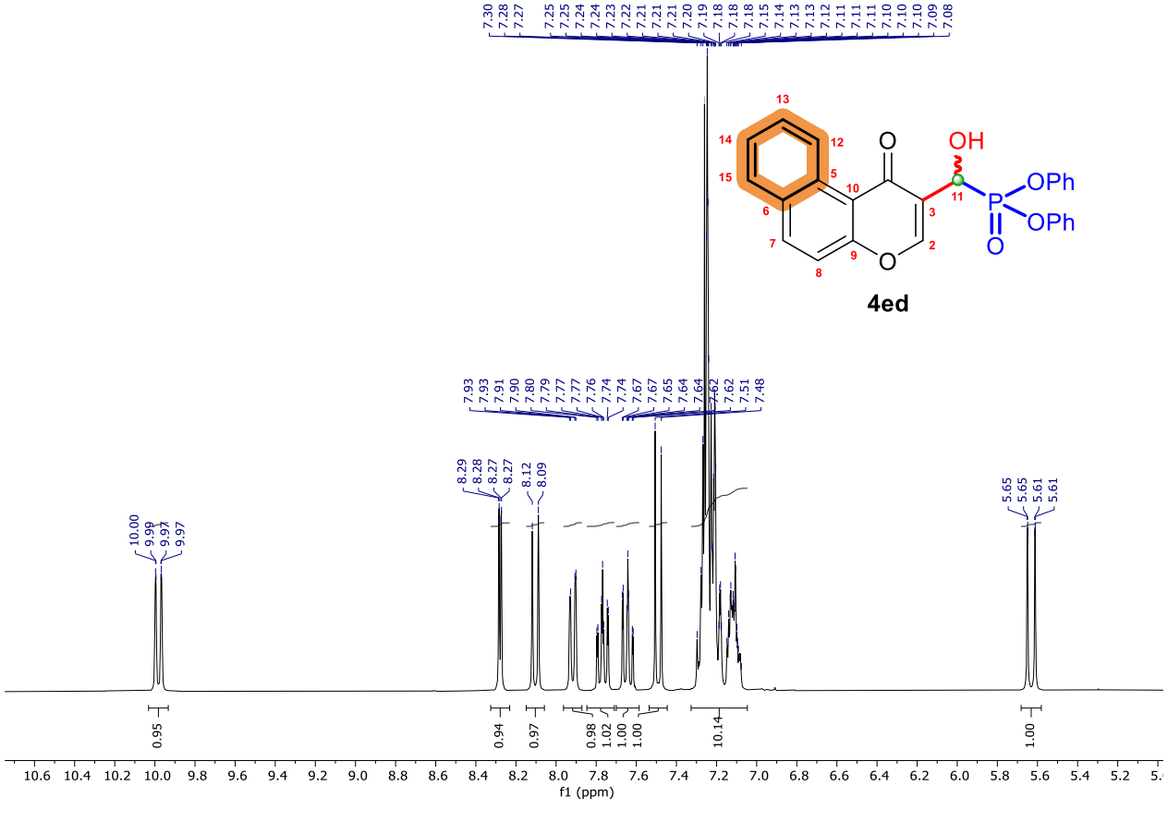

Synthesis | DOI 10.1055/a-2815-1115 |

Figure S34. $^{13}C\{^{1}H\}$ NMR (75 MHz, $CDCl_3$) spectrum of **4ed**.

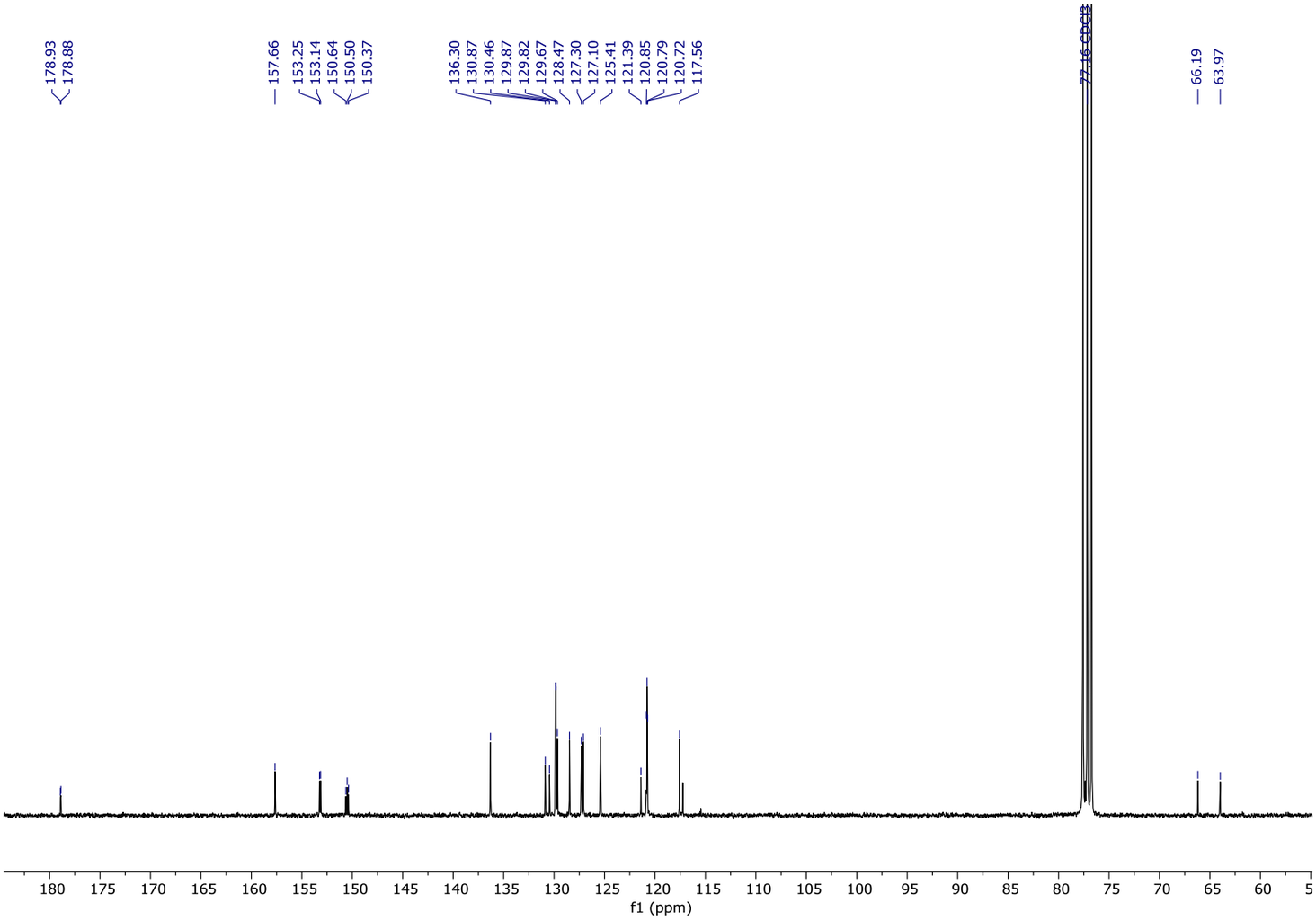

Figure S35. $^{31}P\{^{1}H\}$ NMR (121 MHz, $CDCl_3$) spectrum of **4ed**.

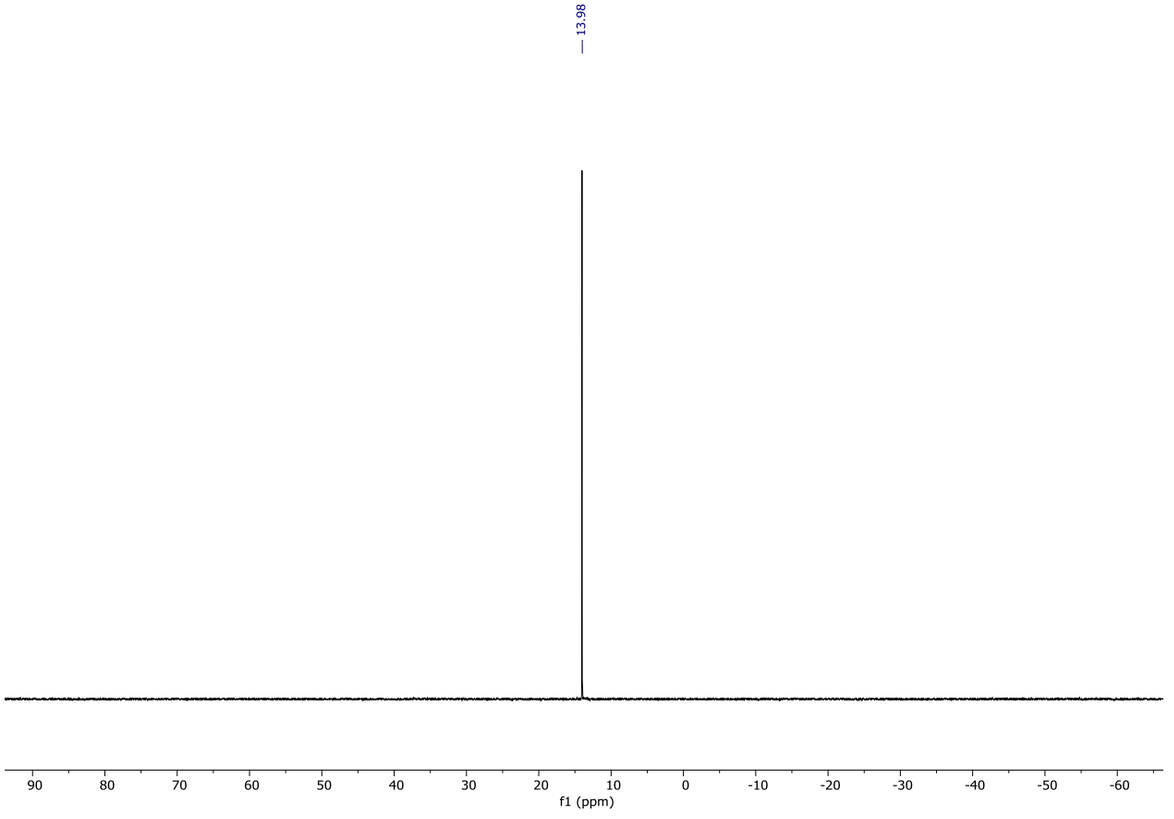

Figure S36. ^{1}H NMR (300 MHz, $CDCl_3$) spectrum of diphenyl (hydroxy(4-oxo-4*H*-benzo[*h*]chromen-3-yl)methyl)phosphonate (**4fd**).

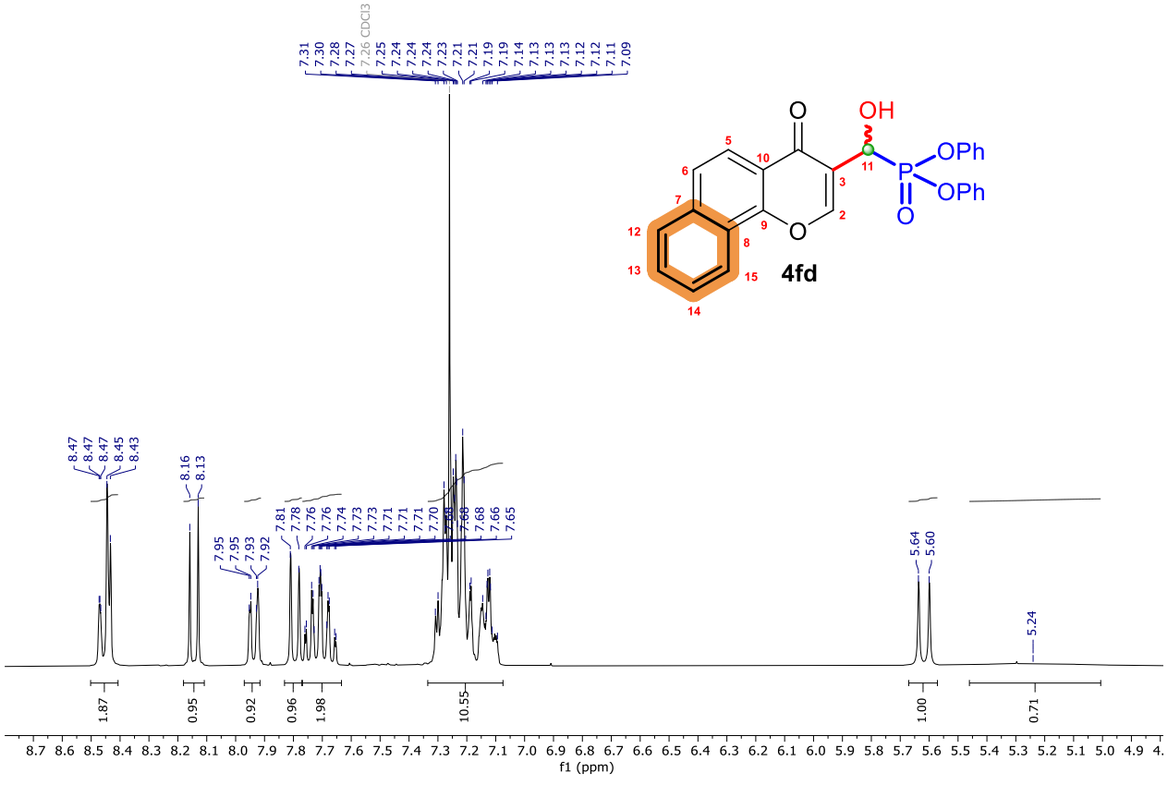

Figure S37. $^{13}C\{^{1}H\}$ NMR (75 MHz, $CDCl_3$) spectrum of **4fd**.

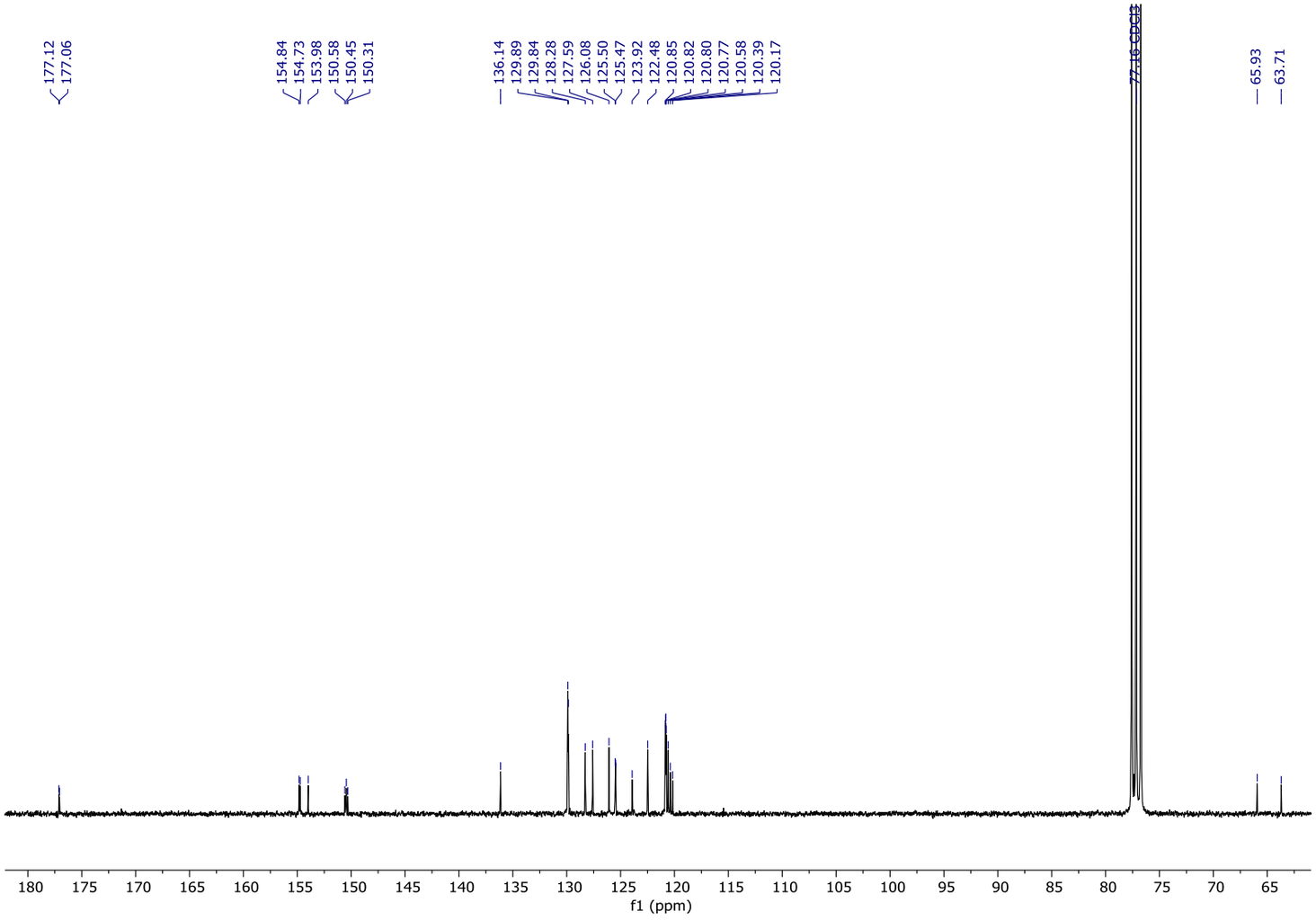

Synthesis | DOI 10.1055/a-2815-1115 |

Figure S38. $^{31}P\{^{1}H\}$ NMR (121 MHz, $CDCl_3$) spectrum of **4fd**.

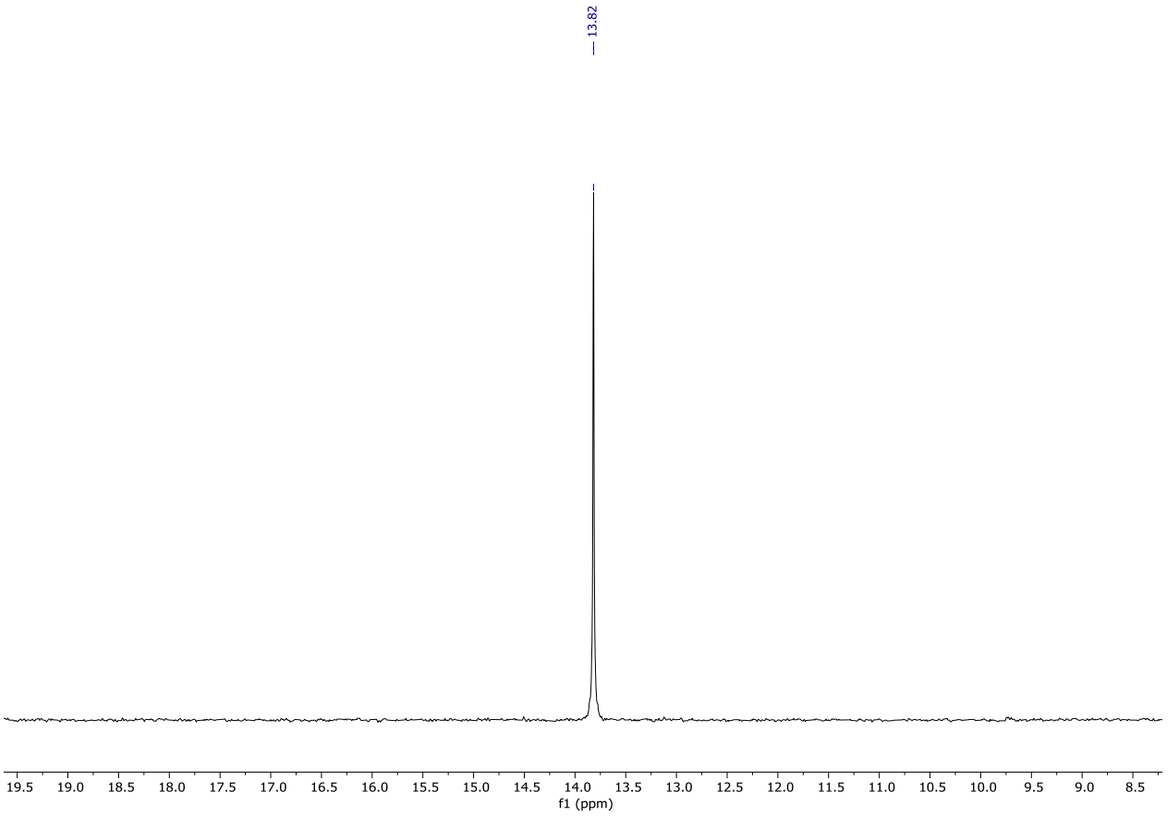

Figure S39. ^{1}H NMR (300 MHz, $CDCl_3$) spectrum of diphenyl (hydroxy(6-nitro-4-oxo-4*H*-chromen-3-yl)methyl)phosphonate (**4gd**).

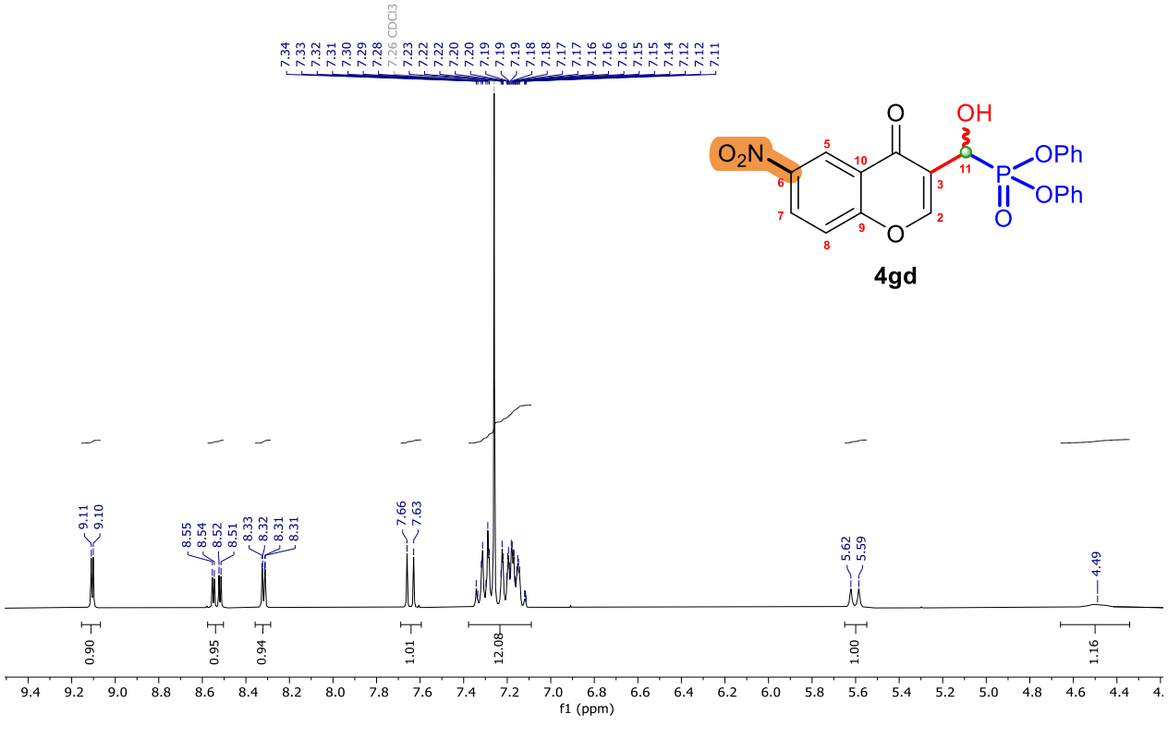

Figure S40. $^{13}C\{^{1}H\}$ NMR (125 MHz, $CDCl_3$) spectrum of **4gd**.

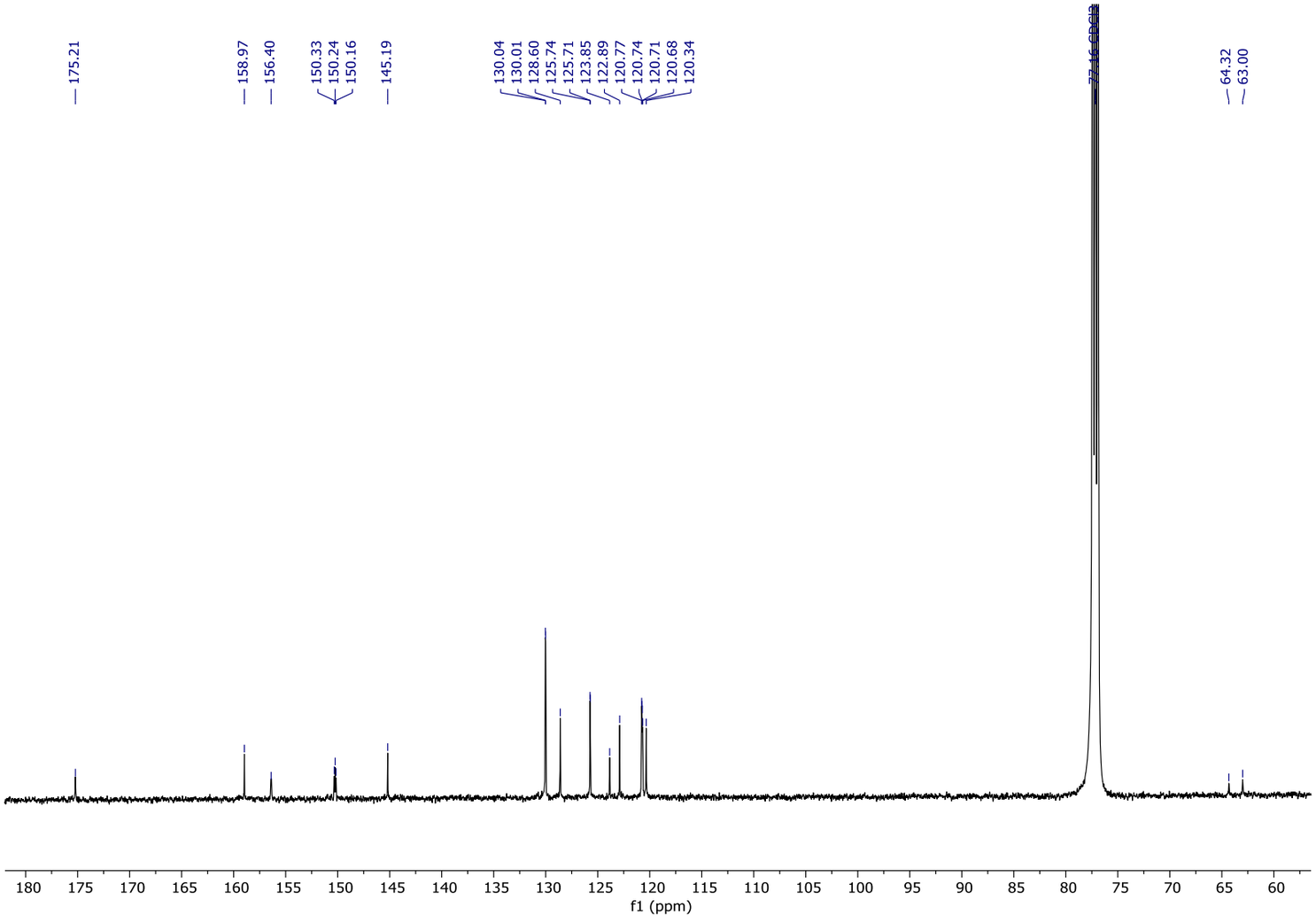

Figure S41. $^{31}P\{^{1}H\}$ NMR (121 MHz, $CDCl_3$) spectrum of **4gd**.

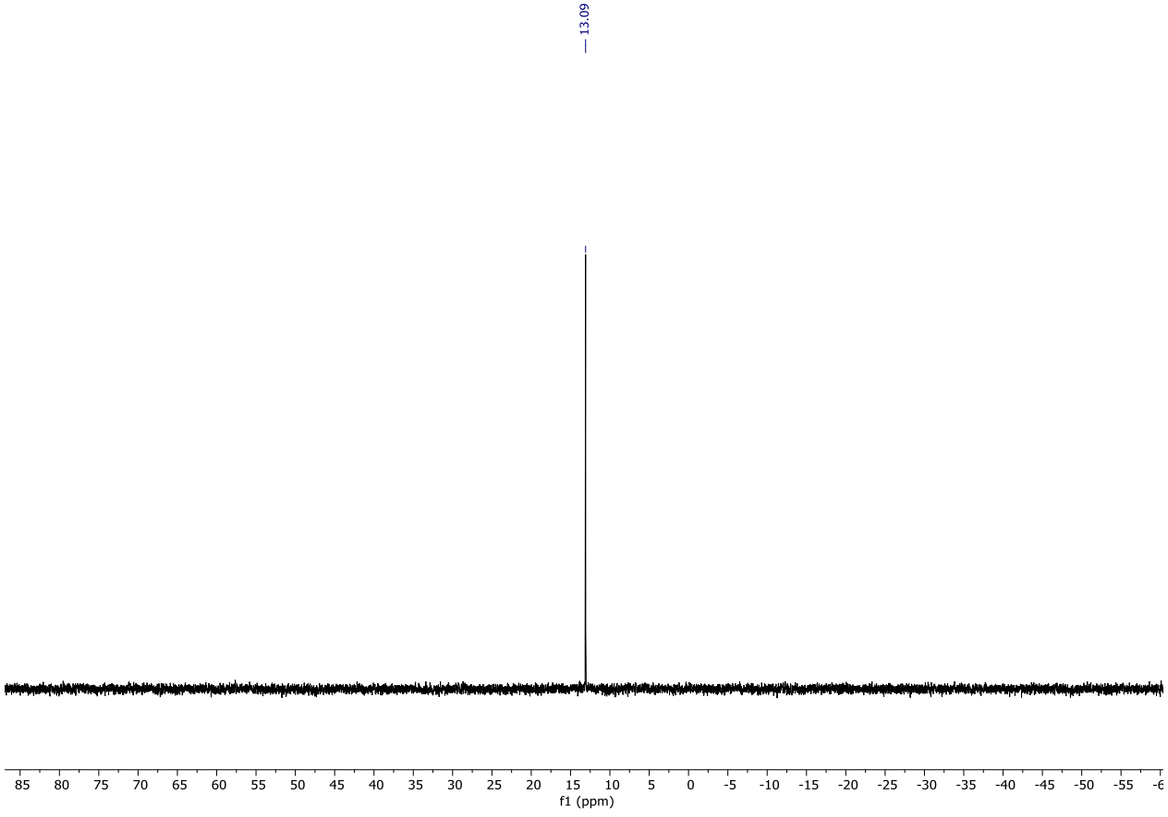

Figure S42. ^{1}H NMR (300 MHz, $CDCl_3$) spectrum of diphenyl (hydroxy(6-bromo-4-oxo-4*H*-chromen-3-yl)methyl)phosphonate (**4hd**).

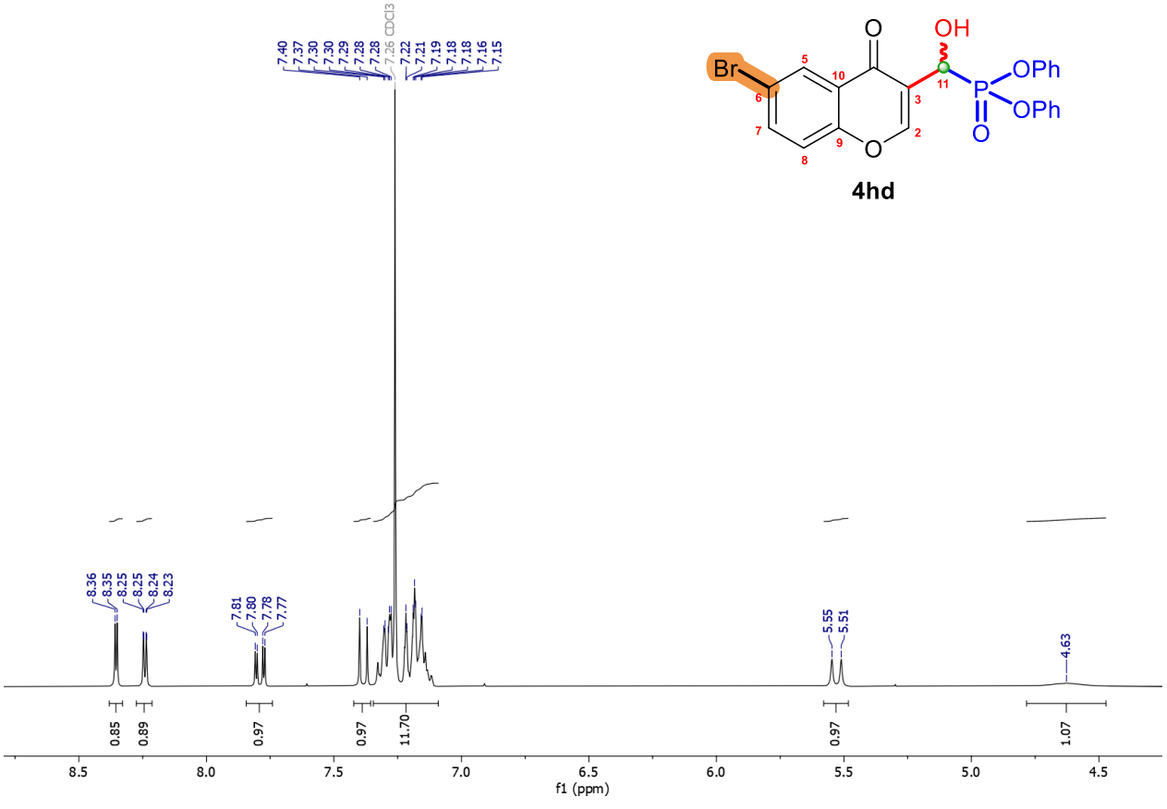

Synthesis | DOI 10.1055/a-2815-1115 |

Figure S43. $^{13}C\{^{1}H\}$ NMR (100 MHz, $CDCl_3$) spectrum of **4hd**.

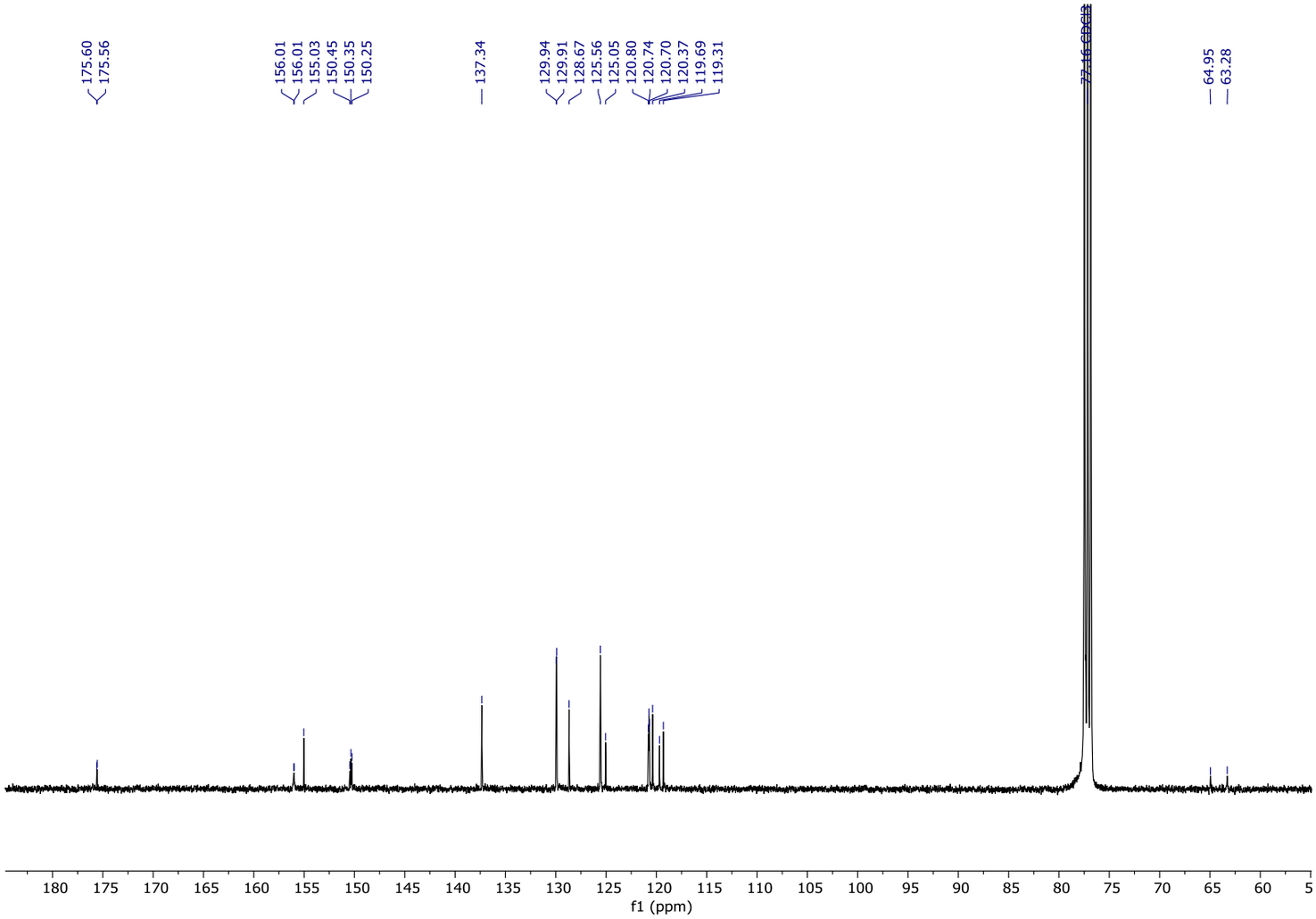

Figure S44. $^{31}P\{^{1}H\}$ NMR (121 MHz, $CDCl_3$) spectrum of **4hd**.

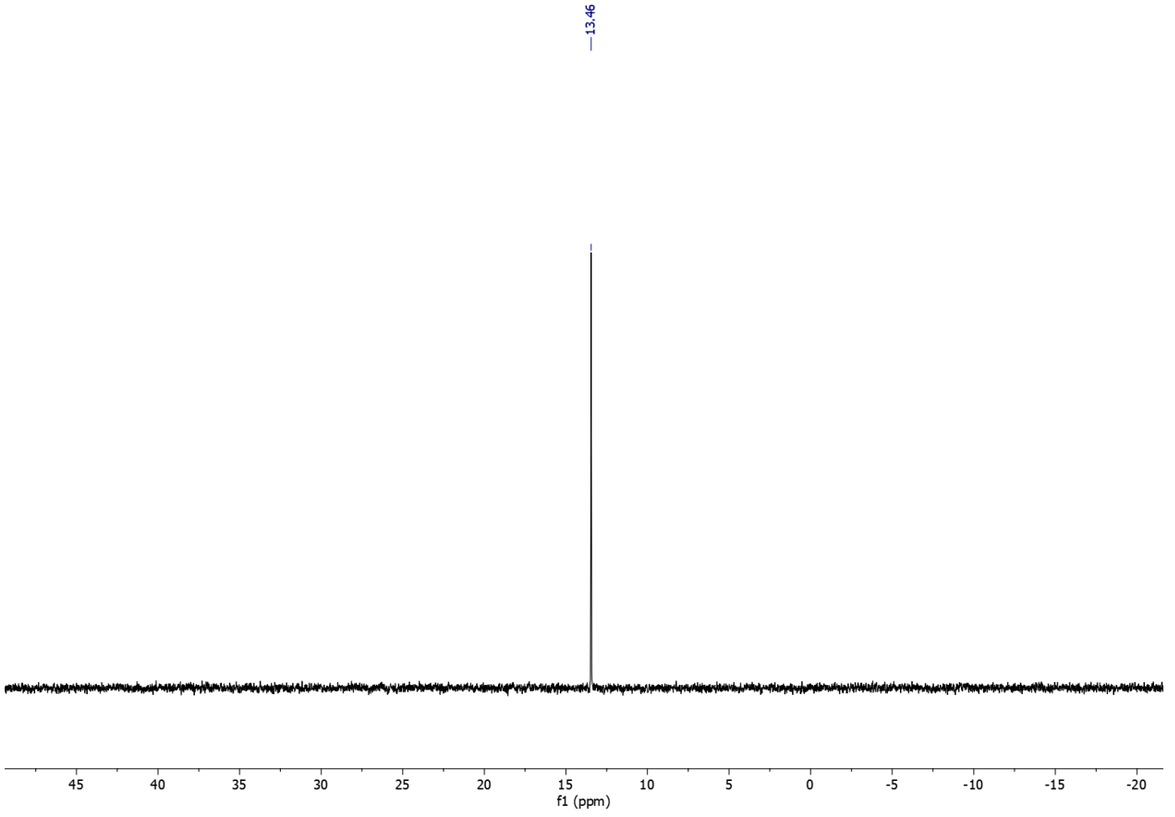

Figure S45. ^{1}H NMR (300 MHz, $CDCl_3$) spectrum of diphenyl (hydroxy(6-chloro-4-oxo-4*H*-chromen-3-yl)methyl)phosphonate (**4id**).

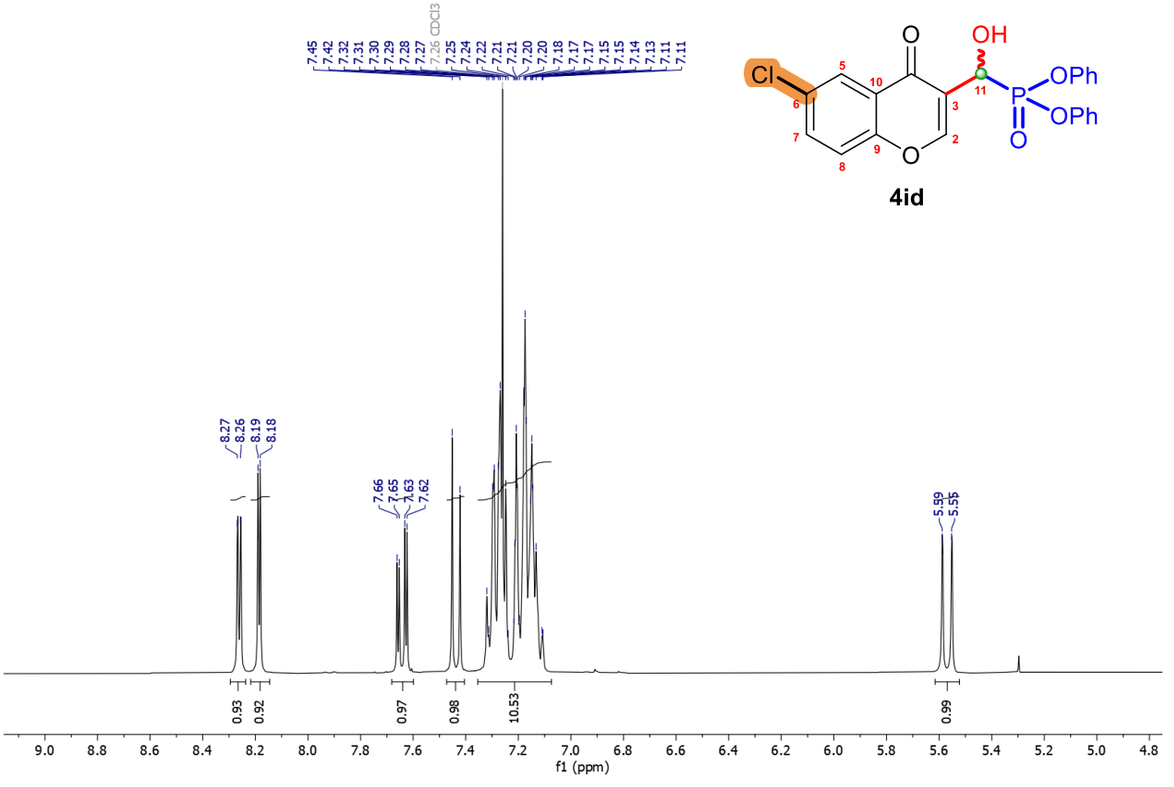

Synthesis | DOI 10.1055/a-2815-1115 |

Figure S46. $^{13}C\{^{1}H\}$ NMR (75 MHz, $CDCl_3$) spectrum of **4id**.

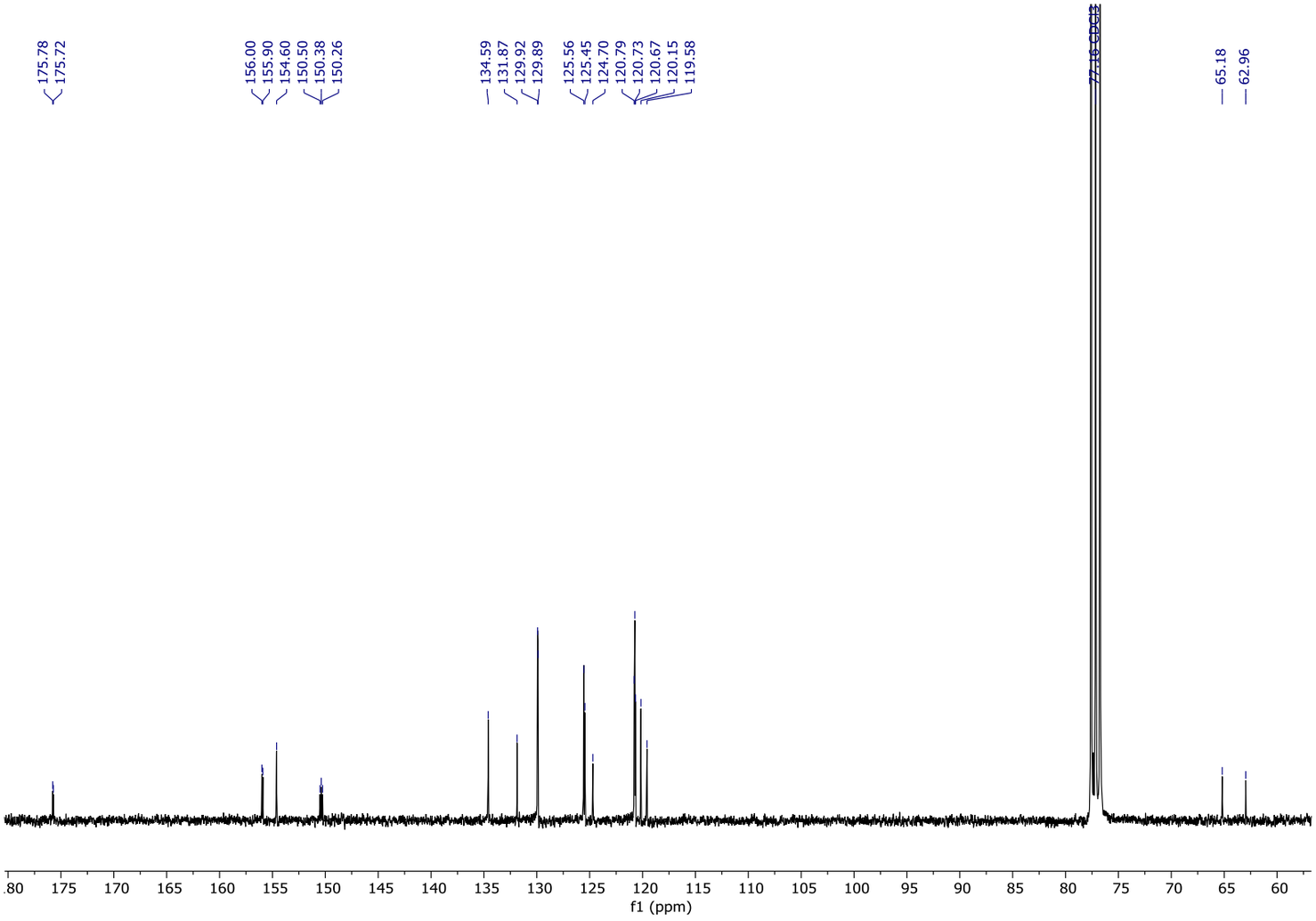

Figure S47. $^{31}P\{^{1}H\}$ NMR (121 MHz, $CDCl_3$) spectrum of **4id**.

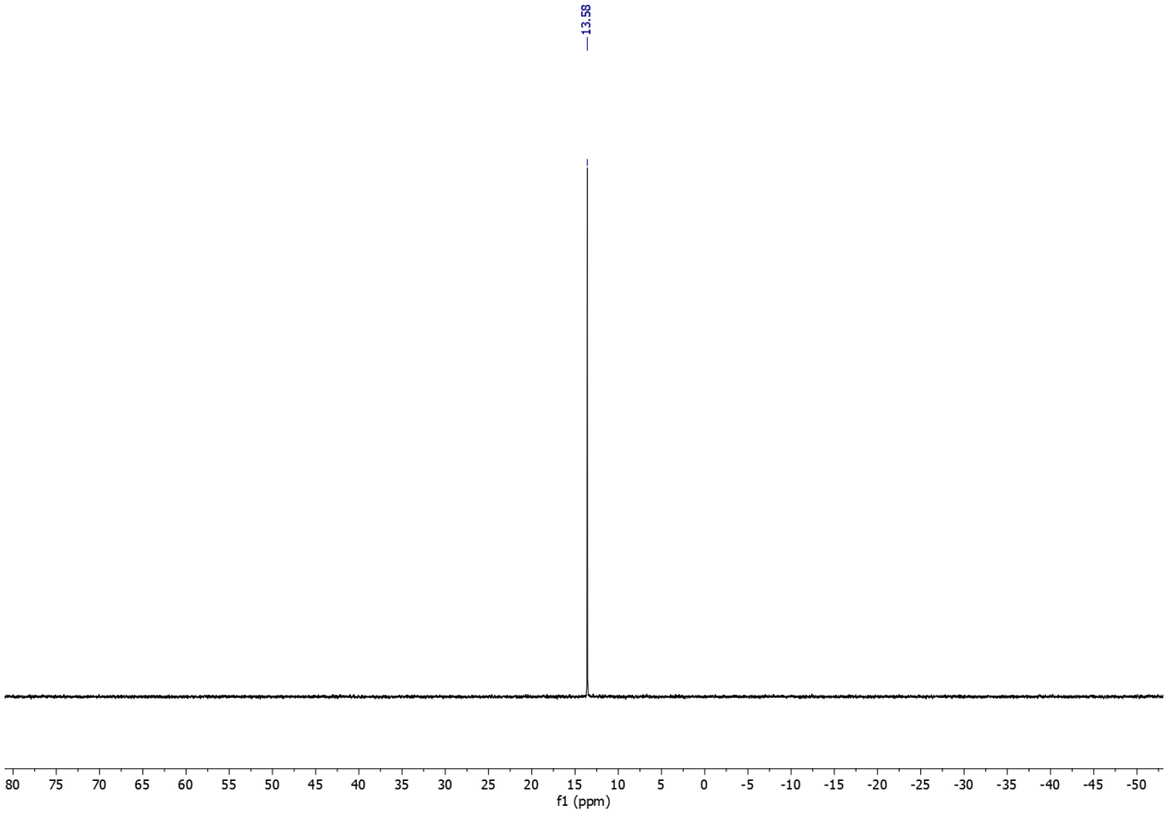

Figure S48. ^{1}H NMR (300 MHz, $CDCl_3$) spectrum of diphenyl (hydroxy(6,8-dichloro-4-oxo-4*H*-chromen-3-yl)methyl)phosphonate (**4jd**).

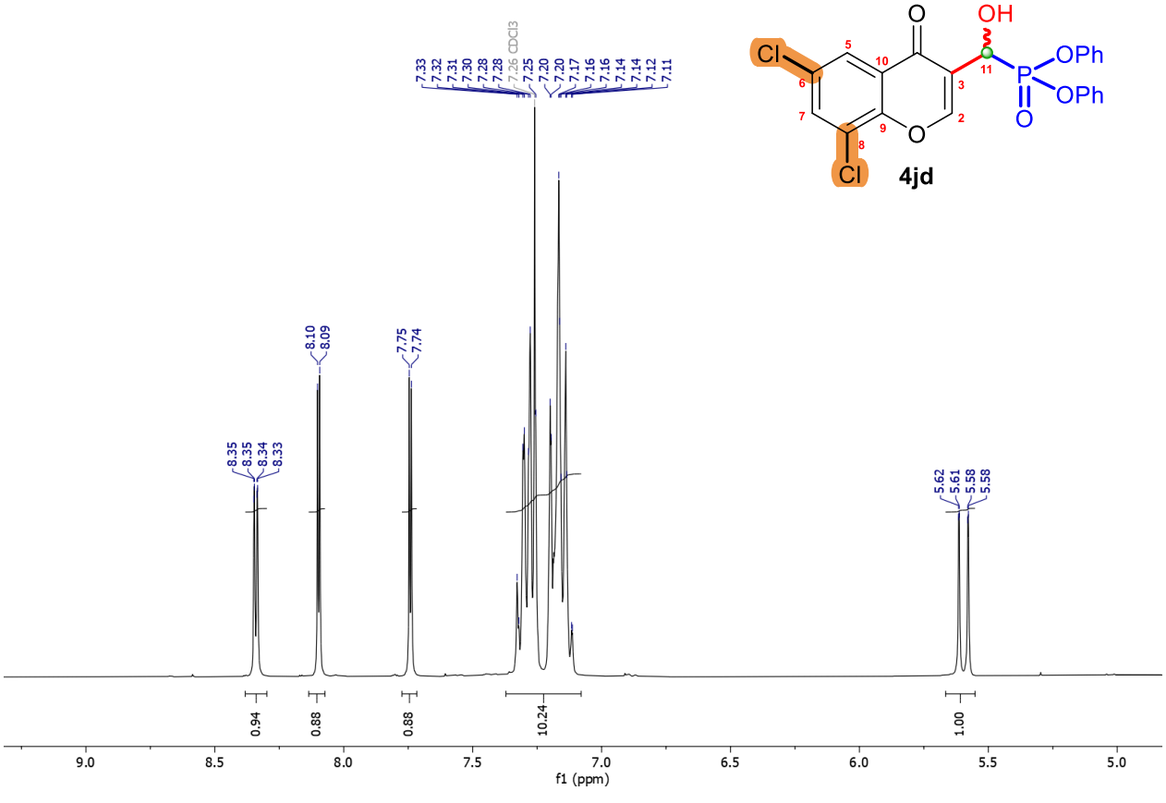

Figure S49. $^{13}C\{^{1}H\}$ NMR (75 MHz, $CDCl_3$) spectrum of **4jd**.

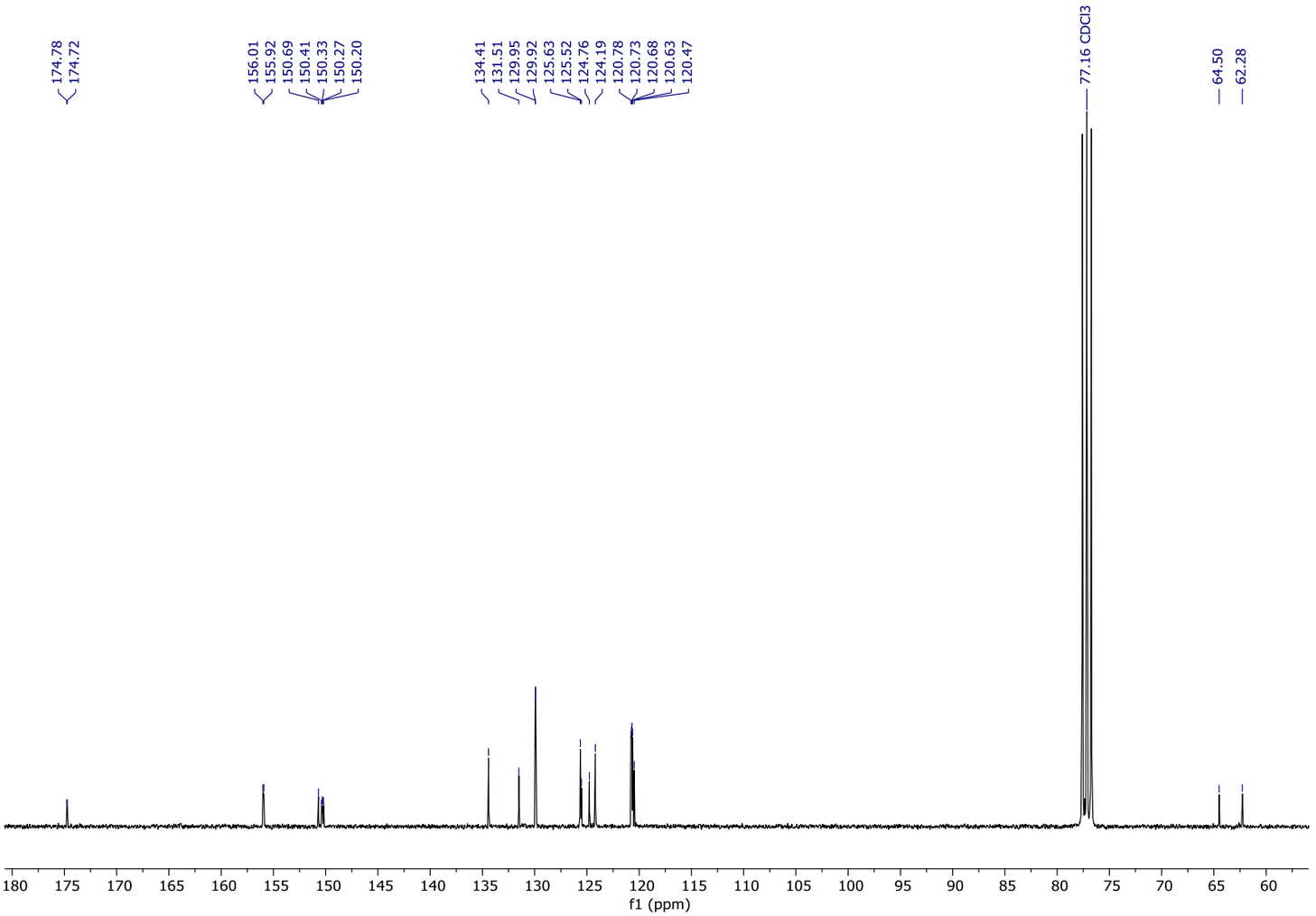

Figure S50. $^{31}P\{^{1}H\}$ NMR (121 MHz, $CDCl_3$) spectrum of **4jd**.

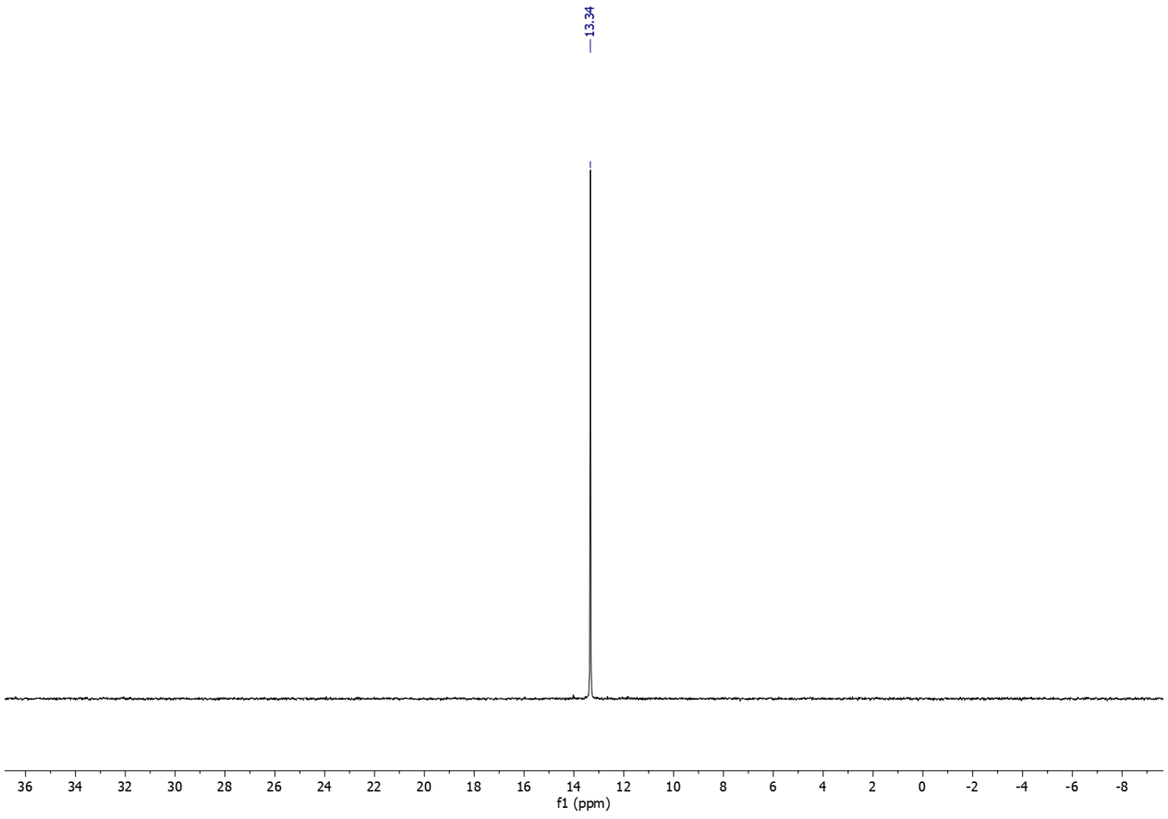

4. Naproxen dibenzyl phosphonates (least polar) (*S*,*S*)-6aa and (most polar) (*R*,*S*)-6aa

Figure S51. ^{1}H NMR (300 MHz, $CDCl_3$) spectrum of (*S*,*S*)-**6aa**.

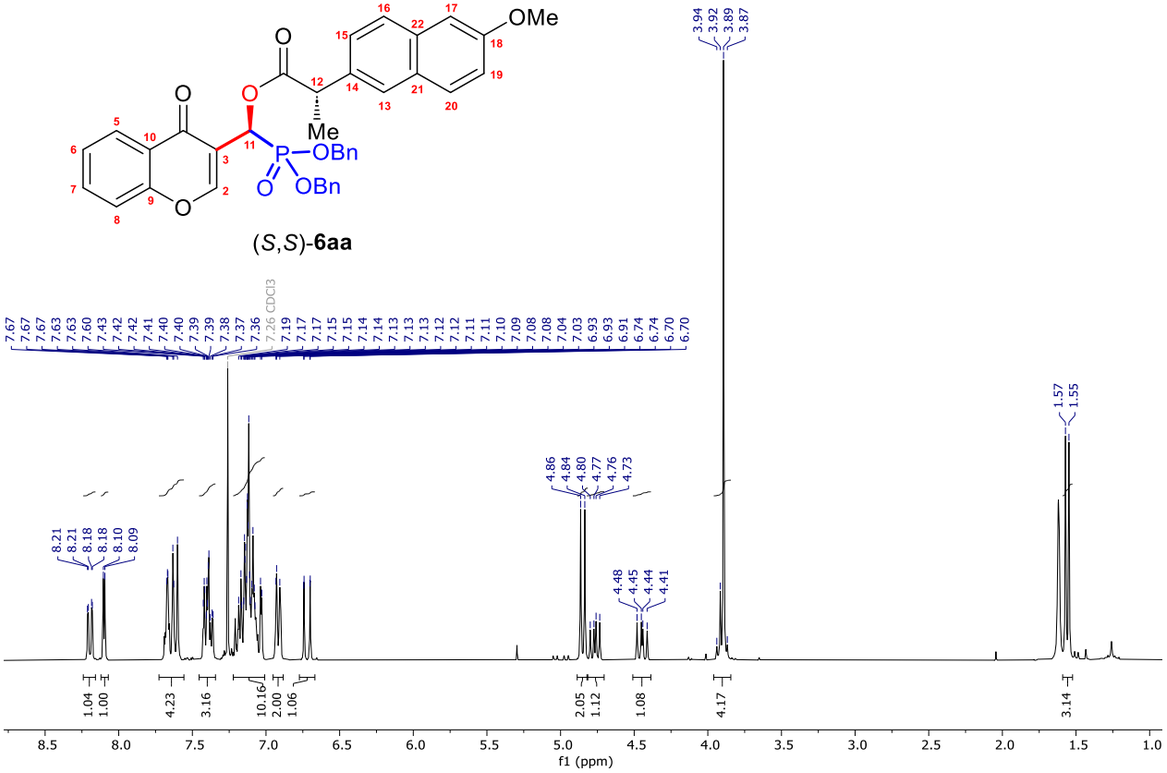

Synthesis | DOI 10.1055/a-2815-1115 |

Figure S52. $^{13}C\{^{1}H\}$ NMR (75 MHz, $CDCl_3$) spectrum of (*S,S*)-**6aa**.

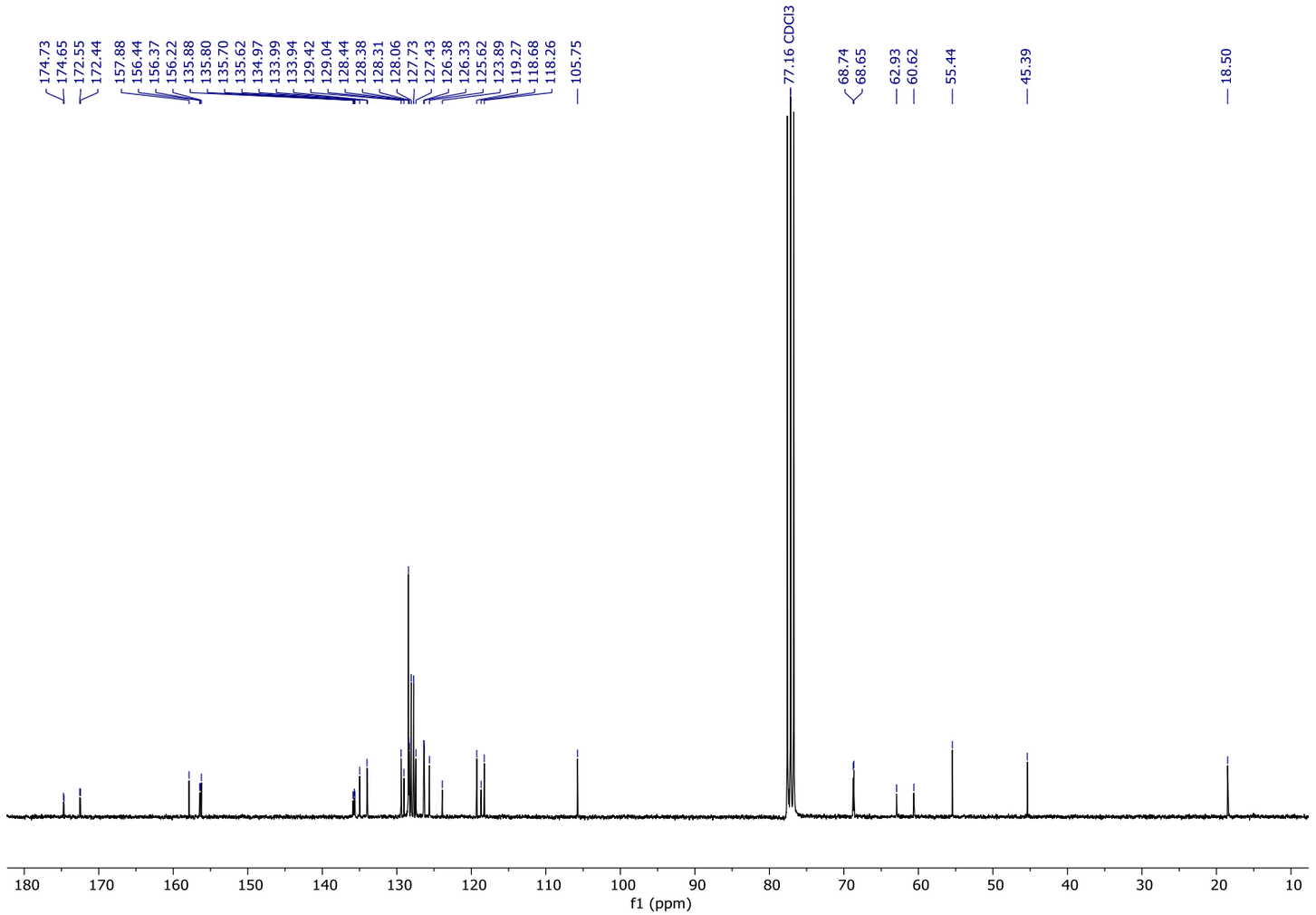

Figure S53. $^{31}P\{^{1}H\}$ NMR (121 MHz, $CDCl_3$) spectrum of (*S,S*)-**6aa**.

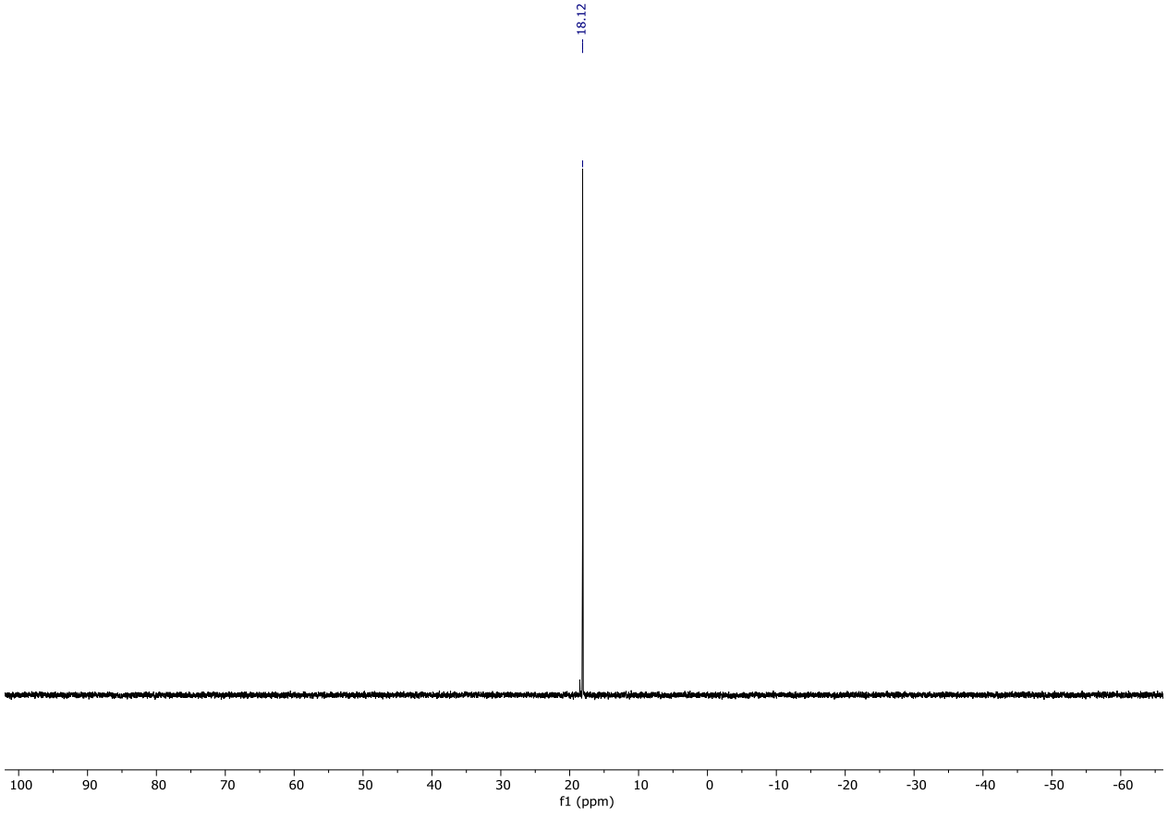

Figure S54. ^{1}H NMR (300 MHz, $CDCl_3$) spectrum of (*R,S*)-**6aa**.

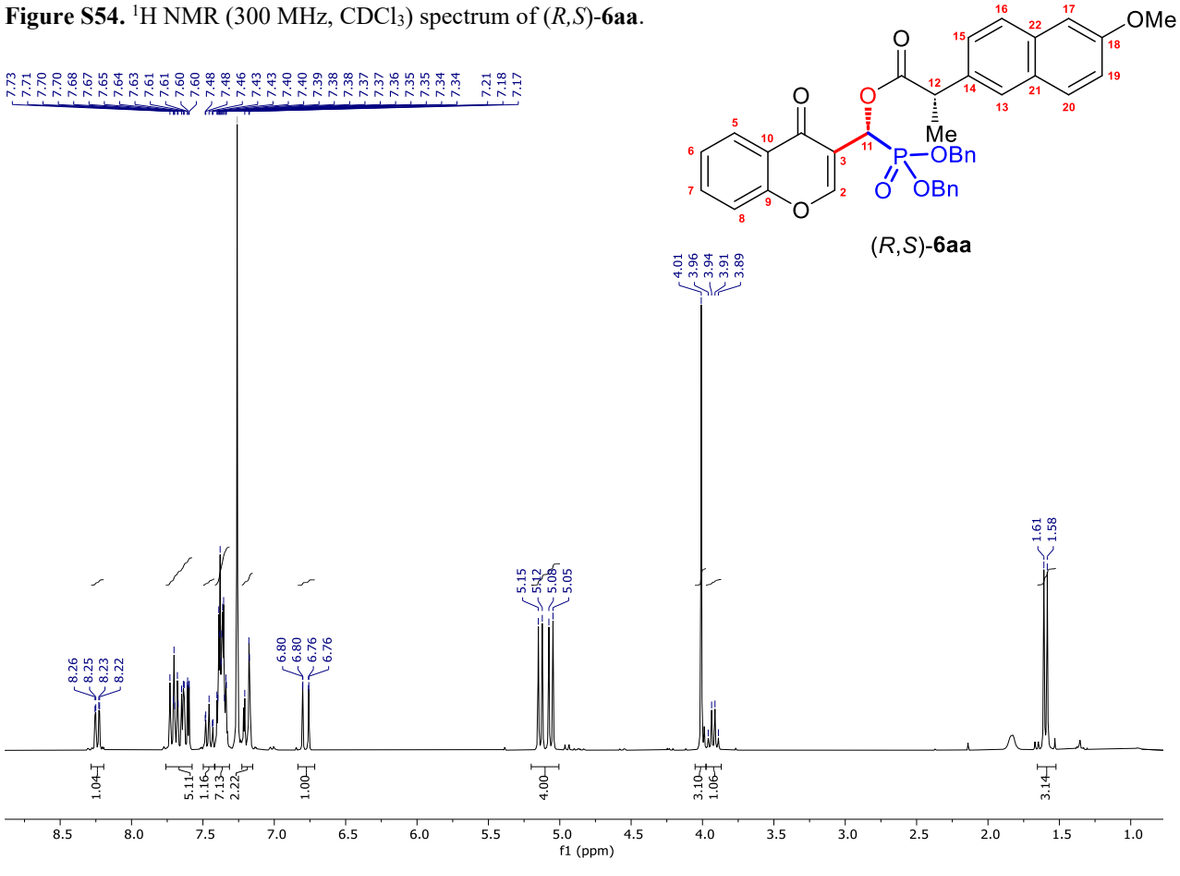

Synthesis | DOI 10.1055/a-2815-1115 |

Figure S55. $^{13}C\{^{1}H\}$ NMR (75 MHz, $CDCl_3$) spectrum of (*R,S*)-**6aa**.

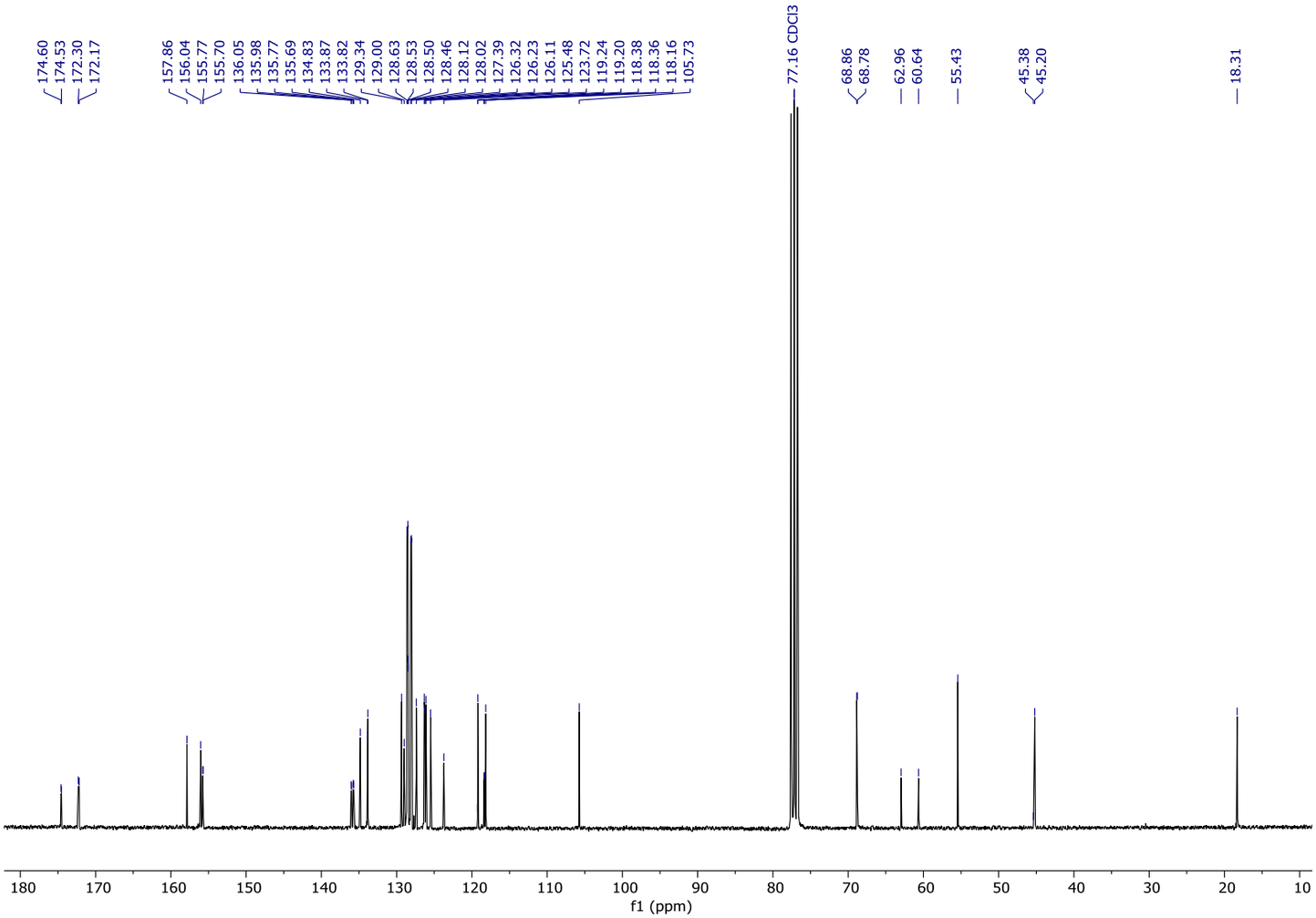

Figure S56. $^{31}P\{^{1}H\}$ NMR (121 MHz, $CDCl_3$) spectrum of (*R,S*)-**6aa**.

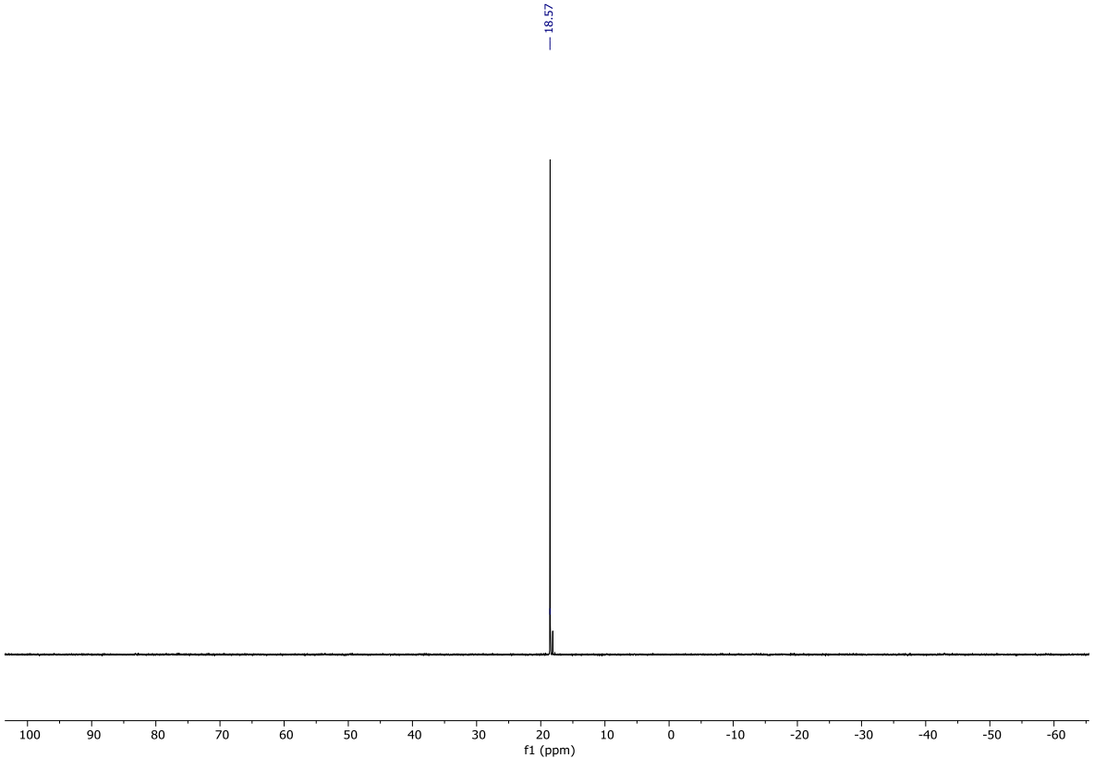

5. Calculation of the diastereomeric ratio (dr) in the synthesis of naproxen dibenzyl phosphonates mixture (*S,S*)-6aa and (*R,S*)-6aa

Figure S57. ^{1}H NMR (300 MHz, $CDCl_3$) spectrum of the mixture of (*S,S*)-**6aa** and (*R,S*)-**6aa**.

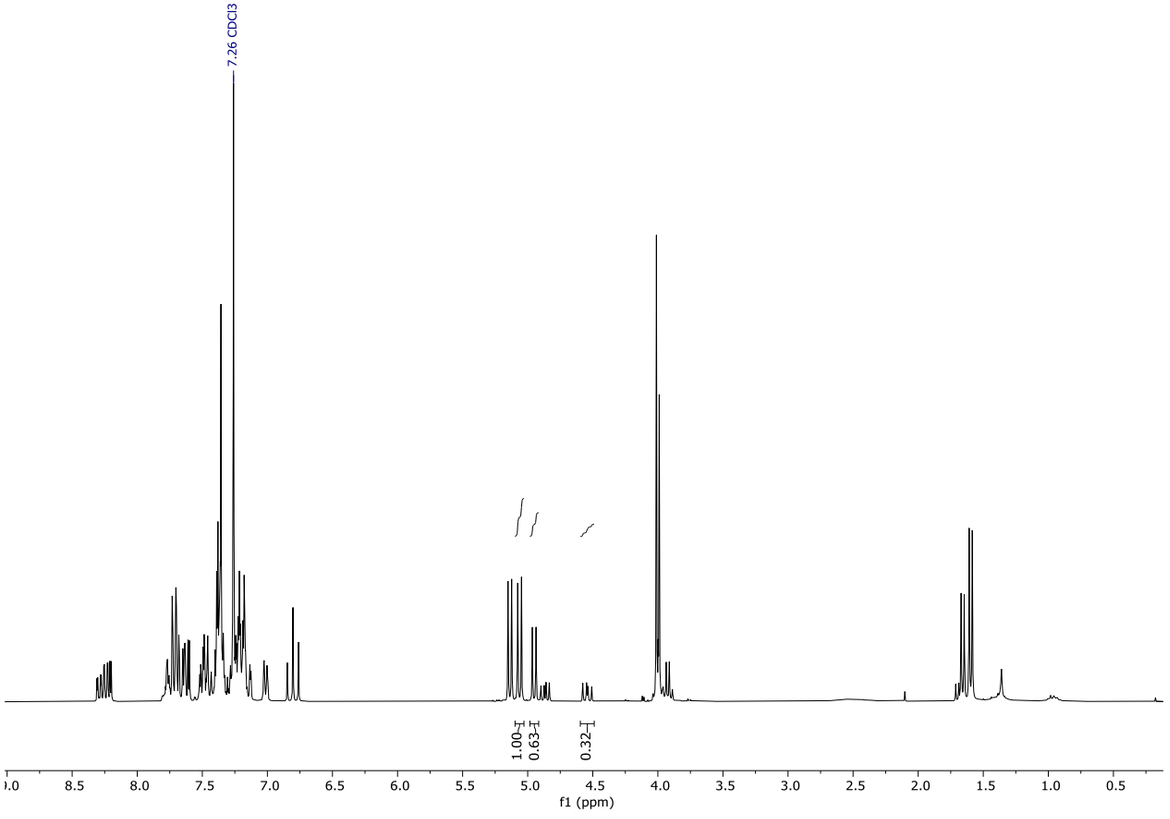

6. HPLC chromatograms

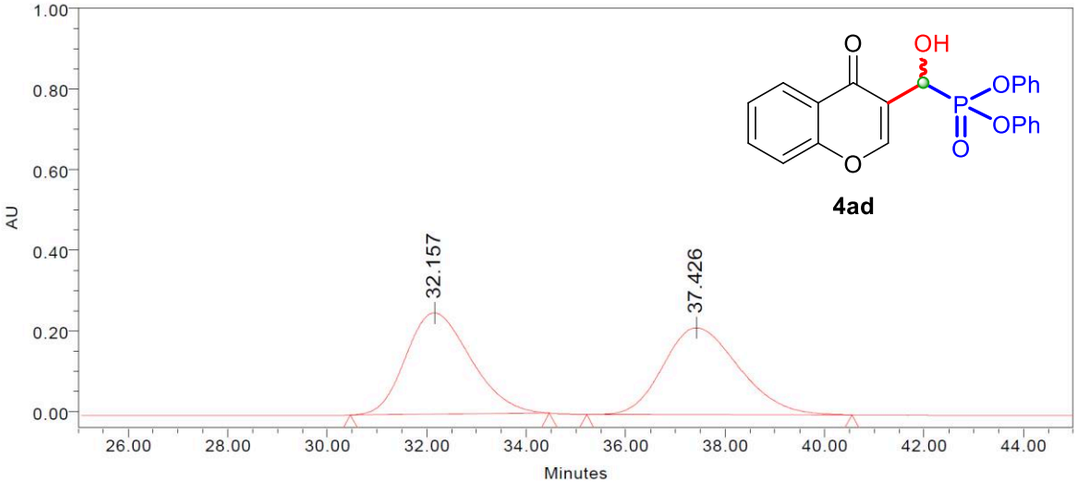

Processed Channel: PDA 241.3 nm

	Processed Channel	Retention Time (min)	Area	% Area	Height
1	PDA 241.3 nm	32.157	22843920	49.99	251529
2	PDA 241.3 nm	37.426	22852153	50.01	215675

Figure S58. Racemic mixture of diphenyl (hydroxy(4-oxo-4*H*-chromen-3-yl)methyl)phosphonate (**4ad**) on Daicel Chiralpak column IC (*n*-heptane/*i*PrOH = 80:20, flow rate 1 mL min^{-1}).

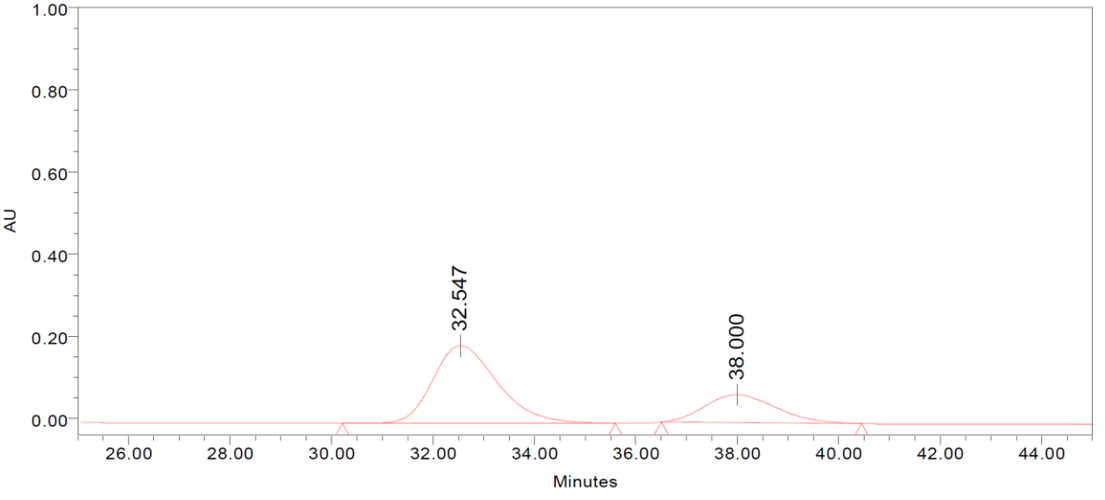

Processed Channel: PDA 241.3 nm

	Processed Channel	Retention Time (min)	Area	% Area	Height
1	PDA 241.3 nm	32.547	16648726	71.67	188361
2	PDA 241.3 nm	38.000	6581459	28.33	67746

Figure S59. Enantioselective mixture (43% ee) of diphenyl (hydroxy(4-oxo-4*H*-chromen-3-yl)methyl)phosphonate (**4ad**).

Synthesis | DOI 10.1055/a-2815-1115 |

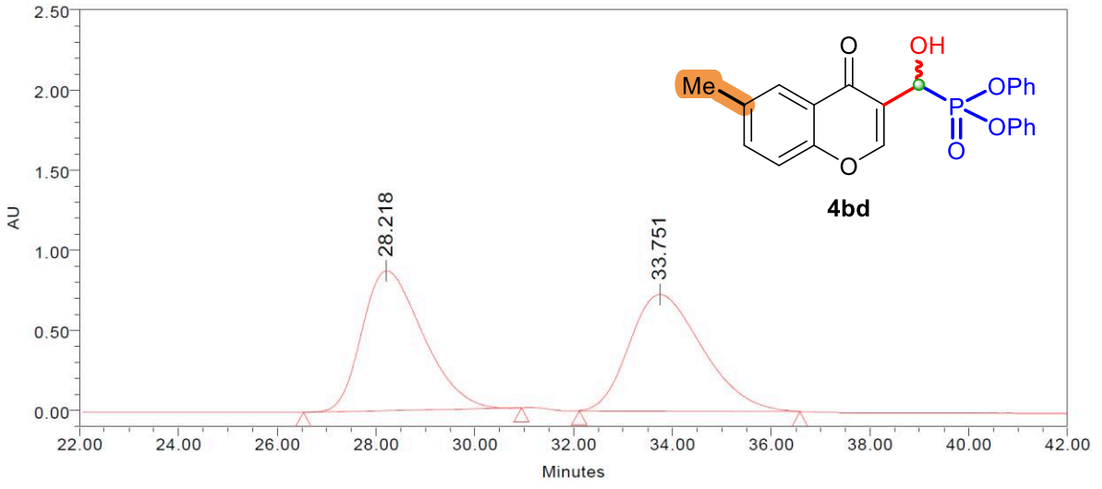

Processed Channel: PDA 231.5 nm

	Processed Channel	Retention Time (min)	Area	% Area	Height
1	PDA 231.5 nm	28.218	74796544	49.99	873071
2	PDA 231.5 nm	33.751	74826928	50.01	726956

Figure S60. Racemic mixture of diphenyl (hydroxy(6-methyl-4-oxo-4*H*-chromen-3-yl)methyl)phosphonate (**4bd**) on Daicel Chiralpak column IC (*n*-heptane/*i*PrOH = 70:30, flow rate 1 mL min^{-1}).

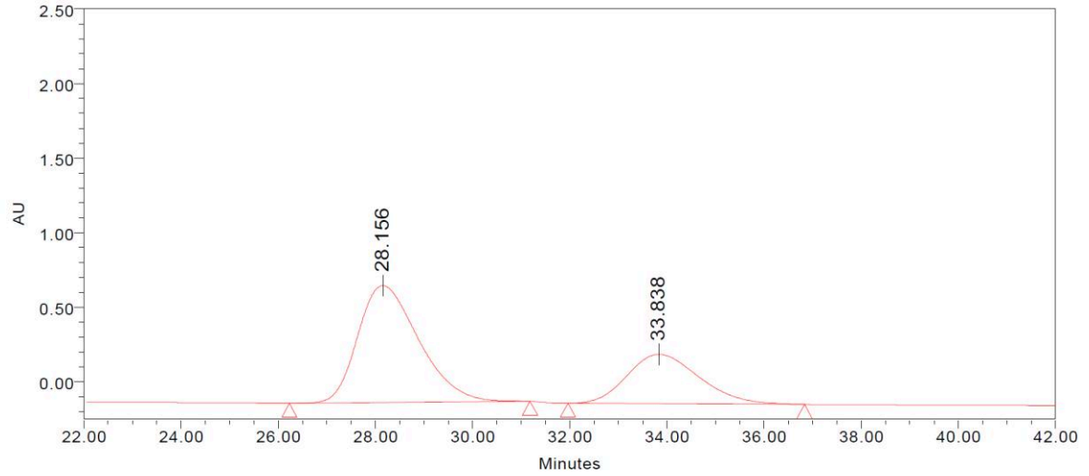

Processed Channel: PDA 231.5 nm

	Processed Channel	Retention Time (min)	Area	% Area	Height
1	PDA 231.5 nm	28.156	68207810	66.56	784120
2	PDA 231.5 nm	33.838	34265455	33.44	331371

Figure S61. Enantioselective mixture (33% ee) of diphenyl (hydroxy(6-methyl-4-oxo-4*H*-chromen-3-yl)methyl)phosphonate (**4bd**).

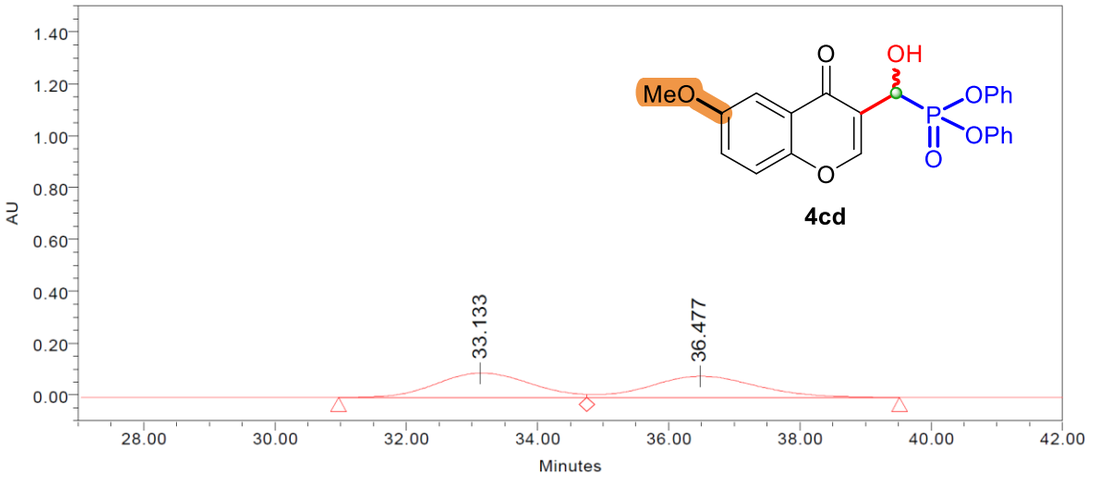

Processed Channel: PDA 238.2 nm

	Processed Channel	Retention Time (min)	Area	% Area	Height
1	PDA 238.2 nm	33.133	9291483	50.29	93509
2	PDA 238.2 nm	36.477	9182851	49.71	81238

Figure S62. Racemic mixture of diphenyl (hydroxy(6-methoxy-4-oxo-4*H*-chromen-3-yl)methyl)phosphonate (**4cd**) on Daicel Chiralpak column IC (*n*-heptane/*i*PrOH = 70:30, flow rate 1 mL min^{-1}).

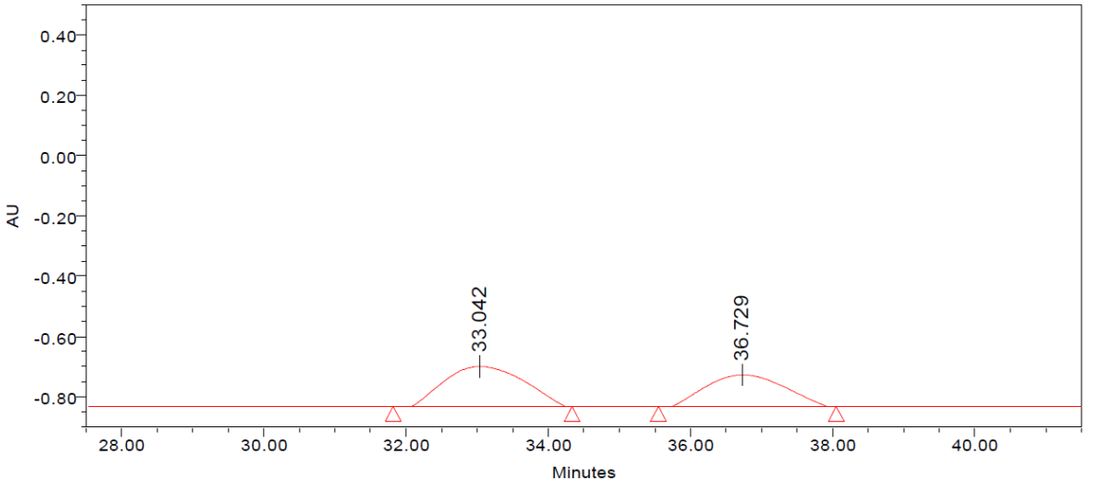

Processed Channel: PDA 238.5 nm

	Processed Channel	Retention Time (min)	Area	% Area	Height
1	PDA 238.5 nm	33.042	10470570	56.18	133695
2	PDA 238.5 nm	36.729	8167875	43.82	105769

Figure S63. Enantioselective mixture (12% ee) of diphenyl (hydroxy(6-methoxy-4-oxo-4*H*-chromen-3-yl)methyl)phosphonate (**4cd**).

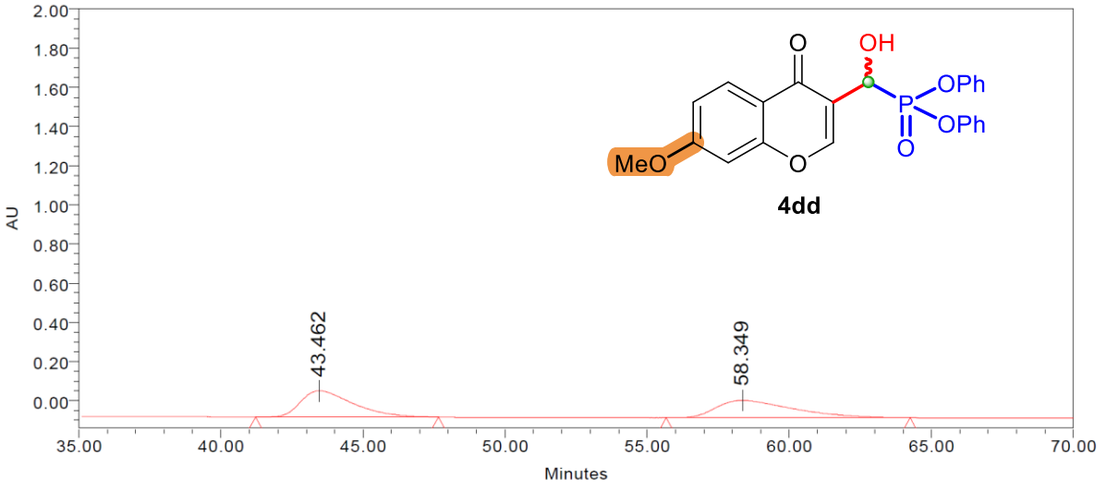

Processed Channel: PDA 210.7 nm

	Processed Channel	Retention Time (min)	Area	% Area	Height
1	PDA 210.7 nm	43.462	17003823	50.63	133592
2	PDA 210.7 nm	58.349	16579463	49.37	88281

Figure S64. Racemic mixture of diphenyl (hydroxy(7-methoxy-4-oxo-4*H*-chromen-3-yl)methyl)phosphonate (**4dd**) on Daicel Chiralpak column ID (*n*-heptane/*i*PrOH = 60:40, flow rate 1 mL min^{-1}).

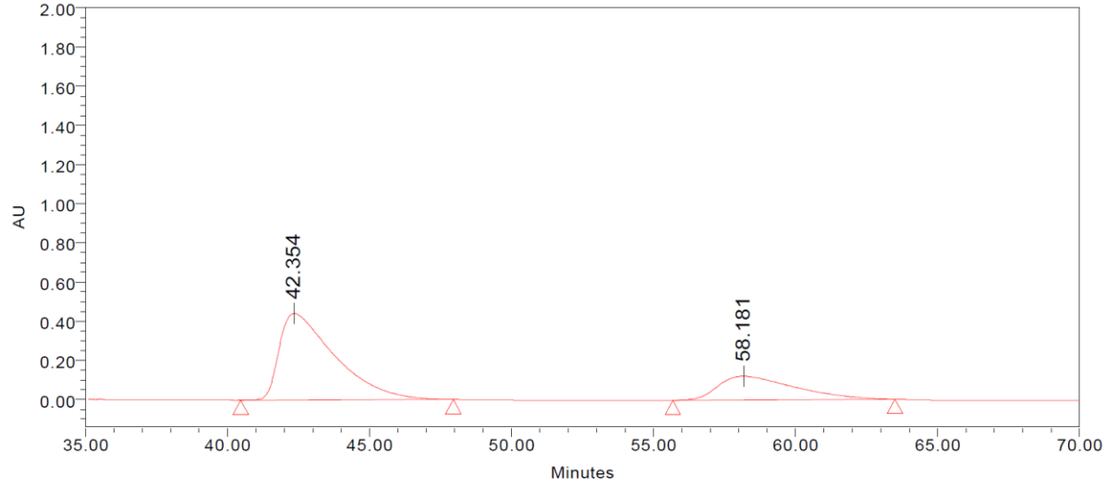

Processed Channel: PDA 210.7 nm

	Processed Channel	Retention Time (min)	Area	% Area	Height
1	PDA 210.7 nm	42.354	59952345	72.62	441685
2	PDA 210.7 nm	58.181	22603151	27.38	120402

Figure S65. Enantioselective mixture (45% ee) of diphenyl (hydroxy(7-methoxy-4-oxo-4*H*-chromen-3-yl)methyl)phosphonate (**4dd**).

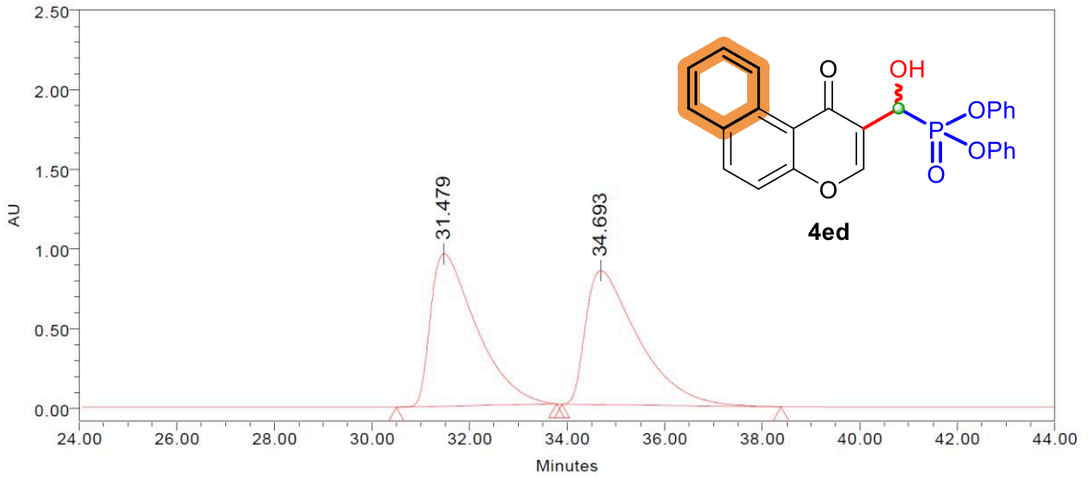

Processed Channel: PDA 260.9 nm

	Processed Channel	Retention Time (min)	Area	% Area	Height
1	PDA 260.9 nm	31.479	62820327	49.94	957944
2	PDA 260.9 nm	34.693	62966630	50.06	841114

Figure S66. Racemic mixture of diphenyl (hydroxy(4-oxo-4*H*-benzo[*f*]chromen-3-yl)methyl)phosphonate (**4ed**) on Daicel Chiralpak column IA (*n*-heptane/*i*PrOH = 60:40, flow rate 1 mL min^{-1}).

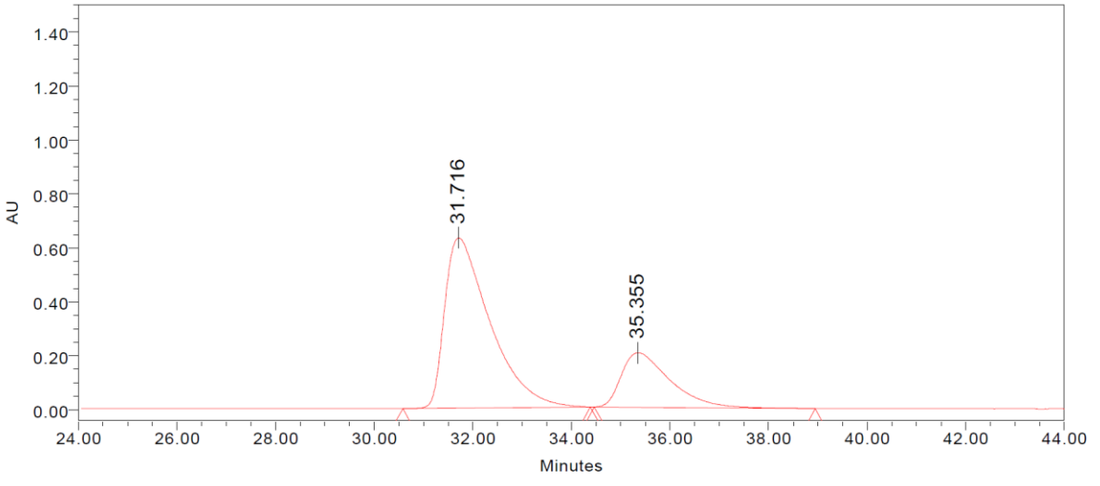

Processed Channel: PDA 260.9 nm

	Processed Channel	Retention Time (min)	Area	% Area	Height
1	PDA 260.9 nm	31.716	40281217	74.51	631182
2	PDA 260.9 nm	35.355	13778568	25.49	202303

Figure S67. Enantioselective mixture (49% ee) of diphenyl (hydroxy(4-oxo-4*H*-benzo[*f*]chromen-3-yl)methyl)phosphonate (**4ed**).

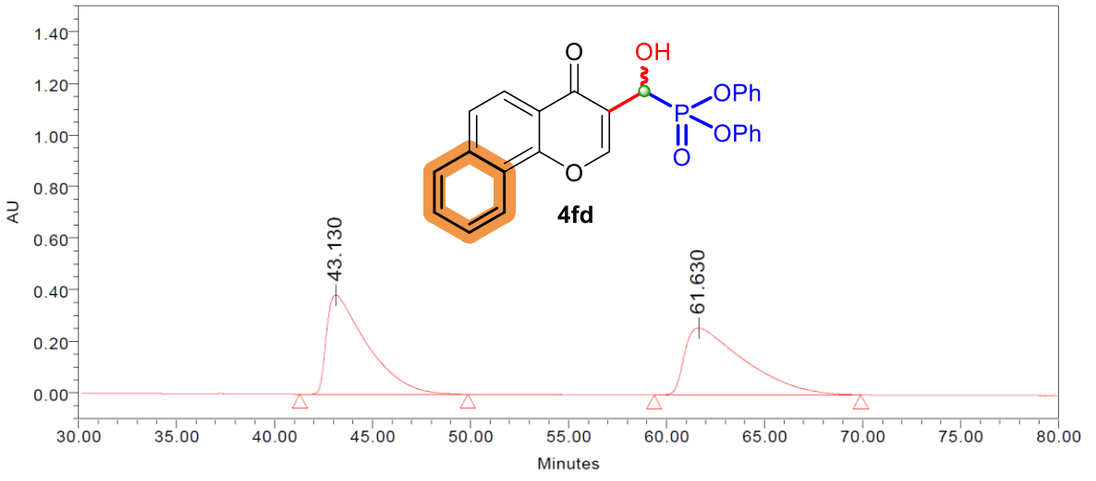

Processed Channel: PDA 231.8 nm

	Processed Channel	Retention Time (min)	Area	% Area	Height
1	PDA 231.8 nm	43.130	55123937	50.06	384196
2	PDA 231.8 nm	61.630	55000020	49.94	259072

Figure S68. Racemic mixture of diphenyl (hydroxy(4-oxo-4*H*-benzo[*h*]chromen-3-yl)methyl)phosphonate (**4fd**) on Daicel Chiralpak column ID (*n*-heptane/*i*PrOH = 70:30, flow rate 1 mL min^{-1}).

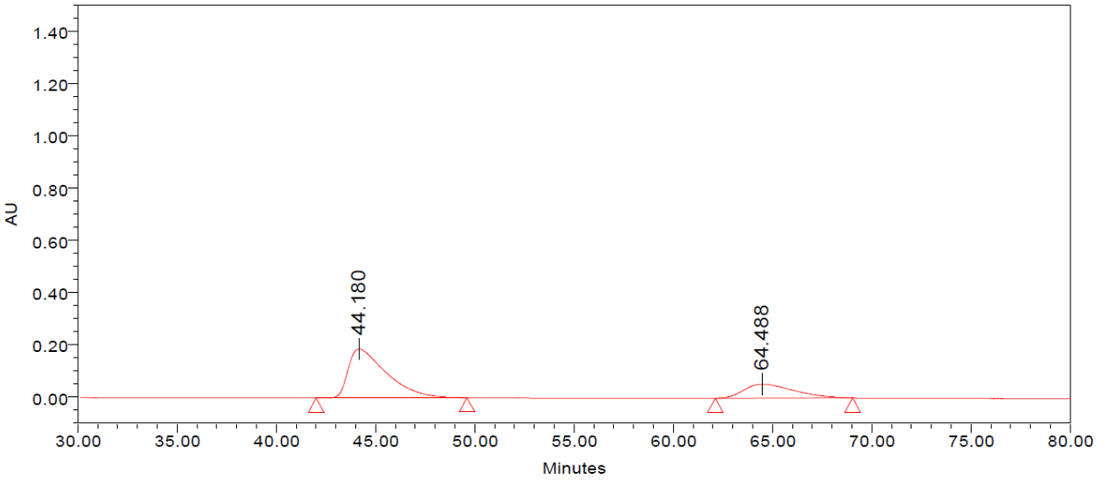

Processed Channel: PDA 231.8 nm

	Processed Channel	Retention Time (min)	Area	% Area	Height
1	PDA 231.8 nm	44.180	24908626	72.83	187158
2	PDA 231.8 nm	64.488	9294727	27.17	53519

Figure S69. Enantioselective mixture (46% ee) of diphenyl (hydroxy(4-oxo-4*H*-benzo[*h*]chromen-3-yl)methyl)phosphonate (**4fd**).

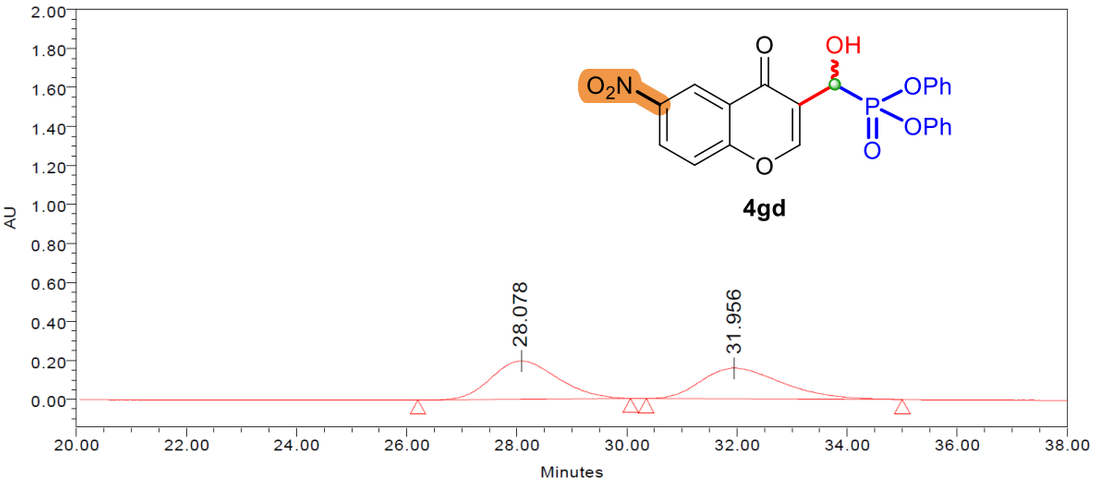

Processed Channel: PDA 210.4 nm

	Processed Channel	Retention Time (min)	Area	% Area	Height
1	PDA 210.4 nm	28.078	16498117	50.42	196389
2	PDA 210.4 nm	31.956	16223827	49.58	158058

Figure S70. Racemic mixture of diphenyl (hydroxy(6-nitro-4-oxo-4*H*-chromen-3-yl)methyl)phosphonate (**4gd**) on Daicel Chiralpak column IC (*n*-heptane/*i*PrOH = 70:30, flow rate 1 mL min^{-1}).

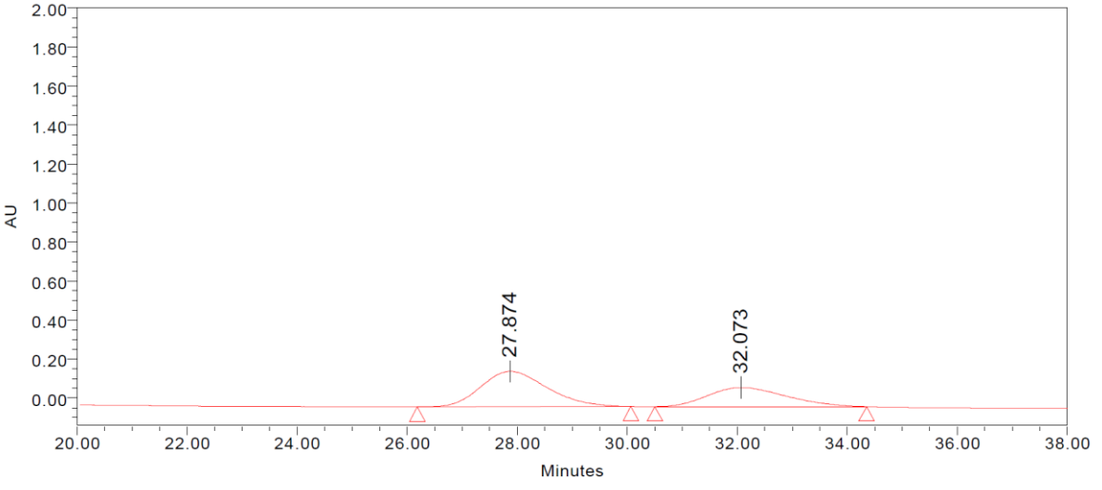

Processed Channel: PDA 210.4 nm

	Processed Channel	Retention Time (min)	Area	% Area	Height
1	PDA 210.4 nm	27.874	15259913	60.97	181348
2	PDA 210.4 nm	32.073	9768441	39.03	98195

Figure S71. Enantioselective mixture (22% ee) of diphenyl (hydroxy(6-nitro-4-oxo-4*H*-chromen-3-yl)methyl)phosphonate (**4gd**).

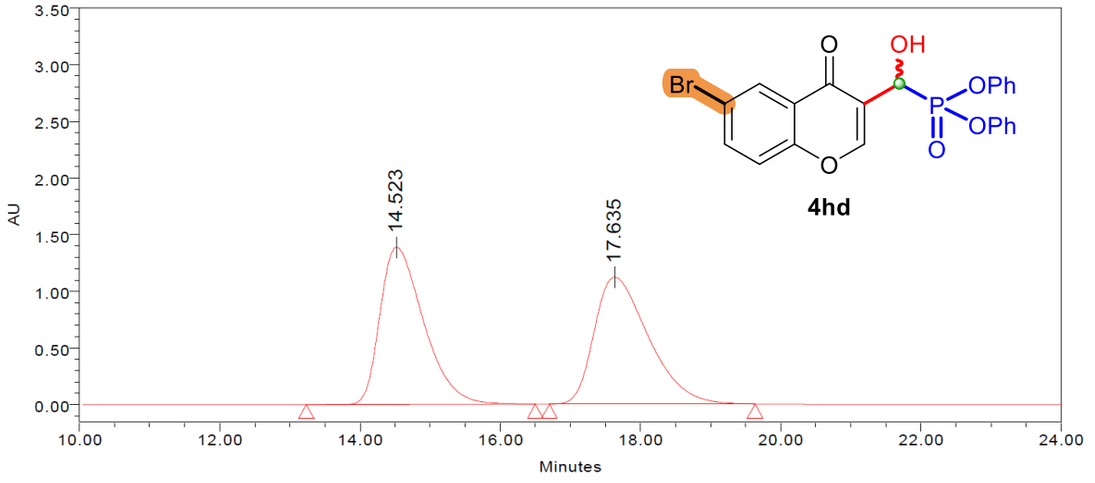

Processed Channel: PDA 316.5 nm

	Processed Channel	Retention Time (min)	Area	% Area	Height
1	PDA 316.5 nm	14.523	60077718	49.92	1387412
2	PDA 316.5 nm	17.635	60259065	50.08	1121257

Figure S72. Racemic mixture of diphenyl (hydroxy(6-bromo-4-oxo-4*H*-chromen-3-yl)methyl)phosphonate (**4hd**) on Daicel Chiralpak column IC (*n*-heptane/*i*PrOH = 70:30, flow rate 1 mL min^{-1}).

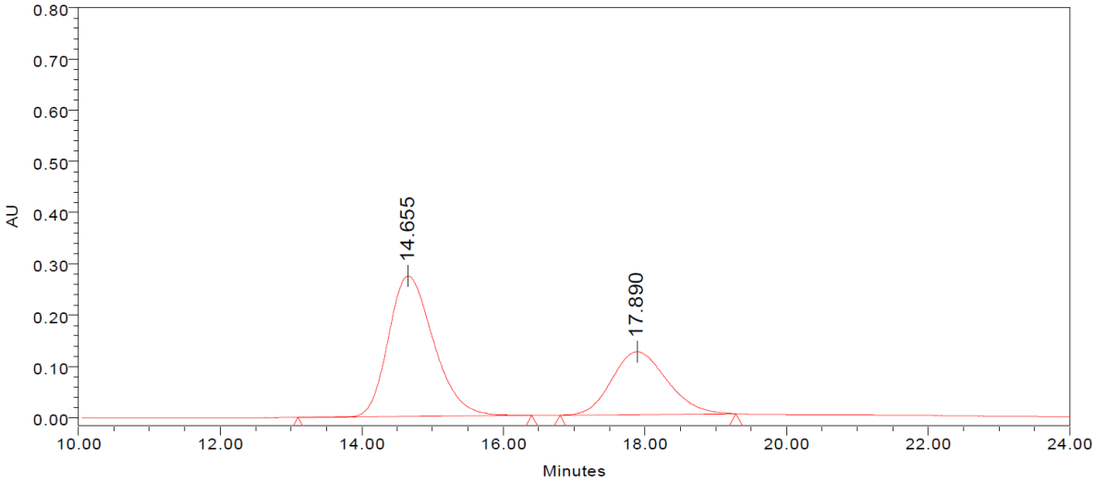

Processed Channel: PDA 316.5 nm

	Processed Channel	Retention Time (min)	Area	% Area	Height
1	PDA 316.5 nm	14.655	12165369	64.79	274121
2	PDA 316.5 nm	17.890	6610831	35.21	122715

Figure S73. Enantioselective mixture (30% ee) of diphenyl (hydroxy(6-bromo-4-oxo-4*H*-chromen-3-yl)methyl)phosphonate (**4hd**).

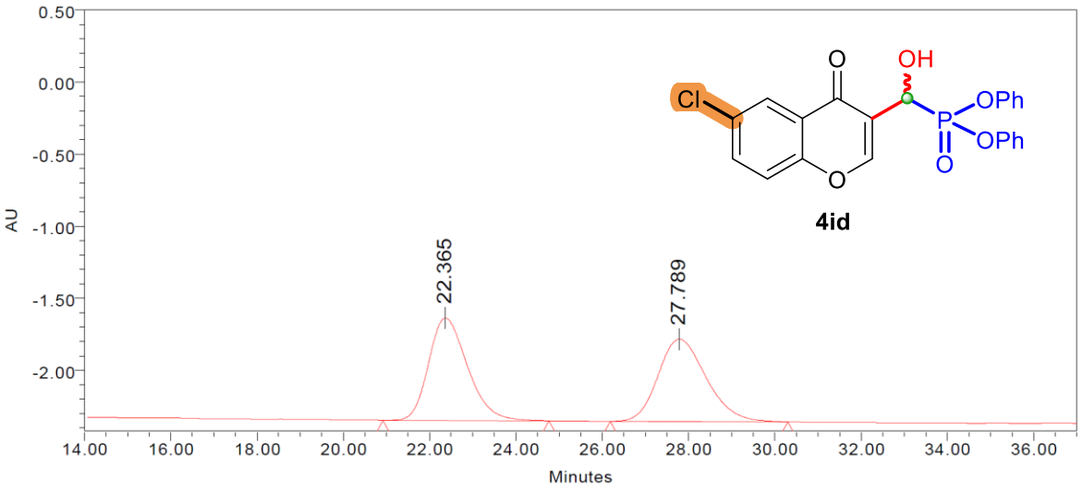

Processed Channel: PDA 233.8 nm

	Processed Channel	Retention Time (min)	Area	% Area	Height
1	PDA 233.8 nm	22.365	44426338	50.00	710575
2	PDA 233.8 nm	27.789	44433368	50.00	572152

Figure S74. Racemic mixture of diphenyl (hydroxy(6-chloro-4-oxo-4*H*-chromen-3-yl)methyl)phosphonate (**4id**) on Daicel Chiralpak column IC (*n*-heptane/*i*PrOH = 80:20, flow rate 1 mL min^{-1}).

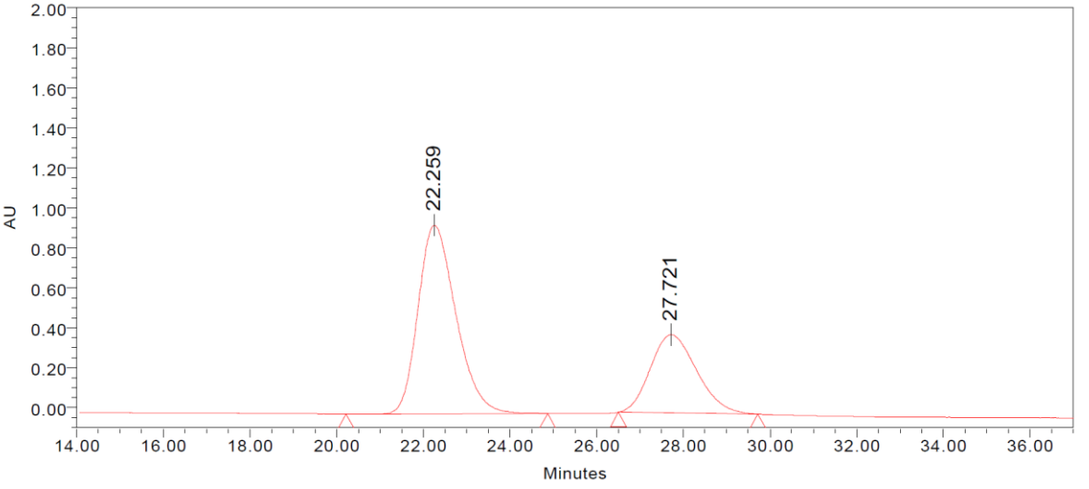

Processed Channel: PDA 233.8 nm

	Processed Channel	Retention Time (min)	Area	% Area	Height
1	PDA 233.8 nm	22.259	57170074	66.31	943374
2	PDA 233.8 nm	27.721	29047951	33.69	391713

Figure S75. Enantioselective mixture (33% ee) of diphenyl (hydroxy(6-chloro-4-oxo-4*H*-chromen-3-yl)methyl)phosphonate (**4id**).

Synthesis | DOI 10.1055/a-2815-1115 |

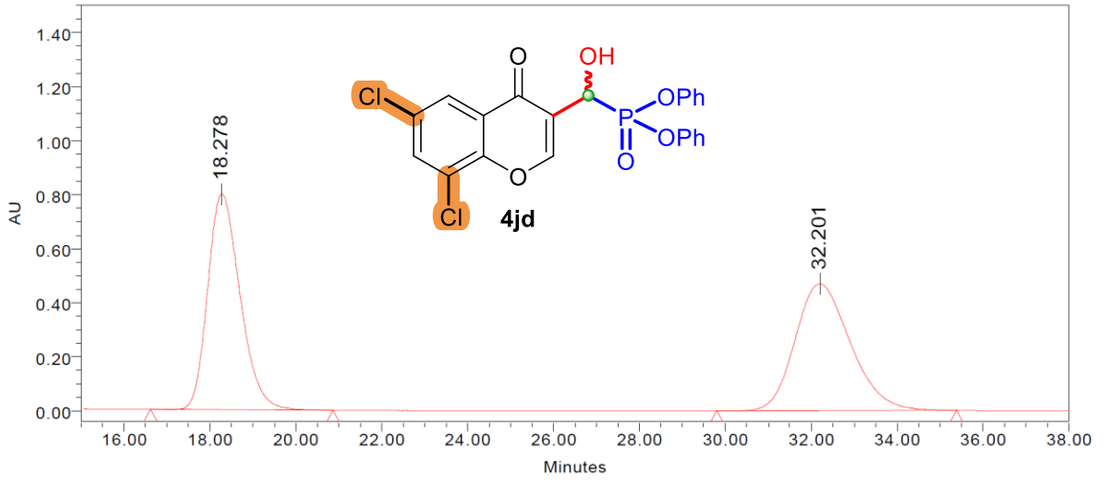

Processed Channel: PDA 236.2 nm

	Processed Channel	Retention Time (min)	Area	% Area	Height
1	PDA 236.2 nm	18.278	41851365	49.98	798629
2	PDA 236.2 nm	32.201	41881741	50.02	468741

Figure S76. Racemic mixture of diphenyl (hydroxy(6,8-dichloro-4-oxo-4*H*-chromen-3-yl)methyl)phosphonate (**4jd**) on Daicel Chiralpak column IC (*n*-heptane/*i*PrOH = 80:20, flow rate 1 mL min^{-1}).

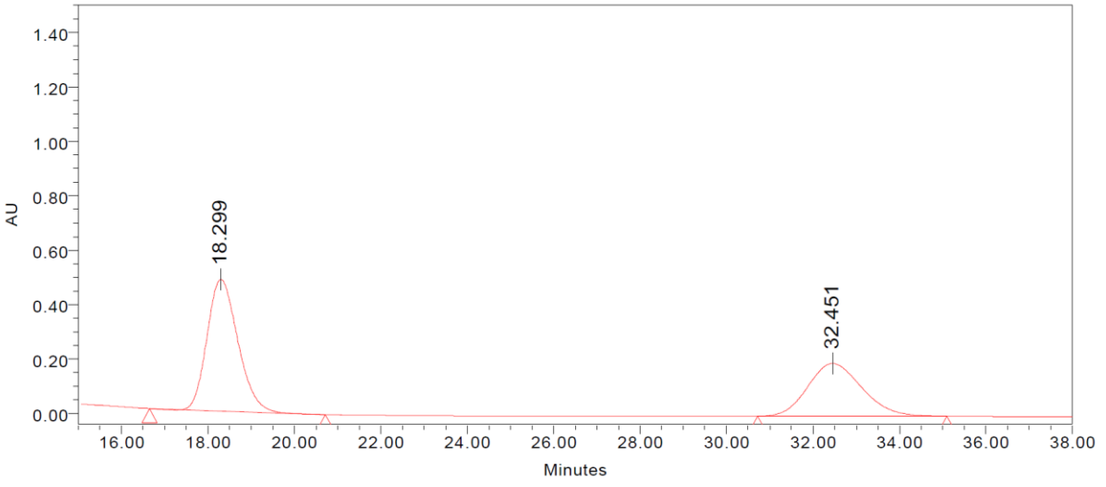

Processed Channel: PDA 236.2 nm

	Processed Channel	Retention Time (min)	Area	% Area	Height
1	PDA 236.2 nm	18.299	24083218	58.77	484423
2	PDA 236.2 nm	32.451	16896021	41.23	193971

Figure S77. Enantioselective mixture (18% ee) of diphenyl (hydroxy(6,8-dichloro-4-oxo-4*H*-chromen-3-yl)methyl)phosphonate (**4jd**).